NASA Contractor Report 187114

Study of Orifice Fabrication Technologies for the Liquid Droplet Radiator

David B. Wallace, Donald J. Hayes,
and J. Michael Bush
MicroFab Technologies, Inc.
Plano, Texas

May 1991

Prepared for
Lewis Research Center
Under Contract NAS3-25275

NASA

National Aeronautics and
Space Administration

NASA
National Aeronautics and Space Administration

Report Documentation Page

1. Report No.	2. Government Accession No.	3. Recipient's Catalog No.
NASA CR-187114		

4. Title and Subtitle
Study of Orifice Fabrication Technologies for the Liquid Droplet Radiator

5. Report Date
May 1991

6. Performing Organization Code

7. Author(s)
David B. Wallace
Donald J. Hayes
J. Michael Bush

8. Performing Organization Report No.

10. Work Unit No.
506-41-51

9. Performing Organization Name and Address
MicroFab Technologies, Inc.
1104 Summit Avenue, Suite 110
Plano, Texas 75074

11. Contract or Grant No.
NAS3-25275

13. Type of Report and Period Covered
Contractor Report Final

12. Sponsoring Agency Name and Address
National Aeronautics and Space Administration
Lewis Research Center
Cleveland, Ohio 44135

14. Sponsoring Agency Code

15. Supplementary Notes
Project Manager, K. Alan White, Power Technology Division,
NASA Lewis Research Center

16. Abstract

Eleven orifice fabrication technologies potentially applicable for a liquid droplet radiator are discussed. The evaluation is focused on technologies capable of yielding 25-150μm diameter orifices with trajectory accuracies below 5 milliradians, ultimately in arrays of up to 4000 orifices. An initial analytical screening considering factors such as trajectory accuracy, manufacturability, and hydrodynamics of orifice flow is presented. Based on this screening, four technologies were selected for experimental evaluation. A jet straightness system used to test 50-orifice arrays made by electro-discharge machining (EDM), Fotoceram, and mechanical drilling is discussed. Measurements on orifice diameter control and jet trajectory accuracy are presented and discussed. Trajectory standard deviations are in the 4.6-10.0 milliradian range. Electroforming and EDM appear to have the greatest potential for Liquid Droplet Radiator applications. Finally, the direction of a future development effort is discussed.

17. Key Words (Suggested by Author(s))	18. Distribution Statement
Orifice Fabrication; Liquid Droplet Radiator; Radiator	Unclassified - Unlimited Subject Categories 20, 31

19. Security Classif. (of this report)	20. Security Classif. (of this page)	21. No of pages	22. Price*
Unclassified	Unclassified	55	A04

*For sale by the National Technical Information Service, Springfield, Virginia 22161

Table of Contents

1.0 Summary

Eleven (11) fabrication methods were identified, described, and evaluated for their suitability to fabricate the large scale (10^5-10^6 holes per system) orifice arrays required for an operational Liquid Droplet Radiator (LDR). The methods were ranked based on past experience with jet straightness, projected experience, manufacturability, pressure drop, hydrodynamic characteristics, and diameter control. When various finishing processes were factored into the evaluation, the resulting rankings were as follows:

1. Electroform
2. Soluble Core Glass Fibers
3. Fotoceram
4. Microchannel Plates
5. Punching
   Chemical Milling
7. Mechanical Drilling and Finishing
8. Laser Drilling and Finishing
   Mechanical Drilling
10. Laser Drilling
    EDM and Finishing
12. EDM
13. E-Beam Drilling

Based on the results of the evaluation, four (4) methods (and five vendors) were selected for experimental evaluation. An orifice plate was designed and parts were purchased from the five vendors. During the evaluation of these orifice plates, two more vendors and fabrication methods were added to the experimental study, bringing the totals to six (6) methods and seven (7) vendors.

A drop generator and jet straightness test system were designed and fabricated. All seven orifice plate types were evaluated for orifice diameter control and jet straightness performance. Twenty-one (21) orifice plates were measured for orifice diameter control, nineteen (19) were qualitatively evaluated for jet straightness performance, and eleven (11) were quantitatively evaluated for jet straightness performance. Best overall results were obtained with the Stork-Veco electroform orifice plates. The Creare EDM and NASA mechanically drilled results were almost as good as the Stork-Veco results. Recommendations are made for further development efforts and specific Phase III tasks are described.

2.0 Introduction

Before the Liquid Droplet Radiator (LDR) can be demonstrated, a successful method of orifice array fabrication must be developed. Liquid Droplet Radiators are expected to have a very large number of individual streams in their final configuration. Straightness of the streams is very critical and even a few misdirected jets can result in serious fluid loss. The straightness required will not allow any jet to be 5mrad or more out of straightness. Even though jet straightness is the most difficult specification, the arrays must meet other requirements. To date, almost all of the LDR work has been focused on the heat transfer performance of LDR's. The objective of this study is to evaluate existing orifice fabrication methods, and to recommend the method or methods most suitable for production of LDR orifice plates.

In order for a fabrication technology to be acceptable, it must satisfy a number of requirements. These requirements can be broken into three main areas: functionality, reliability, and manufacturability. Functionally, the orifice array must be able to meet the drop size, frequency and straightness requirements. It must perform acceptably over the required temperature range. It must be made of a material that is inert to the fluids jetted. Reliability requirements demand that no degradation of the functionality be observable over the life of the LDR. This puts additional requirements on the design and materials. Since an LDR system may contain up to several million orifices, a fabrication process that can be scaled up to volume production is required.

Typical specifications for an orifice array are given in Table I. The actual requirements will vary from one application to another. The goal is to find one or more orifice array technologies that will satisfy all of the requirements.

Table I:
Typical Orifice Array Specifications

Diameter	50 - 200μm
Diameter Tolerances	~5%
No. of Orifices	12 rows X 400
Typical	20 rows X 250
Temperature Range	25°C to 425°C
Jet Straightness	<5 mrad
c to c spacings	>5 x diameter
Plugged holes	<1%

An evaluation and testing program comprises a system of criteria and tests which will measure the orifice arrays against the specification. Jet straightness is the most critical performance criterion and is also the most difficult to test. Therefore jet straightness performance was the focus for both analytical and experimental evaluations.

Some of the factors that affect jet straightness include orifice shape, surface finish, flow characteristics in the orifice area, rigidity of the substrate, particle generation and cleaning, and surface wetting characteristics. Some of these are discussed in detail below.

Phase I of this effort reviewed orifice array fabrication technologies, structural and hydrodynamic influences on jet straightness, testing and selection criterion, and vendor evaluations and recommendations. In Phase II, vendors were selected, orifice plates designed and purchased, a drop generator was designed and fabricated, and orifice plates tested for jet straightness.

3.0 Phase I: Analytical Evaluation of Jet Straightness Effects, Pressure Drop Considerations, Fabrication Methods Survey, and Vendor Survey

3.1 Analytical Evaluation of Jet Straightness Effects

Even if an orifice array is fabricated such that all of the orifices are geometrically equivalent and each orifice is perfectly symmetric, errors in jet straightness can occur due to structurally and hydrodynamically induced effects. The general nature of these errors are discussed below and their relation to specific orifice array fabrication methods is discussed in section 3.3.

3.1.1 Structurally Induced Straightness Effects

It is highly desirable to use multiple row orifice plates in a Liquid Droplet Radiator in order to minimize radiator and catcher size and weight. Heat transfer analysis indicates that up to twenty (20) rows of orifices could be employed and not materially degrade heat transfer efficiency. However, bending of the orifice plate will cause a row-to-row jet straightness error to occur. The magnitude of this error will depend on the operating conditions of the array (i.e. pressure), and will be a significant factor in determining the choice of an orifice plate fabrication method and/or the number of rows in an orifice plate.

The analysis discussed here is presented in non-dimensional form in order to be useful for any operating condition, material property, plate thickness, and number of rows. General conclusions resulting from this analysis will be discussed in this section. In the sections on the individual orifice plate fabrication methods, specific results will be pointed out.

Analytical Development

The deviation from perfect straightness of a multi-row array of jets due to bending of the orifice plate under manifold pressure was examined by modeling the orifice plate as a uniform beam clamped at both ends and under a uniformly distributed load. Initially, the effect of the holes was ignored, both in determining the load and the strength of the beam. The effect of the holes will be discussed at the end of this section.

Using the assumptions in the previous paragraph, an analytical solution of the shape of the beam exists. The angle of rotation of the beam as a function of position is given in equation (1).[1]

$$\Theta = \frac{W}{Et^2}(-xL^2+3x^2L-2x^3) \qquad (1)$$

Θ = *absolute angle of beam at x*
W = *unifom pressure value*
E = *beam material elastic modulus*
L = *beam length*

Figure 1 shows a schematic of the structural analysis configuration and shows the general shape of the beam.

For a multiple row orifice plate, the beam length (which would probably be referred to as the orifice plate width) would be a function of the number of rows and the orifice diameter. From heat transfer considerations, the center-to-center distance between orifices, or the pitch, P, must be greater than or equal to 5 times the orifice diameter. For this analysis, a ratio of pitch to orifice diameter of 5 will be utilized. This represents a best case from a structurally induced straightness effects standpoint.

In addition to the distance between orifice rows, there must be some distance between the outside rows and

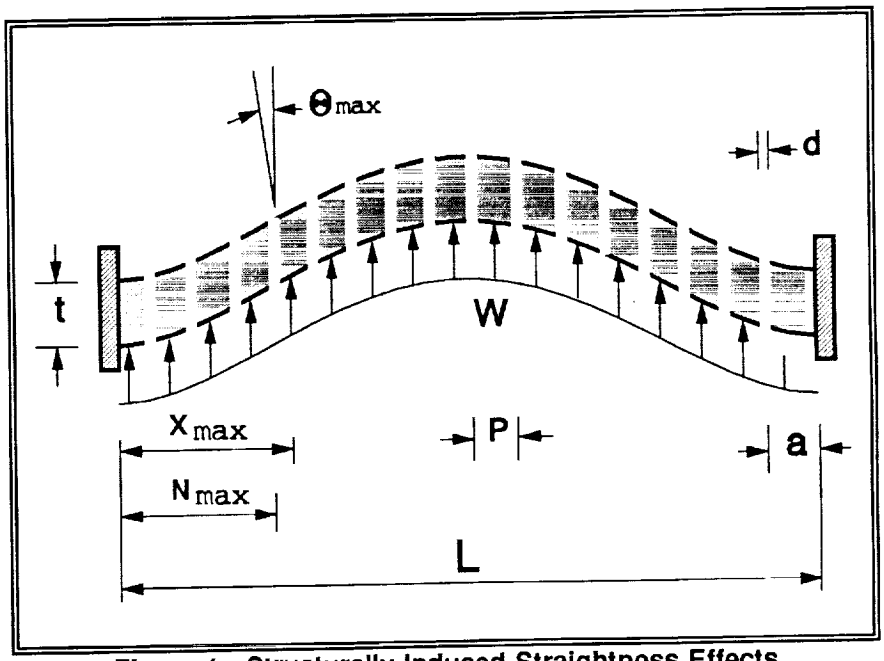

Figure 1: Structurally Induced Straightness Effects Analysis Configuration

the end of the plate. This distance, referred to as the margin, a, was set to twice the pitch in this analysis.

Overall beam length (plate width) is then given by equation (2).

Using the values for pitch and margin discussed above, the length of the beam may be expressed as a function of orifice diameter. Dividing both sides of equation (2) by the orifice diameter, d, equation (3) is obtained in non-dimensional form.

Using the values discussed above for the pitch and margin (shown in equations (4) and (5)), and substituting in equation (3), equation (6) is obtained.

Figure 2 shows the value of L/d as a function of the number of orifice rows on the plate. To use equation (6) in equation (1), the beam length must be expressed in terms of the plate thickness, as in equation (7).

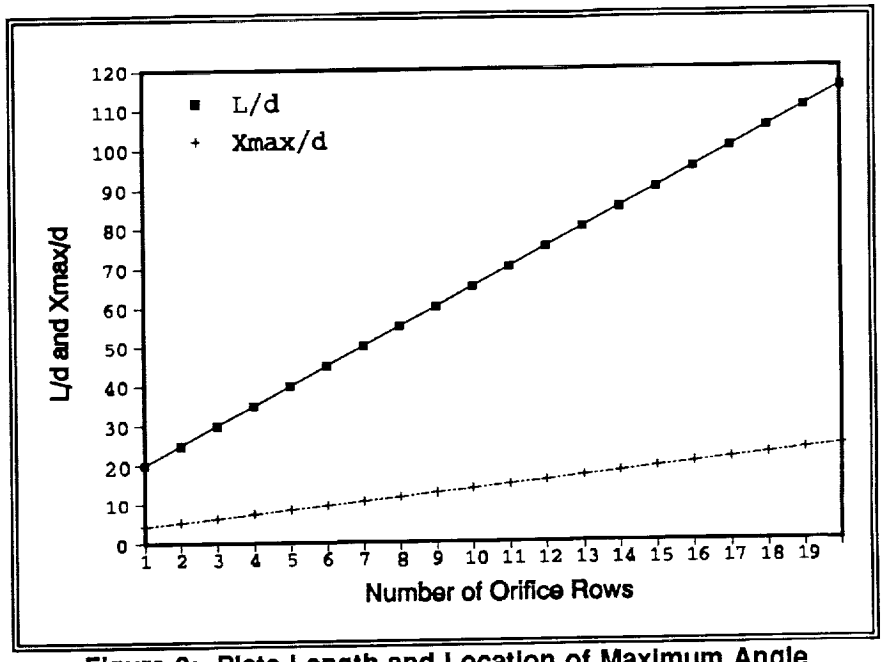

Figure 2: Plate Length and Location of Maximum Angle vs. Number of Orifice Rows

$$L = 2a + [N_{row}-1] \tag{2}$$

L = *beam length(plate width)*
a = *margin(distance from edge of plate to 1st row*
P = *pitch(distance between orifice rows)*

$$\frac{L}{d} = 2\frac{a}{d} + \frac{P}{d}[N_{row}-1] \tag{3}$$

$$\frac{P}{d} = 5.0 \tag{4}$$

$$\frac{a}{d} = 10.0 \tag{5}$$

$$\frac{L}{d} = 20 + 5[n_{row}-1] = 15 + 5N_{row} \tag{6}$$

Equations (6) and (7) may now be used in equation (1) to evaluate beam deflection as a function of *thickness ratio (t/d), number of rows (N_{row}), load to strength ratio (W/E).*

$$\frac{\frac{L}{d}}{\frac{t}{d}} = \frac{15+5N_{row}}{\frac{t}{d}} \qquad \frac{L}{t} = \tag{7}$$

From a system design viewpoint, only the maximum angle of the beam is of interest: more precisely, the maximum absolute angle of one of the orifice rows. The location of the maximum absolute angle is given as in equation (8).

$$\frac{X_{max}}{L} = 0.5[1\pm0.577] \tag{8}$$

The smaller of the two maxima is shown in Figure 2 as a function of the number of orifice rows.

$$X_N = a + [i_{row}-1]P \tag{9}$$

X_N = *location of* i_{row}
i_{row} = *row number*

In general, there will not be an orifice located at the maximum angle location. Solving equations (1), (6), and

(7) at the locations of the orifice rows, an expression (equation (9)) for the row number with the maximum absolute angle is obtained. Figure 3 shows this row number as a function of the number of orifice rows in the array.

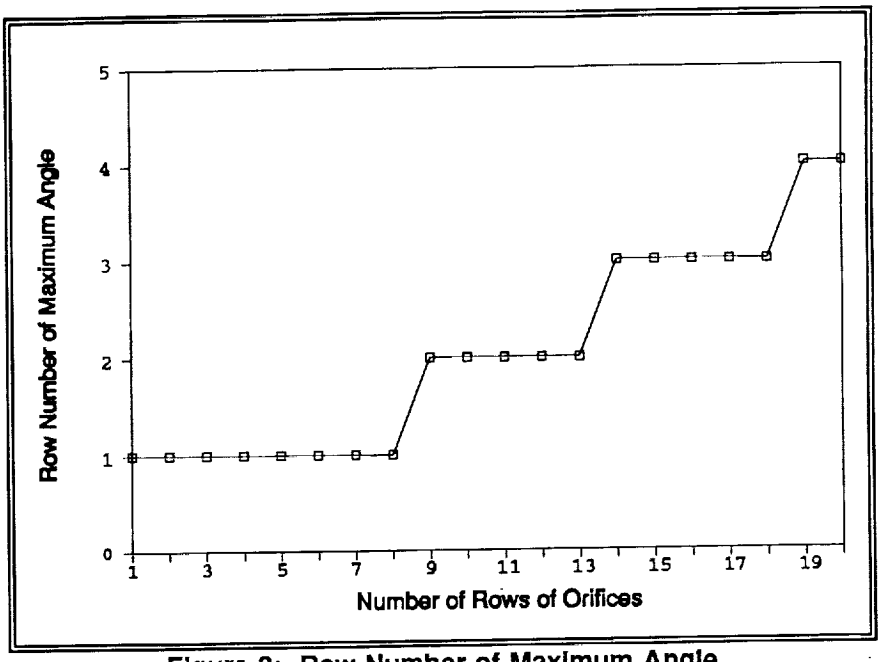

Figure 3: Row Number of Maximum Angle vs. Number of Orifice Rows

Parametric Evaluation

A parametric evaluation of structurally induced jet straightness effects was performed over the range of expected values of t/d, W/E, and N_{row}. The maximum number of rows is limited to approximately 20 by heat transfer considerations. Orifice plate thickness ratio (t/d) for the manufacturing processes considered ranged from 0.4 to 10. Operating pressures were assumed to be in the 20 to 100 psi range. Elastic moduli for the manufacturing processes considered range from $8x10^6$psi (glass) to $28x10^6$psi (steel). Given these ranges, equations (1), (6), and (7) were solved for the maximum absolute angle at an orifice row location using the values shown below.

N_{row} = 1,2,3,4,5,6,,7,...,18,19,20
t/d = 0.4,0.6,1,2,4,7,10
W/E = 0.000001,0.000004,0.000007

The results of the evaluation are shown in Figure 4 through Figure 9. Note that there are two figures for each W/E case and the only difference between them is the maximum angle scale.

Discussion

The results of the parametric evaluation study are shown in Figure 4 through Figure 9 using two sets of scales to illustrate the magnitude of structurally induced straightness effects relative to two maximum overall jet straightness criteria: 5 mrad and 1 mrad. Since other factors will contribute to the overall jet straightness, the allowable error due to structural effects must be less than the total error. Because the error is coherent (i.e., all jets in that row will have the same structurally induced jet straightness error), it will add arithmetically to all the other jet straightness error sources, rather than adding statistically if it were a random error source. This implies that structurally induced straightness errors must be much less than the total straightness criterion. Depending on the magnitude of the other sources of error, the allowable structurally induced error could vary significantly. However, based on previous experience with orifice plate tolerance allocations, it is likely that 10-20% of the total error would be allocated to structurally induced effects. Assuming a 20% allocation, an allowable error of 1 mrad would be assigned to structurally induced effects if the total allowed error is 5 mrad, and 0.2 mrad if the total allowed error is 1 mrad. These are the values indicated on Figure 4 through Figure 9 as the maximum allowable error.

By examining Figure 4 through Figure 9, several general conclusions may be made:

(1) Even for a low loading/high stiffness/large straightness error case (W/E=0.000001, H_{max}=5 mrad), only the highest thickness ratios (t/d=7 and t/d=10) would allow 20 orifice rows to be employed. For the lower straightness criteria and low loading/high stiffness, only a t/d=10 would allow 20 orifice rows.

(2) Orifice plates with thickness ratios less than 1 can only be employed in single row configurations.

(3) For a high loading/low stiffness case at the lower straightness criterion, the number of rows will be limited to 10 or less.

(4) Thickness ratio dominates the structurally induced straightness error because of its cubic

relation to H, as opposed to the linear effect of W/E. However, in the real case, an increase in orifice plate thickness would probably increase the operating pressure required to produce a given jet velocity, so some of the benefit of a thicker plate would be lost. This would be an especially important effect for orifice plate types that would add the additional thickness by increasing the length of the minimum diameter section. For a given orifice type, the dependence of operating pressure on thickness could be modeled and an optimum thickness obtained.

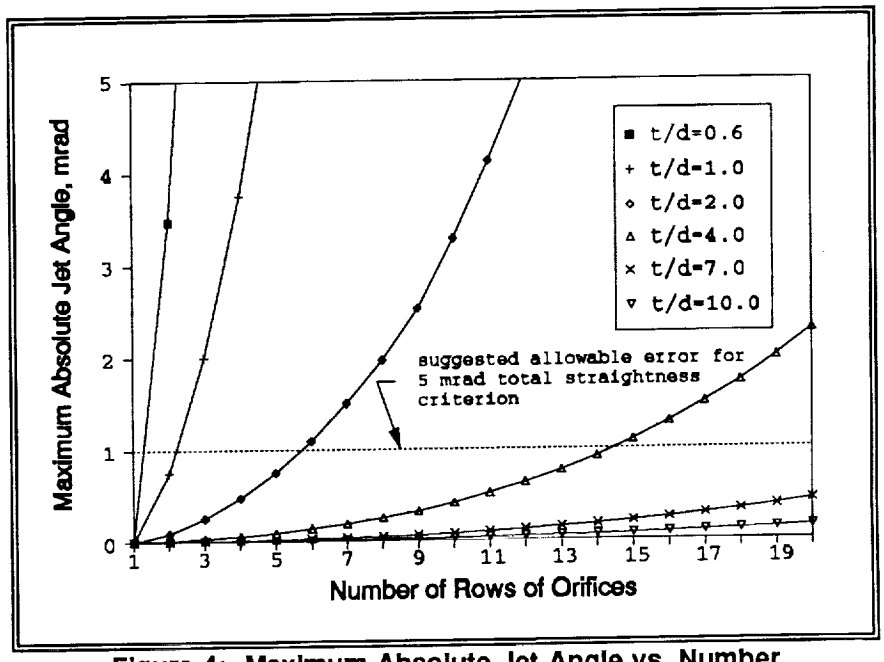

Figure 4: Maximum Absolute Jet Angle vs. Number of Orifice Rows: P/d=5, a/d=10, W/E=10^{-6}

Effect of Holes

The placement of holes in the orifice plate reduces the stiffness of the beam from the value used in deriving equation (1). However, the loading of the beam is reduced. For this analysis, it will be assumed that to first order the reduced stiffness and the reduced pressure offset one another.

The stresses in the plate, however, are much more influenced by the holes than is the deflection. For a beam under uniform load, the moment distribution is given by equation (10).[1] The maximum moment occurs at x=0. The maximum bending stress at any location on the beam is given in equation (11).

The stress calculated using equation (11) will be increased due to stress concentration around the holes. The stress for a single row of holes is increased by a factor of k/{1-d/P}, where k ranges from 1.1 to 1.85 as a/b increases from 0 to 0.7.[2]

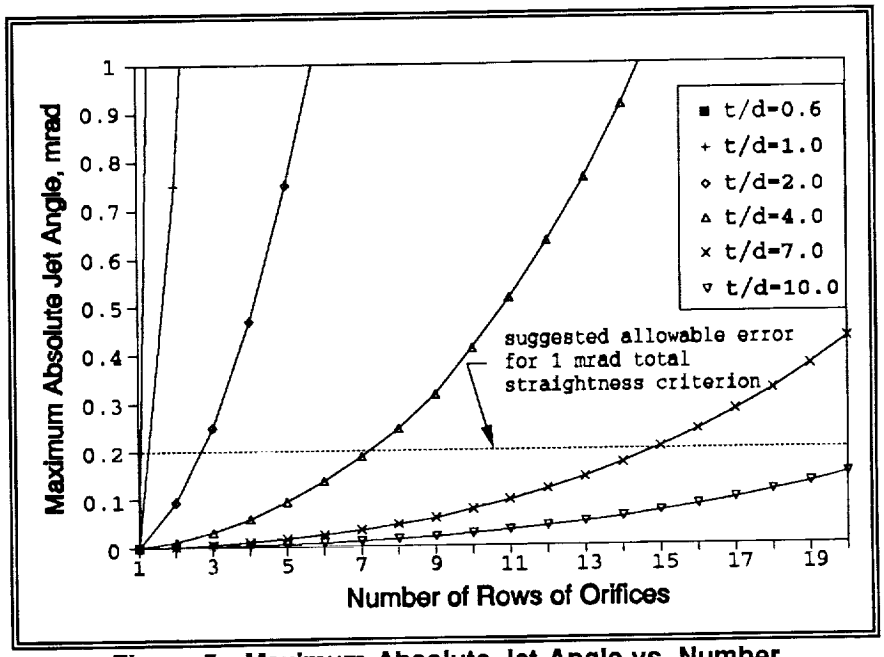

Figure 5: Maximum Absolute Jet Angle vs. Number of Orifice Rows: P/d=5, a/d=10, W/E=10^{-6}

$$M = \frac{W}{12}[6Lx - 6x^2 - L^2] \qquad (10)$$

M = *moment at location x*

$$\frac{Mt}{2I} = \frac{W}{2t^2}[6Lx - 6x^2 - L^2] \qquad (11)$$

I = *moment of inertia*

For a matrix of holes, two types are relevant to stress concentration analysis: rectangular and triangular. Figure 10 illustrates the two types of configurations.

From stress concentration factors determined for plates under tension (as opposed to bending), the rectangular array results in less stress concentration than the triangular array, which would have a better view factor for radiation heat transfer. Both have a minimum factor of 4. For a rectangular array with closely spaced holes, the stress concentration factor may be as high as 10 and for a triangular array as high as 25. Thus, stress concentration effects will probably dominate any fatigue failure analysis.

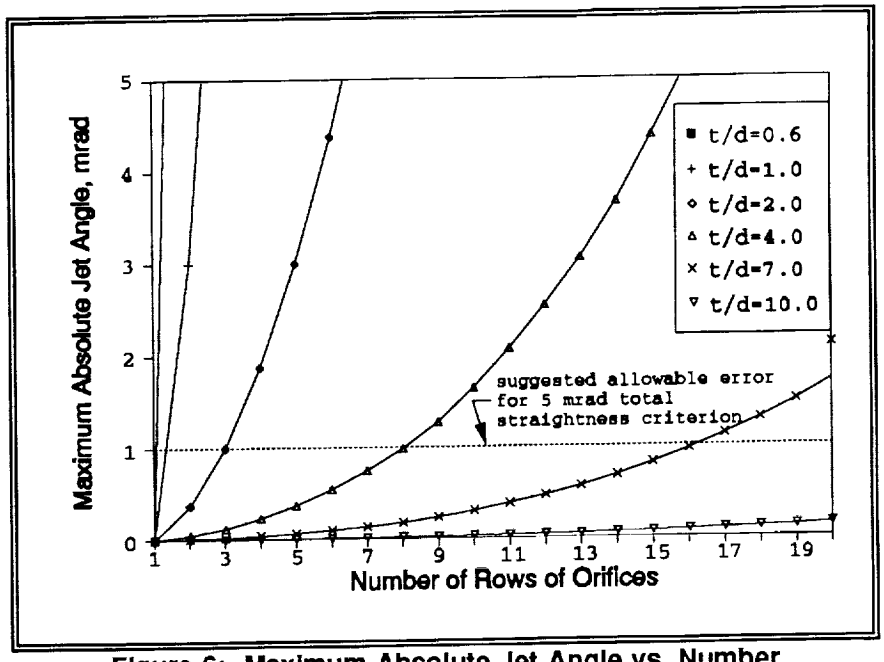

Figure 6: Maximum Absolute Jet Angle vs. Number of Orifice Rows: P/d=5, a/d=10, W/E=4x10^{-6}

3.1.2 Hydrodynamically Dependent Straightness Effects

If an orifice plate manufacturing process could produce orifices whose side walls were all parallel, the resulting jets would not necessarily all be parallel. The phenomena that would cause the jets to be non-parallel will be referred to here as hydrodynamically induced straightness effects. These in general are caused in four ways:

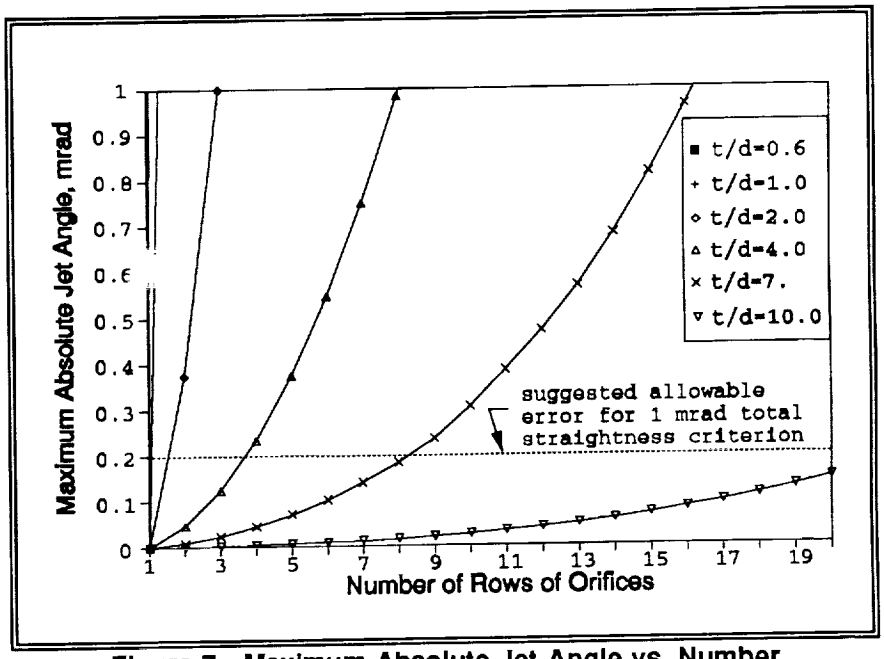

Figure 7: Maximum Absolute Jet Angle vs. Number of Orifice Rows: P/d=5, a/d=10, W/E=4x10^{-6}

(1) Asymmetric surface finish/roughness.

(2) Misalignment of two parts (i.e. orifice plate and back-up plate) or two processes (e.g. drilling the cone in a mechanical broaching process).

(3) Asymmetric flow separation from symmetric geometries.

(4) Asymmetric wetting of the exterior surface of the orifice plate.

The importance of all four of the above phenomena is a function of the flow passage geometry and Reynolds number. In general, the liquid metal LDR configurations will have much higher Reynolds numbers, but given the number of working fluids under consideration, the possible Reynolds number range is distributed over three orders of magnitude. Table II[3] shows the properties for six fluids and the Reynolds number for each for a 10m/s jet exiting from a 0.004 inch (100μm) orifice.

Asymmetric Surface Finish/Roughness

Asymmetric surface roughness will cause the velocity profile across the flow at the exit of the orifice to be

asymmetric, which in turn can cause the average of the velocity component normal to the desired flight path to be non-zero. After separation from the orifice, the momentum of the fluid in the jet will redistribute and the jet will have a component of velocity normal to the desired flight path, directed away from the maximum roughness surface.

At very high Reynolds numbers viscous effects will not be important, and at very low Reynolds numbers, the flow at the exit of the orifice will be parallel, even if it is asymmetric. Both very high and very low Reynolds numbers result in the component of velocity normal to the flight path being zero.

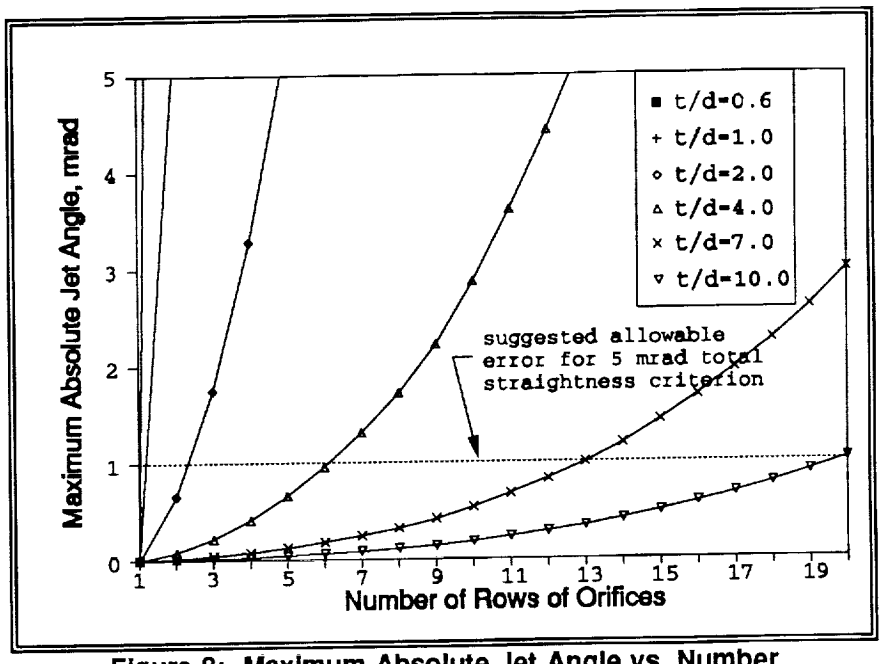

Figure 8: Maximum Absolute Jet Angle vs. Number of Orifice Rows: P/d=5, a/d=10, W/E=7x10^{-6}

For the case where the Reynolds number is such that the boundary layer is approaching the diameter of the flow channel, the effect of non-uniform roughness, whether distributed or discrete, will be a maximum. This will occur when the l/d of the constant diameter section is equal to approximately 0.02*Re, and thus will probably be important only for the applications using low vapor pressure oils.

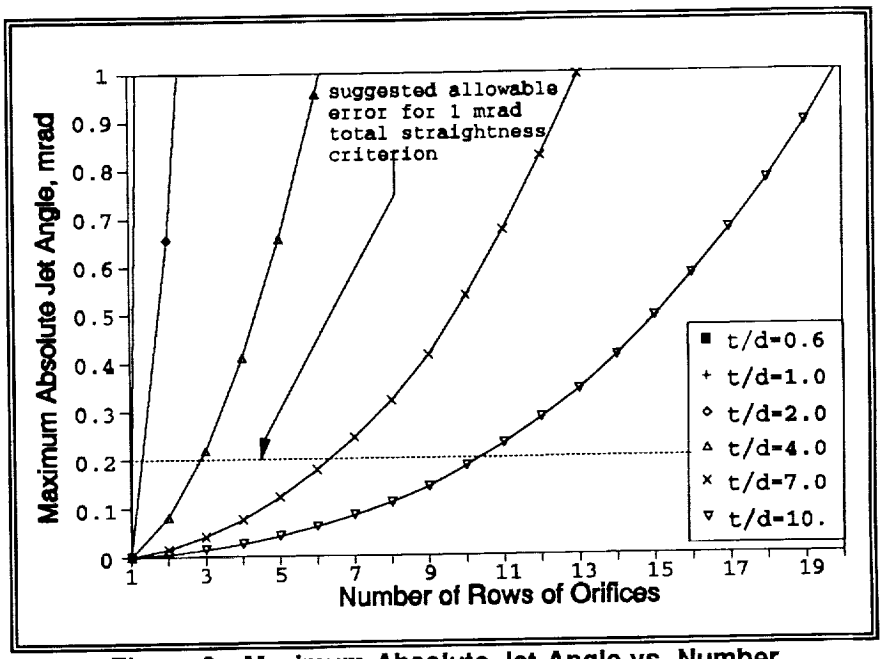

Figure 9: Maximum Absolute Jet Angle vs. Number of Orifice Rows: P/d=5, a/d=10, W/E=7x10^{-6}

Misalignment of Two Part or Two Process Orifice Plates

If an orifice plate assembly is made of two parts, such as a pure Ni electroform or a low t/d thickness ratio soluble core glass orifice plate bonded to a relatively thick backup plate, or if the orifice plate is made by a two step process, such as the pre-drilling of the cone in the mechanical broaching and drilling processes, there will be some misalignment between the two parts or process steps. This misalignment will result in an asymmetry in the flow due to inertial and/or viscous effects.

Misalignment of the two parts or processes would cause the mean flow to negotiate a pair of turns that would result in a velocity component normal to the desired flight path downstream of the final turn. At very high Reynolds numbers this effect would be compensated for if the section downstream of the turning is straight: the longer the l/d of this section, the less the effect of the turning will be "remembered" at the exit of the orifice. Since inertial effects dominate at high Reynolds number, the decay of the effects of turning would be similar to the decay of a disturbance in any field described by an elliptic partial differential equation.

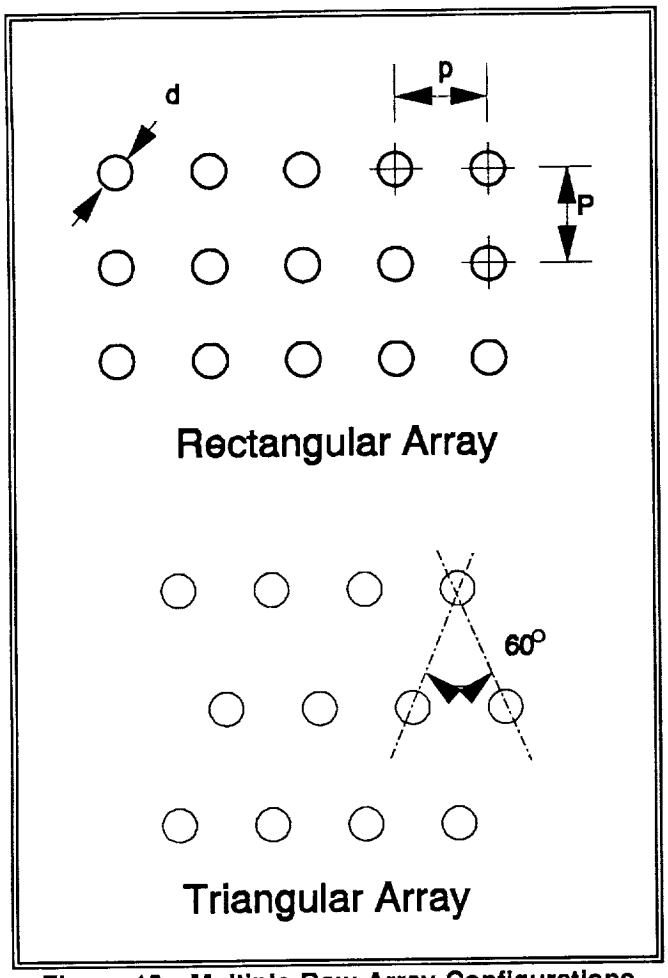

Figure 10: Multiple Row Array Configurations

Therefore, downstream l/d's of greater than 2-3 should minimize this effect.

At moderate Reynolds numbers where the boundary layer is less than the channel width, but significant enough to affect the mean flow, the asymmetric distribution of viscous effects will interact with the inertial effects. In addition, this non-uniform distribution of viscous effects will be "remembered" downstream of the turning for a distance that depends on Reynolds number. Again, a straight section downstream of turning, on the order of 2-4 diameters, will decrease the effect of the misalignment. Quantifying this effect is obviously highly dependent on the geometry and Reynolds number.

Asymmetric Flow Separation from Symmetric Geometries

Even in a perfectly symmetric channel, the flow can be non-uniform. This is usually illustrated by the unstable or multi-stable flow in a diffuser where the flow separates from one or both walls. Many of the orifice plate processes considered here produce very sharp corners at the entry to the orifice plate and asymmetric separation downstream of these corners, even if the orifice geometry is perfectly symmetric.

This phenomenon will be significant at moderate to high Reynolds numbers, since the corner will be smoothed by a viscous layer that is large enough. At the Reynolds numbers expected with some of the liquid metals (10,000 to 40,000) this phenomenon could be significant and therefore should be investigated analytically for the configurations of interest.

Asymmetric Wetting of the Exterior Surface of the Orifice Plate

As with the above phenomenon, asymmetric wetting of the exterior surface of the orifice plate can cause an otherwise perfectly straight flow to be deflected. This can conceivably occur even if the surface finish is uniform due to the hysteresis between leading and lagging contact angles. In practice, a non-uniform surface finish is usually the cause.

Previous experience with soluble core glass orifice plates at a Weber number of around 50 indicates that this phenomenon can be very important, especially when a high surface energy material like glass is the orifice plate material.

Table II: Fluid Properties, Reynolds Number and Weber Number for Candidate LDR Fluids

Fluid	Absolute Viscosity (poise)	Density (kg/m^3)	Surface Tension (N/m)	Typical Reynolds Number	Typical Weber Number
Dow 705	0.24	1090	0.037	45	300
Lithium	0.0055	500	0.35	900	14
Gallium	0.0016	6092	0.718	38,000	85
Aluminum	0.029	2300	0.90	770	25
Tin	0.012	6800	0.515	5,500	132
NaK	0.0025	755	0.110	3,000	70

3.2 Pressure Drop Considerations

Both power consumption and structural weight are affected by viscosity induced pressure losses. As with hydrodynamically induced straightness effects, the relative importance of viscosity induced pressure losses will be a function of passage geometry and Reynolds number.

The typical Reynolds numbers listed in Section 2.4.0 for the candidate liquid metals are all greater than 700. At these Reynolds numbers almost all the viscous loss would be due to entry flow effects, so the pressure loss would be affected strongly by entrance geometry and only weakly by the length (i.e, thickness) of the flow passage.

Systems that use low vapor pressure oils (typical Reynolds number of 45) would have a much greater interaction between orifice shape and viscous loss than would liquid metal systems because of the much smaller Reynolds number. In order to quantify this variation in viscous losses between different orifice plate types, a pressure loss coefficient was estimated for each type of plate using the orifice flow model shown in (12).[4]

$$C_p = [K + \frac{K'}{Re} + \frac{64l}{Re\,d}]$$

$$C_p = \frac{actual}{ideal}\ pressure \qquad (12)$$

l = *length at diameter d*
d = *orifice diameter*
Re = *Reynolds number based on d and average jet velocity*
K, K' = *loss constants*

For the Reynolds number range of interest, the term with K' can be neglected. For each orifice plate type, an *l*/d equal to average of the minimum and maximum values possible was used in Equation (13). For smooth and continuous contractions, K was estimated as 1.5[5] For sudden contractions (*l*/d = 0), K was estimated to be 2.3.[6] The pressure coefficient computed from (12) was multiplied by ten and used as ranking for the pressure drop category.

3.3 Fabrication Methods Evaluation

Based upon prior experience at both Microfab and NASA and upon initial literature searches, eleven fabrication methods were investigated during Phase I of this effort. The methods selected are shown in Table III and will be discussed in detail in Section 3 of this report. Some of the fabrication methods investigated have more than one process flow and/or design configuration option. Moreover, the addition of a finishing process to some of the mechanical and thermal material removal processes will be necessary or advantageous to enhance the manufacturability of the nozzle arrays. In this section the eleven fabrication methods are discussed in detail. Specific information includes:

Table III: Orifice Fabrication Methods Investigated

Electroform - Plating
Chemical Milling
Laser Drilling
Electro-Discharge Machining
Mechanical Punching (or broaching)
Mechanical Drilling
Soluble Core Glass Fibers
Multichannel Plates
Electron Beam Machining
Ion Drilling
Fotoceram

Description of Method
Geometric Sketch
Materials
Structurally Induced Straightness Effects
Hydrodynamically Induced Straightness Effects
Past Experience at Achieving 5 mrad Straightness
Straightness Estimate
Direction of Effort to Improve Straightness

3.3.1 Electroform - Plating

Description of Method

Figure 11 outlines the typical process steps for the electroform process. The starting material can be purely a mandrel where the Ni nozzles are electroformed and then removed, or in some cases, the Ni is electroformed onto Cu, BeCu or other starting material to form a bimetallic nozzle structure. In either case, the electroform metal (for orifice plates this is usually Ni or a Ni rich alloy) is plated onto the substrate or mandrel. This process begins by using a photolithography technique to define a pattern of circular disks of photoresist on a metal substrate.

Figure 11 a shows a substrate material coated on both sides with a thin layer of photoresist material. A spin coating process is used on small parts and a dip process is usually used on large parts.

Once the photoresist is ready, a matched pair of photomasks are aligned above and below the substrate. The photomask contains clear and opaque features that define the pattern to be created in the photoresist layer. The areas in the photoresist exposed to the U.V. light are polymerized and are made insoluble to a specific solvent known as a developer. This type of photoresist is known as a negative photoresist.

After exposure to U.V. light and the development of the resist, a pattern shown in Figure 11c exists. Now the part is ready for Ni plating.

The plating occurs everywhere except where the photoresist pattern exists. To obtain high quality parts, the plating rate, uniformity, and time must be controlled very tightly. The plating solution, usually a nickel sulfumate or a Watts nickel solution, is monitored for pH and for assay of certain chemicals. In doing so, the plater can control the film stresses, surface finish, and plating rates. Figure 11d shows the part after plating.

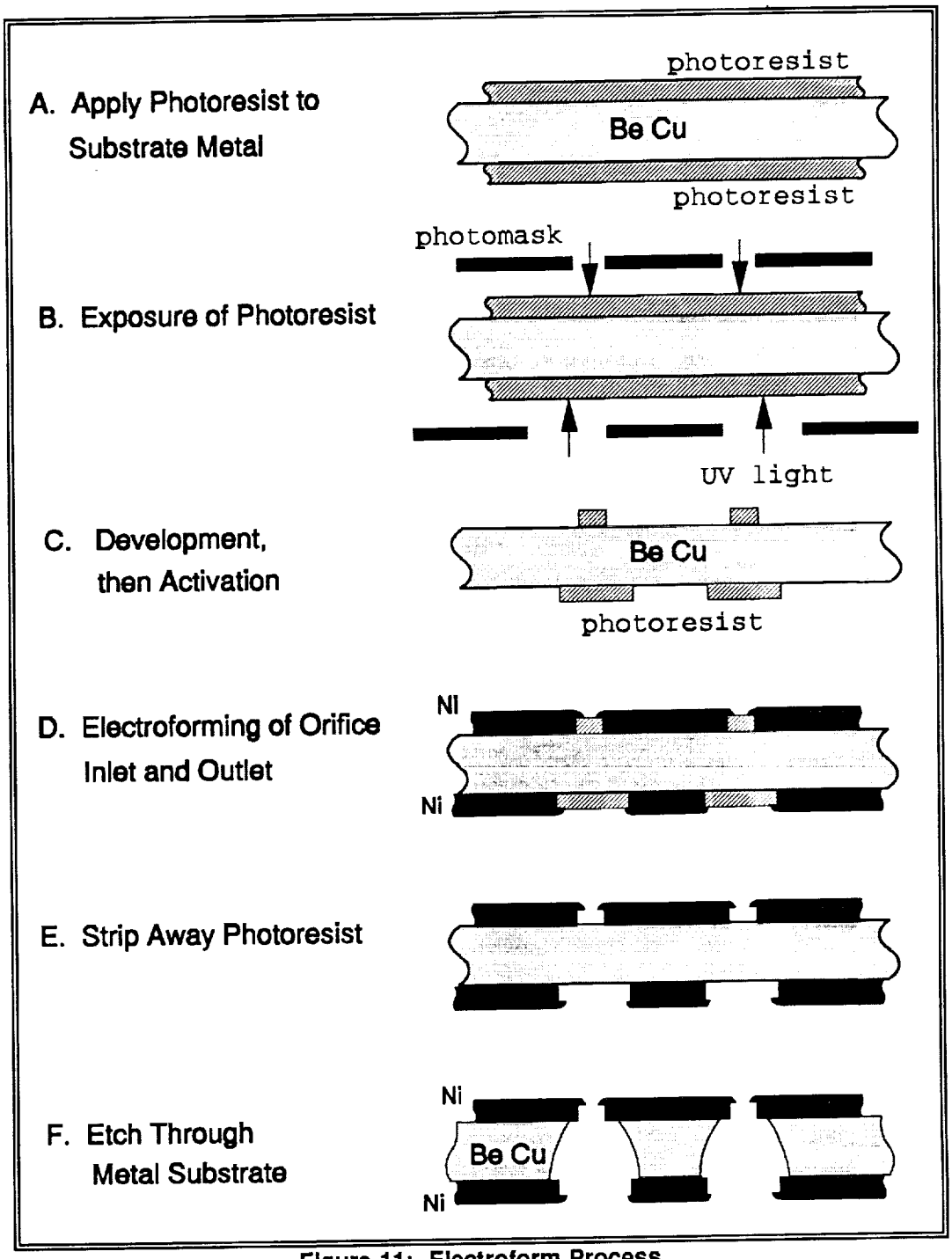

Figure 11: Electroform Process

Next, the photoresist is removed (see Figure 11e) and Ni is used as a mask and the substrate metal is etched away inside the cavity as shown in Figure 11f. The final orifice geometry obtained is shown in Figure 12.

Materials

The nozzles are typically formed of pure nickel or a nickel alloy. The nozzle cavity can be either nickel, or a Bimetallic where Cu or BeCu is used as a starting material. The assay of the nozzles is influenced by the nickel anode material assay, the plating bath chemistry and the mandrel materials.

Structurally Induced Straightness Effects

The two types of electroform orifice plates, pure Ni and bimetallic, would have distinctly different structurally induced straightness characteristics. With a modulus of elasticity approximately half that of steel for both Ni and Be-Cu, the load to strength ratio, W/E, would probably be close to the middle of the range evaluated. Using existing technology, the pure Ni plates would have t/d ratios less than two. A method under current development whereby the photoresist pegs can be made much longer than is currently possible would permit plates to be made with t/d ratios of up to approximately 5. In the former case, use of the pure Ni plates would be restricted to single row configurations. In the latter case, up to 4 rows might be possible.

For the bimetallic configuration, a t/d ratio of 5 probably represents a minimum, and ratios well above 10 are possible. Thus, from a structural standpoint, the bimetallic configuration is to be preferred since it should allow for as many rows as is desired from heat transfer considerations.

Hydrodynamically Induced Straightness Effects

From a hydrodynamic standpoint, the shape of the orifice for electroform orifice plates is probably the worst that could be imagined: not only must the entry flow negotiate a sharp corner greater than 90°, but the flow channel downstream of the corner is divergent and there is no clearly defined detachment location for the jet. The divergent channel could result in asymmetric flow separation and the lack of a clearly defined detachment point could result in non-uniform wetting effects.

The above paragraph indicates that, by inspection, electroform orifice plates could have poor jet straightness due to hydrodynamic effects. Experience, however, indicates the opposite. Electroform plates are the most common type of orifice plate used in ink jet printing systems, and by implication their jet straightness performance is acceptable. Although drop-on-demand systems do not require small values of jet straightness to produce acceptable print quality, continuous systems do, and the experience of Microfab personnel confirms that electroform orifice plates can have acceptable jet straightness despite the inherent shape. This is probably due to a high degree of uniformity, both of the geometry and the surface finish, resulting from the plating process. Also ink jet printing systems operate at moderate Reynolds and Weber numbers. An obvious area of concern is that electroform plate performance would change at the higher Reynolds numbers and lower Weber numbers associated with some of the liquid metal applications.

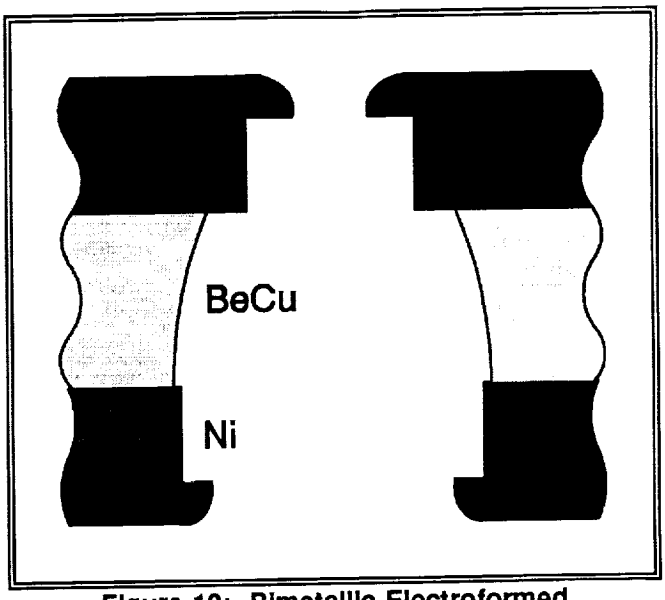

Figure 12: Bimetallic Electroformed Orifice Geometry

Past Experience At Achieving 5 mrad Straightness

This method of nozzle fabrication has been used to produce single nozzles and nozzle arrays at Mead Office Systems, Xerox, IBM and other companies which met straightness conditions of <5 mrad. Our personal experience at Mead Office Systems includes jet straightness results of <3 mrad over large numbers of jets in a single array (>200 nozzles).

Straightness Estimates

Given the ability to plug 1 to 2 percent of the jets in a given array, we feel that jet straightness in the 2 to 3 mrad range is possible with this fabrication method.

Direction of Effort To Improve Straightness

Improvements to the surface quality of the mandrel materials and/or bimetallic starting materials could yield a large number of jets which meet the 2 mrad straightness criterion. In addition, improvements of airborne particulate conditions by changing both filtration and handling procedures could improve both average straightness and the yield of straight jets. Thirdly, the use of thick liquid photoresist (25-50μm) when creating the nozzle mandrels could reduce the nozzle diameter tolerance currently experienced.

3.3.2 Chemical Milling

Description of Method

This process utilizes photolithography (see Figure 11a,b,c) to create an etchant resist pattern or "mask" on the nozzle starting material. In the electroform process, the photoresist was used to define the orifice area (Figure 11c) and expose the surrounding

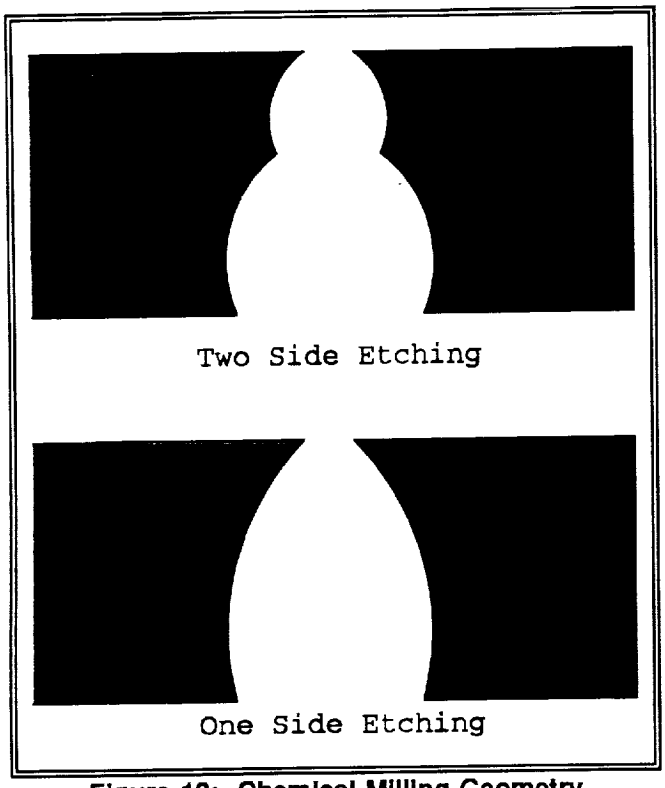

Figure 13: Chemical Milling Geometry

metal. In the chemical milling process, the photoresist is used to protect the surrounding metal and expose the orifice area. Chemical etching removes the metal in the orifice as shown in Figure 13. The subsequent etching process is enhanced by using spray etchers, or by applying an electrical potential between the etchant material and the substrate metal. Thus the term "Photochemical Etching" is sometimes used in describing the process. By varying etchant conditions and the number of etch passes, some control of nozzle wall angle can be achieved.

Materials

The chemical milling process works quite well with most metals. Many formulations of stainless steels would be good candidate materials for producing liquid droplet nozzle arrays.

Structurally Induced Straightness Effects

If stainless steel is used as the plate material, the load to strength ratio should be at the low end of the range evaluated. The thickness of the plate can be selected, allowing high t/d plates to be used, although there is a trade-off between thickness and production time and cost. Chemical milling should therefore allow the number of rows to be selected from heat transfer considerations.

Hydrodynamically Induced Straightness Effects

The two principle areas of concern for chemically milled orifice plates as far as hydrodynamically induced effects are concerned are the sharp entry flow region and the poor, and thus potentially non-uniform, surface finish. A long l/d flow channel would probably decrease any asymmetry associated with the entry flow.

Past Experience at Achieving 5 mrad Straightness

There is no direct experience or accounts of nozzle arrays being fabricated using this technique.

Straightness Estimates

We have no available data on the straightness of chemical milled parts. The quality of the final orifice plates depends on the quality of the starting metal substrate (grain structure, defects, etc.), the photolithography process and the etching process. We feel that it would be extremely difficult to obtain large chemical milled parts with straightness better than 5 mrad.

Direction of Effort To Improve Straightness

Improvements to the surface quality of the starting material would be a good starting point. In addition, improvements of airborne particulate conditions would reduce the nozzle defects that are photolithography induced.

3.3.3 Laser Drilling

Description of Method

The output of a pulsed laser is an intense burst of coherent monochromatic light. Using values typically encountered in pulsed laser drilling, a 1.2 msec pulse of 15J total energy focused on a .005" diameter spot produces an instantaneous power density in excess of 90MW/cm^2. Such an intense pulse will melt and vaporize a small portion of the target work piece. The tremendous volume expansion of the vaporized material generates pressures sufficient to blow the molten material out, creating a hole. Multiple shots at a given spot produce a progressively deeper hole.

The dimensions of a laser drilled hole are a function of the material and part configuration, the pulse length and energy, the beam focus, and the number of shots taken per hole.

The characteristic shape of a laser drilled hole when drilled at the optimum parameters exhibits a tapered or bell-mouthed entrance followed by a nearly uniform diameter through the remainder of the hole. The taper may add 10 percent to the nominal hole diameter. By altering the drilling parameters appropriately, the hole can intentionally be made to taper all the way from entrance to exit or even to have a reverse taper with an

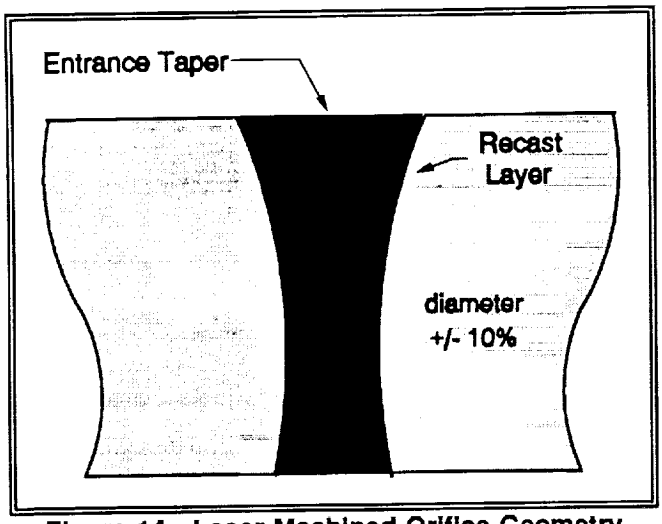

Figure 14: Laser Machined Orifice Geometry

enlarged exit following the bell-mouthed entrance.

Repeatability of hole diameter is a function of the consistency of the operating parameters, primarily energy per shot, focal distance and work piece thickness.

Figure 14 shows how a typical laser drilled hole might appear in cross section in a metal sample. Uncontrollable diameter variations exist, starting with the funnel-shaped entrance to the hole. A thin layer of "recast" clings to the side walls of the hole. This material has been melted and resolidified in such a short time that the frozen metal has a different structure than that of the parent material. Depending on the alloy being drilled, this recast is often of considerable hardness and prone to developing micro-cracks.

The build-up of the recast layer can be minimized by optimizing the operating parameters of the laser. In some cases, finishing operations can be used to remove this recast layer. Since amorphous materials go from the solid phase directly to the vapor phase, they don't show the same recast effect.

Materials

A wide variety of materials can be machined using lasers. Neodymium-doped, Yttrium-Aluminum-Garnet (Nd:YAG) lasers are used to drill holes in metallic materials. All metals can be drilled, including high conductivity ones such as gold, silver and copper. Stainless steel (incl. #316) as well as high melting point metals such as tungsten, molybdenum and niobium, can also be drilled.

CO_2 lasers can be used to drill holes in ceramics and polymers. Excimer Lasers can be used for polymer materials as well as for metals and ceramics.

Structurally Induced Straightness Effects

If stainless steel is used as the plate material, the load to strength ratio should be at the low end of the range evaluated. However, with a maximum t/d of around 5, the number of rows would probably be restricted to 8 or less.

Hydrodynamically Induced Straightness Effects

The two principle areas of concern for laser drilled orifice plates are the sharp entry flow region and the poor, and thus potentially non-uniform, surface finish. The long l/d of the flow channel would probably decrease any asymmetry associated with the entry flow.

Past Experience at Achieving mrad Straightness

We know of no outside groups who have made arrays using laser drilling. The principals at Microfab have had some experience using this technology, but no parts were ever made where the straightness was better than 10 mrad.

Straightness Estimates

These estimates are difficult to make because we feel that to get the straightness <5 mrad will require post processing steps such as electroplating. Based on this assumption, our estimates are as follows:

	Now	1-2 Yr. Effort
Standard Materials	10-20 mrad	10 mrad
Amorphous Materials	5-15 mrad	~5 mrad
Post Processing	?	<5 mrad

Direction of Effort To Improve Straightness

To improve the quality of laser drilled orifice arrays, a number of actions should be taken:

1. Select a laser system that has extremely good control over the power levels.
2. Select a high quality optical system that has been designed specifically for this application.
3. Select the best substrate material for the application and for the ability to obtain clean holes. Amorphous metals may be the best selection.
4. Run designed experiments to study the interaction among the various parameters.
5. Develop a finishing process to obtain clean, smooth surfaces.

3.3.4 Electro-Discharge Machining

Description of Method

Electro-discharge machining, designated EDM, removes metal through the action of high-energy electric sparks on the surface of the work piece. The mechan-

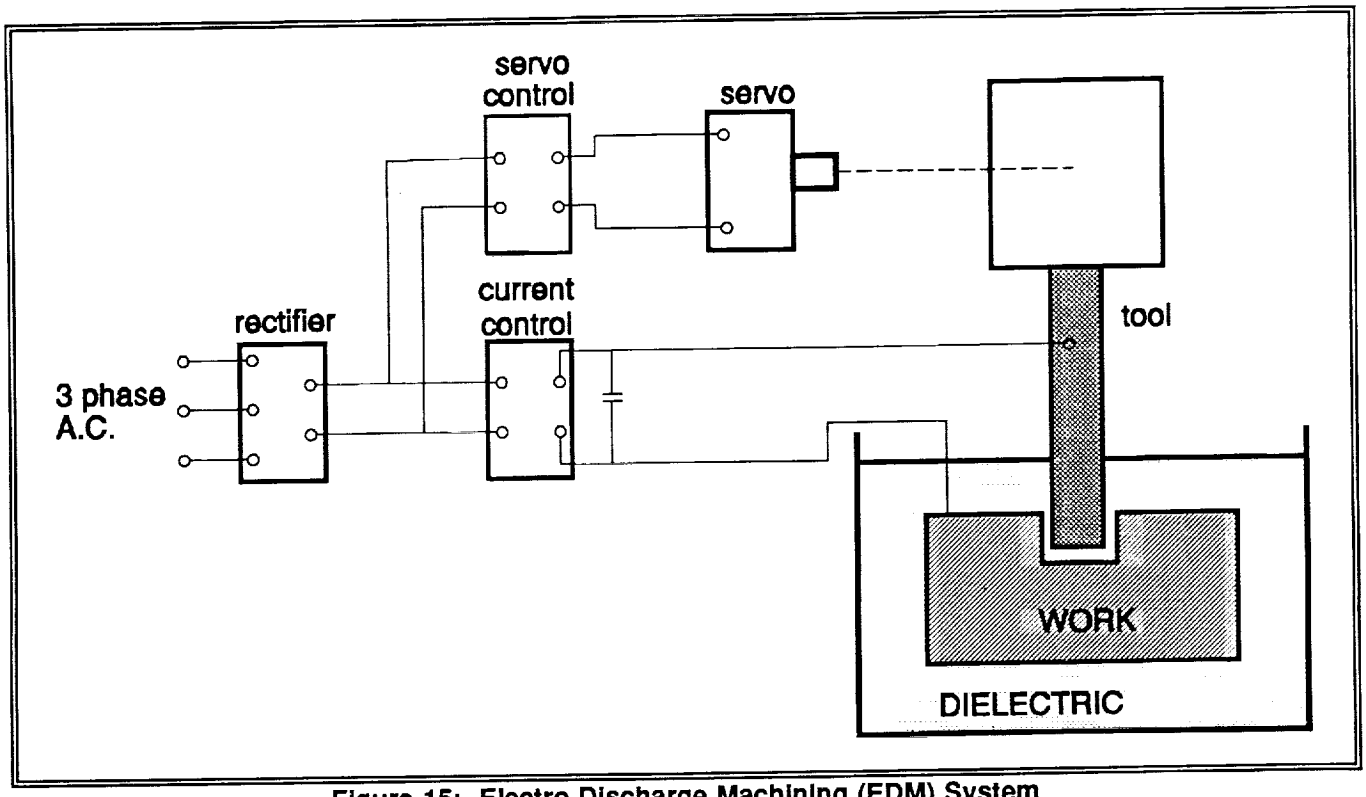

Figure 15: Electro-Discharge Machining (EDM) System

ical setup and the electrical circuit involved are shown in Figure 15. The tool and the work piece are submerged in a fluid having poor electrical conductivity-usually a light oil. A very small gap, of approximately 25μm or less, is maintained between the tool and the work piece by means of a servosystem. When the voltage across the gap becomes sufficiently high, capacitors discharge current across the gap in the form of a spark for an interval of from 10 to 30 msec and with a current density of the order of 1,500 A/mm^2 (10^6 A/in.^{2}). When the voltage has dropped to about 12 volts, the spark discharge is extinguished and the capacitors start to recharge. This cycle is repeated thousands of times per second, and thousands of spark-discharge paths occur between the surface of the tool and its mating work surface. Each discharge removes minute amounts of material from both the tool and the work piece. The resulting workpiece surface is composed of extremely small craters, so small that a surface finish of about 3.81 microns (150 microinches) is obtained on roughing cuts and about 0.762 microns (30 micro-inches) on finishing cuts. A typical EDM orifice geometry is shown in Figure 16.

The mechanism of metal removal by electro-discharge machining is not completely understood and appears to involve more than one phenomenon. Most of the removal is by fusion of minute particles of metal that are thrown from the surface by the thermal action accompanying the highly localized heating and cooling of the metal surface as a consequence of the concentrated release of energy in the spark. However, not all the particles released are fused, particularly in the case of some metals. It appears that highly localized thermal stresses also play a role in the metal-removal process.

As with the laser drilling process, EDM usually requires secondary finishing operations to obtain holes adequate for fluid jet applications. Chemical machining, electropolish machining, and abrasive flow machining are examples of secondary finishing operations.

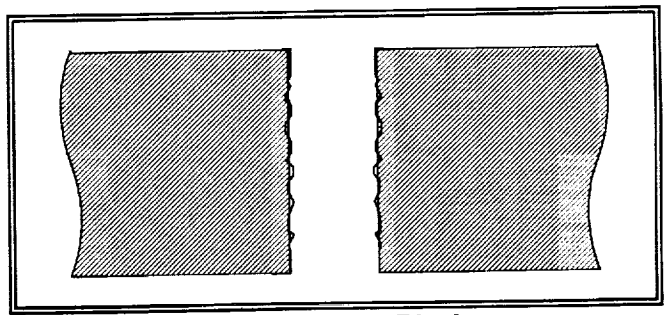

Figure 16: Electro-Discharge Machined (EDM) Orifice Geometry

Electro-discharge machining is best suited for hole diameters 125μm or above. It is capable of a depth to diameter ratio of 10:1. We have sources of precision tungsten wire of 25μm. Tungsten is usually used as the electrode material.

Materials
Electro-discharge machining works for all metals. For this application, a material such as 316 stainless steel is a good selection. The selection process for material should take into account the finishing operation.

Structurally Induced Straightness Effects
As with the laser drilled plates, if stainless steel is used as the plate material, the load to strength ratio should be at the low end of the range evaluated. The maximum thickness for EDM plates would be greater than the laser drilled plates, allowing thickness ratios of up to 10. This would allow the use of as many rows as desired from heat transfer considerations. However, the production time (and cost) would increase almost directly proportionally to the depth to be drilled, making high t/d EDM plates not quite as attractive.

Hydrodynamically Induced Straightness Effects
As with the laser drilled orifice plates, the two principle areas of concern for electro-discharged machined orifice plates as far as hydrodynamically induced effects are concerned are the sharp entry flow region and the potentially non-uniform, surface finish. The long l/d of the flow channel would probably decrease any asymmetry associated with the entry flow.

Past Experience at Achieving 5 mrad Straightness
We know of no straightness information using electro-discharge machining. Panasonic has sold an electro-discharge machine MG-ED01 for creating single ink-jet orifices. This machine is capable of creating orifices (of good quality) below 25μm.

Straightness Estimate
Based upon the quality of holes obtained using the Panasonic MG-ED01, good jet straightness could be obtained. It should be as good as laser drilling.

Direction of Effort to Improve Straightness
To improve the quality of orifice arrays made by the electro-discharge machine method, a number of actions should be taken:

1. Obtain a Panasonic MG-ED01
2. Develop an acceptable process using the MG-ED01
3. Select the best substrate material for the application
4. Run designed experiments to optimize the process parameters
5. Develop a finishing process to improve the quality of the surfaces

3.3.5 Mechanical Punching (or Broaching)

Description of Method
This technology is used for the manufacture of fibers for the clothing industry. In that industry, it is referred to as the spinneret technology. The fabrication process consists of first drilling the taper section of the nozzle and then high speed/high pressure mechanical punching. The surface finish of parts observed has been outstanding. It is not known whether secondary operations were performed on those parts. The method has flexibility in the taper length, taper angle, and the length to diameter ratio. Length to diameter ratios from 0.5:1 to 5:1 are possible. A typical broached orifice geometry is shown in Figure 17.

Materials
The quality of mechanically punched holes depends upon the mechanical and flow characteristics of the metals. A material of medium hardness is desired. Successful holes are routinely manufactured using stainless steel (316 is a good choice).

Structurally Induced Straightness Effects
If stainless steel is used as the plate material in mechanical broaching processes, the load to strength ratio should be at the low end of the range evaluated. The need to predrill the cone forces the plate to high thickness ratios. Therefore, broached plates should

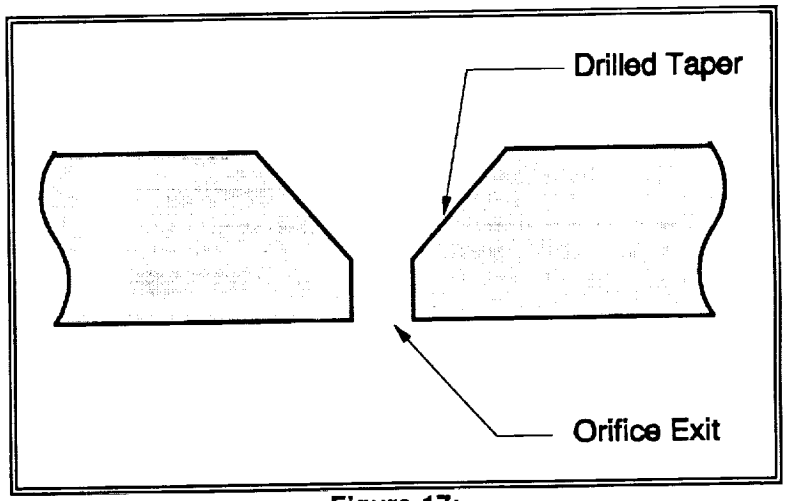

Figure 17:
Mechanically Punched Orifice Geometry

allow for the use of as many rows as desired from heat transfer considerations.

Hydrodynamically Induced Straightness Effects
Mechanical broaching requires the pre-drilling or forming of a cone at the locations where the orifices are to be made. This produces the potential for some misalignment of the two steps, and thus a flow induced jet straightness error. Note that any angle between the axis of the cone and the axis of the broached section will produce a flow pattern similar to a spatial misalignment of the two processes.

Past Experience at Achieving 5 mrad Straightness
We have previously tested 200 jet arrays using plates made by Kasen. These plates had most of the jets <10 mrad, with a few outside this range. Seventy-five percent of the jets were within 5 mrad.

Straightness Estimate
The only data we have is 200 orifice arrays where 75% of the orifices were within 5 mrad and 100% were within 20 mrad. We feel that this could be improved to the point where orifice plates with all jets within 8 to 10 mrad are possible.

Direction of Effort To Improve Straightness
Companies such as Celanese, DuPont, etc. use this spinneret technology to make orifice arrays for pulling fiber consider their processes a trade secret. Since we do not understand the processes it would be necessary to rely on these companies for improvements.

3.3.6 Mechanical Drilling

Description of Method
Certain aspects of drilling can cause considerable difficulty, especially when drilling holes below 0.010" in diameter. Most drilling is done with a tool having two cutting edges. These edges are at the end of a relatively flexible tool and the cutting action takes place within the work piece. This requires that the chips must come out of the hole while the drill is filling a large portion of it. This especially complicates very small hole drilling. Friction between the body of the drill and the wall of the hole results in additional heating. Problems can arise from poor heat removal. Lubrication and cooling are difficult because of the counter flow of the chips.

Even though companies manufacture drills down to 20μm the quality of the cutting edges and the strength of the tools are questionable. High speed drilling is performed reliably in the PC board manufacturing industry. Hole sizes range down to .004" to .016" with aspect ratios of 8:1 or more. Tools are configured as shown in Figure 18. Figure 19 shows a typical mechanically drilled orifice geometry.

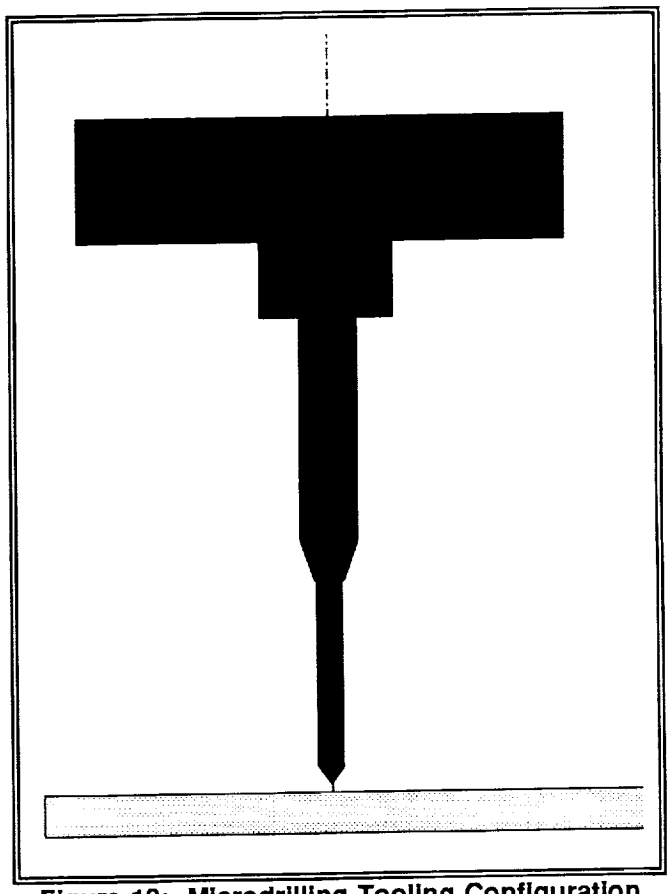

Figure 18: Microdrilling Tooling Configuration

On some of the systems, drilling speeds have reached 200 in/min @ 90,000 RPM. This is in epoxy based PCB's. Multilayer boards containing 16,000 holes of .006" diameter have been successfully drilled on one of these systems. Even though PCB material is not acceptable for the LDR application, these numbers give a sense where the state-of-the-art is.

For the LDR application, small drill bits need to be used drilling into harder materials. This requires slower RPM's, lower feed rates and more specialized bits and machines. Post processing finishing operations may also be required.

Materials
Almost all metals can be mechanically drilled. Stainless steel is a good choice.

Structurally Induced Straightness Effects
As with mechanical broaching, stainless steel can be used as the plate material in drilling processes so the load to strength ratio should be at the low end of the

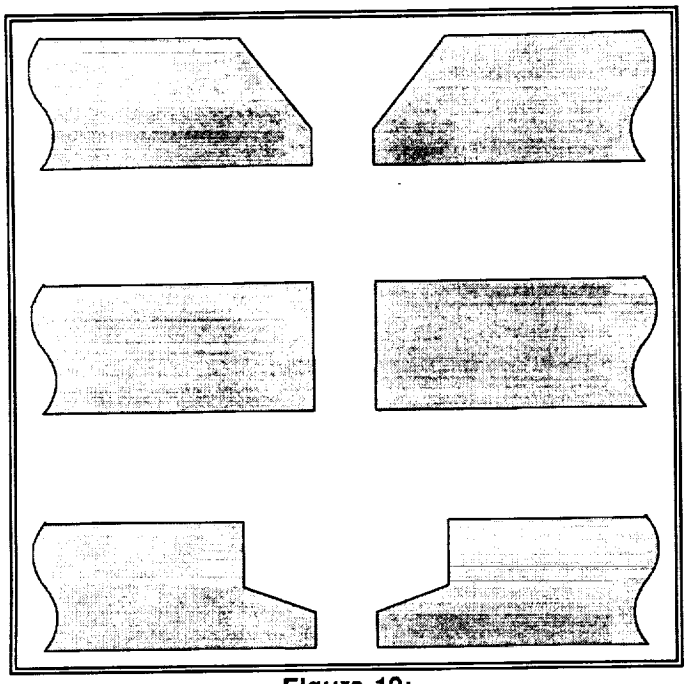

Figure 19:
Mechanically Drilled Orifice Geometries

range evaluated. The need to predrill the cone forces the plate to high thickness ratios so that broached plates should allow for the use of as many rows as desired from heat transfer considerations.

Hydrodynamically Induced Straightness Effects
As with mechanical broaching, mechanical drilling requires the pre-drilling or forming of a cone at the locations where the orifices are to be made. This produces the potential for some misalignment of the two steps, and thus a flow induced jet straightness error. Note that any angle between the axis of the cone and the axis of the broached section will produce a flow pattern similar to a spatial misalignment of the two processes. Also, a drilled orifice plate would have the potential for non-uniformly distributed burrs.

Past Experience at Achieving 5 mrad Straightness
Orifice arrays have been manufactured by a group at Lawrence Livermore Laboratories. With an electropolish finishing operation, they obtained jet straightness numbers <5 mrad. NASA has also manufactured arrays using the mechanical drilling approach. To date, their results are not as encouraging.

Straightness Estimates
Without finishing operations 10-30 mrad would be expected.

Direction of Effort To Improve Straightness
The largest improvements would come from finishing operations.

3.3.7 Soluble Core Glass Fibers

Description of Method
Glass fibers can be manufactured to very high precision. In the fiber optics industry, it is normal to fabricate a fiber which has an inner glass (core) different from the outer glass (clad). In optical fibers the intent is to have a different index of refraction in the core and clad glass. By taking advantage of the manufacturing technology of fiber optics, fibers have been made in which the core glass has a much higher solubility than the clad glass in dilute acids. If the core and clad glass are thermally matched, the core-to-clad diameter ratio for the preform can be reproduced in the fiber. The fibers are then aligned in parallel grooves and sealed in place, as shown in Figure 20. Once the block and fibers are sealed, the block is cross-sectioned into wafers and these wafers are polished and bonded to a supporting plate.

After bonding, the front surface of the plate is lapped and polished, and finally the core glass is etched out to form the orifices. The final orifice geometry is the same as for the Microchannel arrays (see Figure 22).

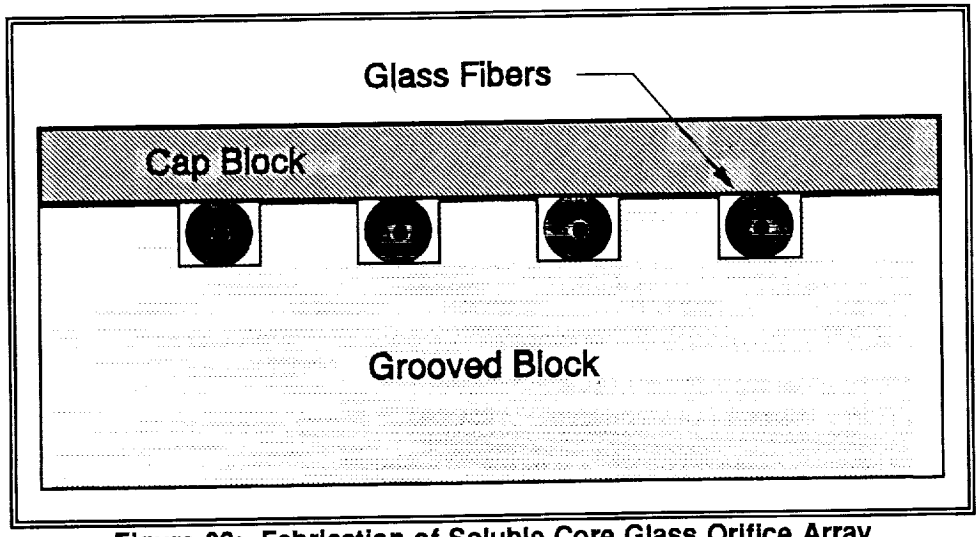

Figure 20: Fabrication of Soluble Core Glass Orifice Array

Materials

Special glasses must be fabricated to obtain the fibers. Special thermal and mechanical matching must exist between clad and core glass. A material such as fotoceram can be used to manufacture the grooved block. Solder glass can be used to seal the fibers in the block.

Because the center-to-center spacings for the LDR application are not critical, grooves may not be necessary. This would eliminate the need for the fotoceram.

Structurally Induced Straightness Effects

With a modulus of elasticity only one third that of steel, the load to strength ratio for soluble core glass plates will be at the high end of the range examined. Thus, even though thickness ratios of up to 10 are possible, the number of rows will probably be limited to 11 or less.

Hydrodynamically Induced Straightness Effects

Soluble core glass orifice plates have very sharp corners in the entry flow region, but the l/d of the flow channel can be long to compensate. Because of the relatively high surface energy of glass, the sharpness of the edge of the orifice at the exit and the surface finish of the outside of the orifice plate have been found by Microfab personnel to be critical to jet straightness performance.

Past Experience at Achieving 5 mrad Straightness

Arrays with all jets <2 mrad have been obtained with this technique.

Straightness Estimates

Arrays can be made using this technique with jet straightness better than 2 mrads. Improving this would be difficult.

Direction of Effort To Improve Straightness

At this time, no company is set-up to utilize this method. The experience base exists at MicroFab.

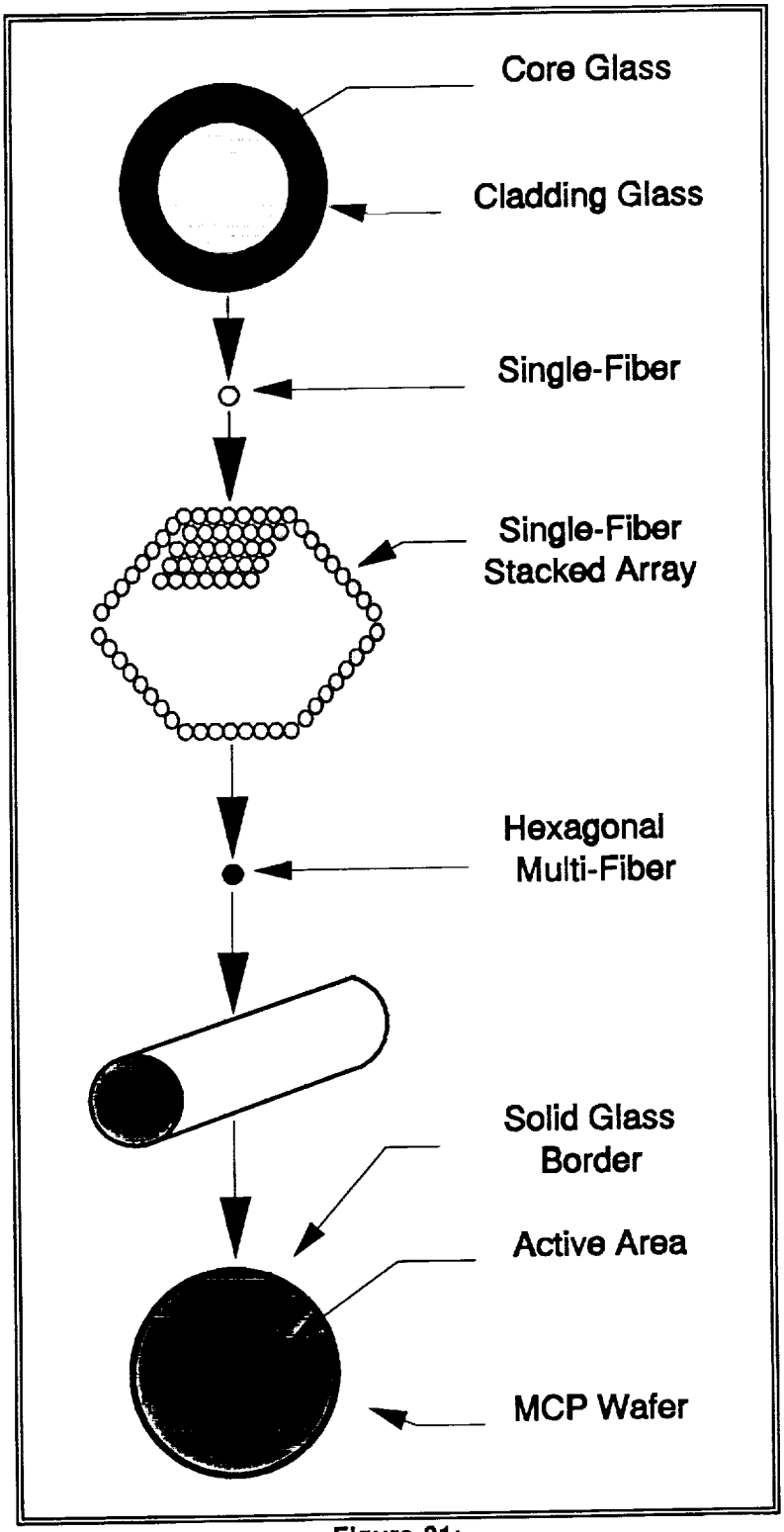

Figure 21:
Fabrication of a Microchannel Orifice Array

3.3.8 Microchannel Plates

Description of Method

The basic steps used are given in Figure 21 (courtesy of Galileo Electro Optics Corporation). Single fibers are drawn as solid glass fibers having two components, an etchable core glass, and a glass cladding which is insoluble in the core glass etchant. The fibers from this first draw are packed together into an array (usually hexagonal), are tacked together thermally, and are drawn again into hexagonal

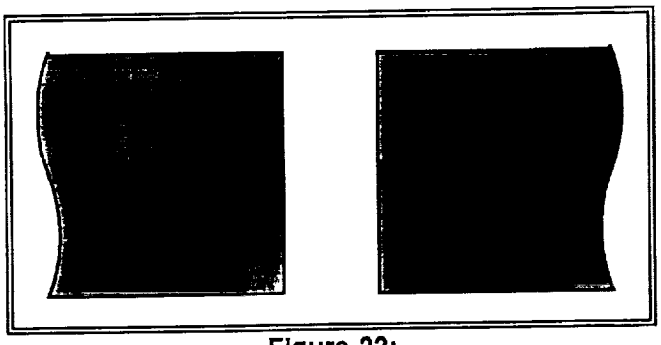

Figure 22:
Microchannel Orifice Geometry

multifibers. These hexagonal multifibers are then stacked again and fused within a glass envelope to form a boule. The boule is then sliced usually at a slight angle (8° to 15°) from the normal to the fiber axes. The resulting wafers then are edged, beveled and polished into thin plates. The soluble core glass is then removed by a suitable chemical etchant. A typical MCP orifice geometry is shown in Figure 22.

Materials
The mechanical plates consist entirely of glass formulations. Although the composition may be varied, a lead oxide glass is most common.

Structurally Induced Straightness Effects
With a modulus of elasticity only one third that of steel, the load to strength ratio for microchannel plates will be at the high end of the range examined. Thus, even though thickness ratios of up to 10 are possible, the number of rows will probably be limited to 11 or less.

Hydrodynamically Induced Straightness Effects
As with soluble core glass orifice plates, microchannel orifice plates would have very sharp corners in the entry flow region, but the l/d of the flow channel can be long to compensate. Because of the relatively high surface energy of glass, the sharpness of the edge of the orifice at the exit and the surface finish of the outside of the orifice plate would be critical to jet straightness performance.

Past Experience at Achieving 5 mrad Straightness
There is no direct experience or accounts of nozzle arrays being fabricated using this technique. However, one would expect that the experience with soluble core fibers at Mead Office Systems, IBM and elsewhere is applicable, due to the process similarities.

Straightness Estimates
This process should yield straightness values as good as the soluble core glass fiber process (2 mrad).

Direction of Effort To Improve Straightness
Improvements to the current lapping/polishing are needed because of the small t/d ratios needed for droplet formation. Typical t/d ratios for microchannel devices are 50:1 whereas 3:1 to 1:1 is more common in ink-jet applications.

3.3.9 Electron Beam Machining

Description Of Method
A beam of electrons (10^8 to 10^9 W/cm^2) colliding with a surface can transform solid materials into the gaseous phase. In order to avoid molten pools resulting from thermal conduction, short bursts are used. This process is similar to laser drilling, using electrons instead of photons. The process works in the following way:

If electrons collide with a solid material at a certain speed, their kinetic energy will be immediately converted to thermal energy. What happens within the work piece after this initial effect depends not only on the electron beam parameters such as total power, power density, duration of impact, etc., but also on the thermal properties of the target, such as heat capacity, melting point and vaporization point, thermal conductivity, heat of fusion, etc. The material can be heated, melted or vaporized.

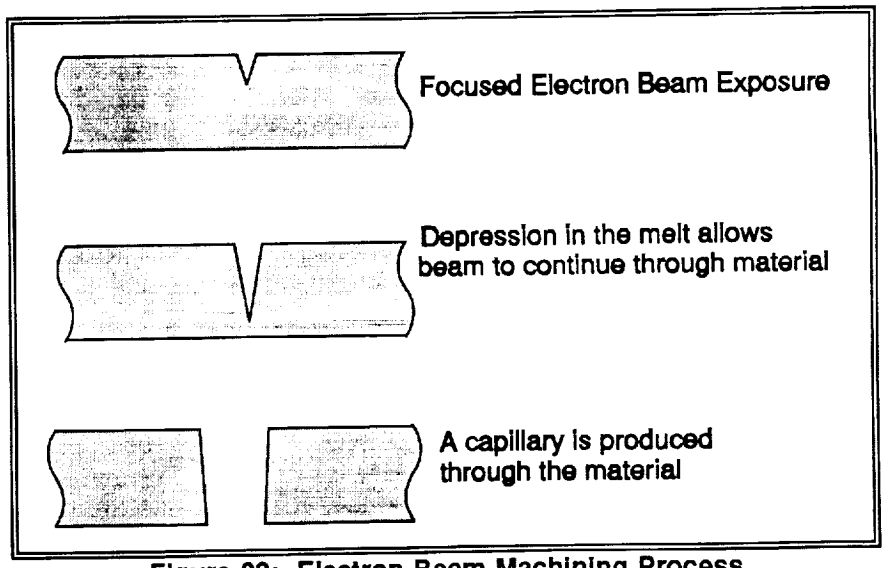

Figure 23: Electron Beam Machining Process

For removing material by Electron Beam machining, there are two different mechanisms. Either the material is evaporated or it is melted and the liquid phase is removed by additional forces.

In general, a combination of fusion and evaporation is used in such a way that the vapor pressure is used as additional force to remove the liquid material.

The pulse interval and thus the time of impact of the beam on the work piece is between 10μs and 10ms. The main task of the process controller is to maintain suitable beam parameters which allow the shape of the molten volume to be controlled as well as the position of maximum temperature (the vapor source) so that the liquid material is ejected completely and rapidly. The main control parameters for shaping the hole are the pulse width for the depth of the hole, the beam current for the diameter of the hole and the power distribution within the beam as well as the position of the focus with respect to the work piece. These parameters can be combined in many ways and each can be varied with respect to time.

Many of the features of the electron beam machined hole are similar to that of the laser drilled hole. Figure 23 shows the typical process for e-beam drilling. In both cases, selection of materials and operating parameters are important. EBM, like laser drilling, may require secondary finishing operations. A typical electron beam machined orifice is shown in Figure 24.

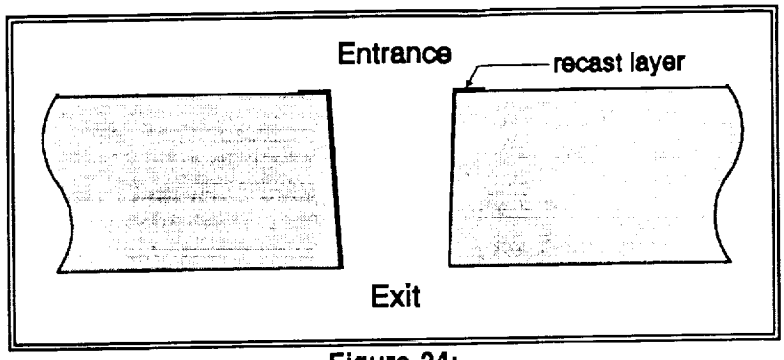

Figure 24:
Electron Beam Machined Orifice Geometry

Materials
A wide variety of materials can be used with this technique. All metals can be machined, including stainless steels and titanium. Since there is a wide range of choices with this technique, these can be evaluated on the basis of reproducible hole formation and debris formation.

Structurally Induced Straightness Effects
As with the EDM plates, if stainless steel is used as the plate material, the load to strength ratio should be at the low end of the range evaluated. The maximum thickness for e-beam plates should be greater than 10, thus allowing the use of as many rows as desired from heat transfer considerations. However, the production time (and cost) would increase almost directly proportionally to the depth to be drilled, making high t/d electron beam plates not quite as attractive.

Hydrodynamically Induced Straightness Effects
As with EDM, the two principle areas of concern for e-beam plates are the sharp entry flow region and the potentially non-uniform, surface finish. The long l/d of the flow channel would probably decrease any asymmetry associated with the entry flow.

Past Experience at Achieving <5 mrad Straightness
There is no direct experience or accounts of nozzle arrays being fabricated using this technique.

Straightness Estimates
This process has the capability of yielding parts like laser drilling, except this is not a large industrial effort to drill small, high quality holes with E-beam. Even with post processing, we feel 5 mrad is out of reach in the foreseeable future.

Direction of Effort To Improve Straightness
There is a current minimum hole diameter limitation of approximately .004". Efforts are in progress to get to the .002" range.

In addition, material choices plus subsequent debris removal (chemical polish, etc.) to improve the surface finish and nozzle shape are required.

3.3.10 Ion Milling

Description of Method
Beams of ions have been used in two ways to form orifices. First, they can be focused and used in the same fashion as electron beams in the previous section. The limited intensity of ion-beam sources have in the past made this method slow. But stable, liquid metal ion sources are changing this situation. Second, unfocused beams can be used to etch away material unprotected with a mask. This is shown in Figure 25. This process is referred to as ion milling. It has been used in the semiconductor related industry for some time. In this process, a beam of accelerated ions (usually argon) bombards the surfaces and imparts

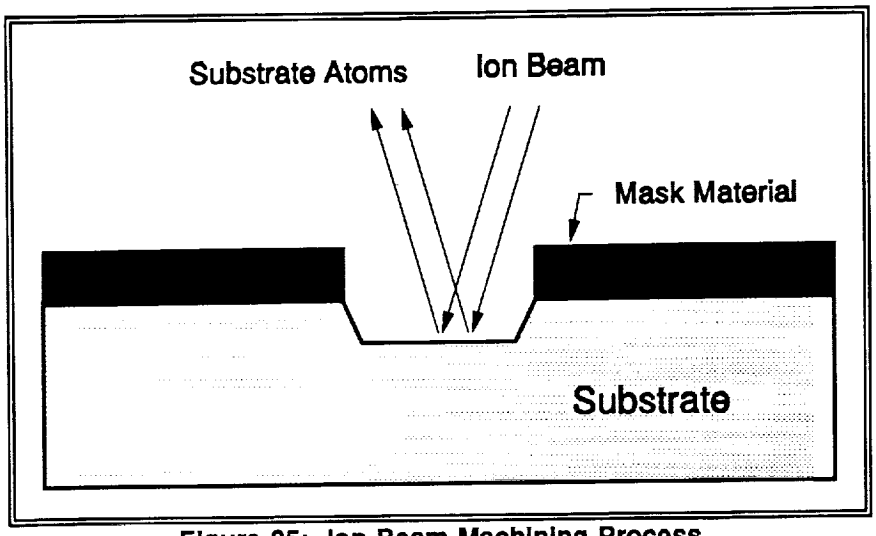

Figure 25: Ion Beam Machining Process

enough energy to the substrate atoms to remove material. The etching rate is a function of five major variables: acceleration voltage, angle of incidence, type of gas employed, type of material milled, and reactive gas influence. Increasing the acceleration voltage raises the milling rates almost linearly. For most materials, maximum milling occurs at an angle 40° - 60° from normal. Ion milling etch rates are slow. Using Argon at 500 volts, normal incidence, and 1mA/cm^2 beam current density, the following etch rates have been obtained:

Stainless steel	250-275 Å/min.
Aluminum	300-600 Å/min.
Titanium	150-350 Å/min.
Glass (Na, Ca)	200-220 Å/min.

At 250 Å/min., it would take approximately 17 hours to drill a 25μm deep hole in stainless steel. This is one of the main drawbacks to ion milling. The second problem is that of finding a masking material that is much more resistant to the ion beam than the substrate material. A typical ion milled orifice geometry is shown in Figure 26.

Materials

Almost any material can be used. The etch rates are very slow and when a mask is used, the etch rate of the mask material must be slower than the substrate.

Structurally Induced Straightness Effects

Because of the slow etch rates, only very low t/d plates are practical if the orifices are made entirely using ion drilling. Therefore, only single row plates could be used. If a secondary process is used to open the entrance, large thickness ratio plates could be made, allowing heat transfer effects to determine the number of rows.

Hydrodynamically Induced Straightness Effects

The combination of low l/d and sharp edge entry flow region would be of concern for an entirely ion milled plate. The formation of a tapered entrance by a secondary process would eliminate entry flow effects, but would create the potential for misalignment of the two processes. The short l/d downstream of the entrance would not be able to eliminate the effects of misalignment.

Past Experience at Achieving 5 mrad Straightness

No past experience is known.

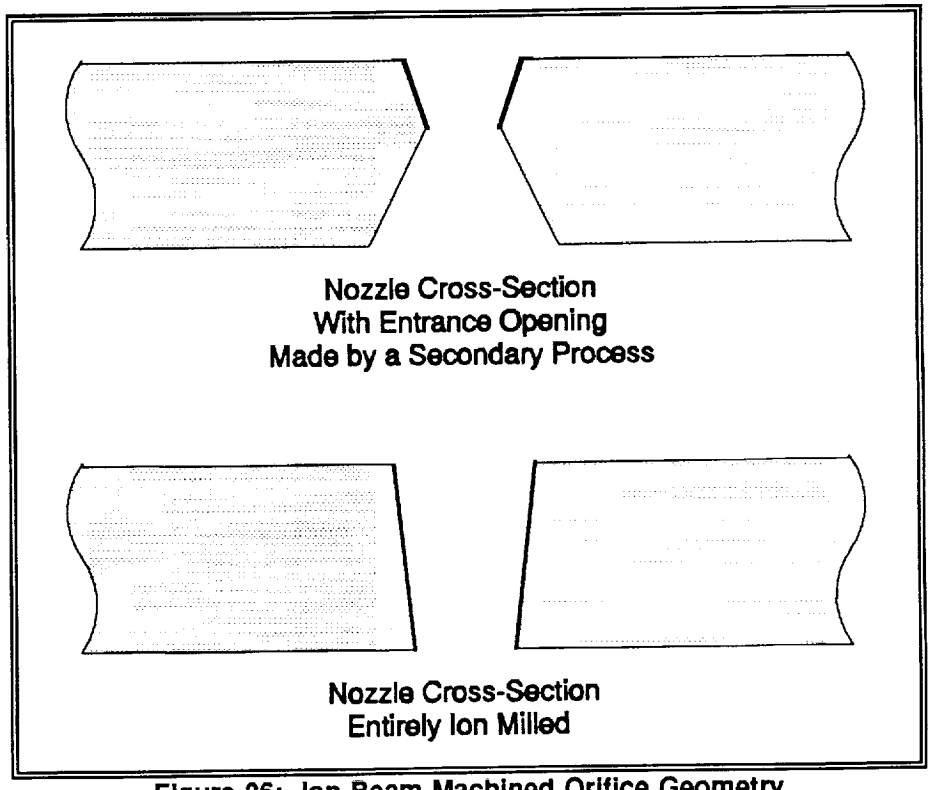

Figure 26: Ion Beam Machined Orifice Geometry

Straightness Estimate
The process combines some form of photolithography with ion milling. Both processes should produce clean, uniform surfaces. Therefore, the potential is good. 5 mrad could be achieved if it were not for the process limitations.

Direction of Effort To Improve Straightness
Because of the low process speed, this method is not recommended.

3.3.11 Fotoceram

Description of Method
Fotoceram glass has one unique property. Where it is exposed to UV light, it crystallizes when heated in a furnace. The use of Fotoceram glass in orifice plate fabrication is as follows:

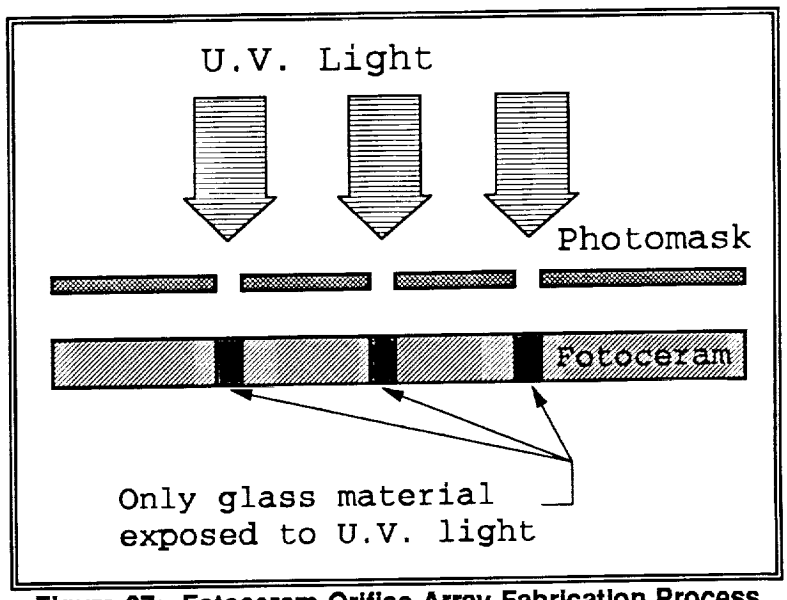

Figure 27: Fotoceram Orifice Array Fabrication Process

A photomask would be made which exposes only the areas where the orifices are desired, as shown in Figure 27. A sketch of the typical process flow is shown in Figure 28. This material is then baked. Crystallization occurs in the exposed areas. These crystallized areas are subject to etch rates 15 to 20 times higher than the uncrystallized material. After etching, the substrate is fired into ceramic form for strength. The main limitation of this method is that shrinkage during the firing process cannot be controlled accurately.

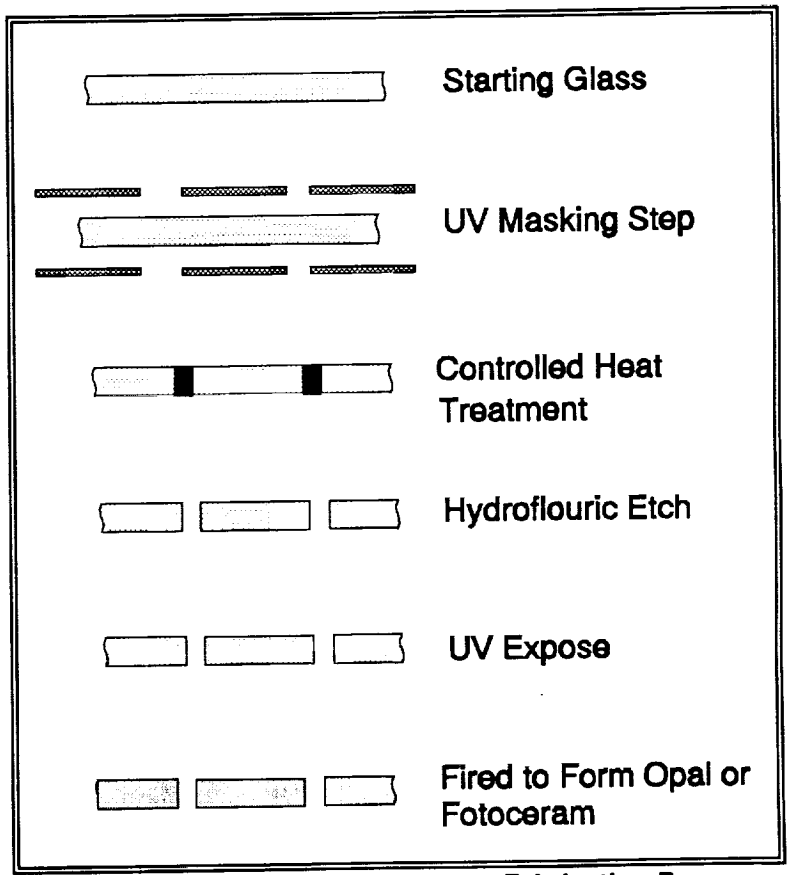

Figure 28: Fotoceram Orifice Array Fabrication Process

Materials
The starting material is a piece of photosensitive glass. It will be fired later to produce Fotoform opal or Fotoceram.

Structurally Induced Straightness Effects
As with microchannel plates, fotoceram plates would have a modulus of elasticity only one third that of steel. Thus the load to strength ratio for fotoceram plates will be at the high end of the range examined, and even though thickness ratios of up to 10 are possible, the number of rows will probably be limited to 11 or less.

Hydrodynamically Induced Straightness Effects
As with soluble core glass orifice plates and microchannel orifice plates, fotoceram would have very sharp corners in the entry flow region. The l/d of the flow channel is more limited for fotoceram, however. Because of the relatively high surface energy of glass, the sharpness of the edge of the orifice at the exit and the surface finish of the outside of the orifice plate would be critical to jet straightness performance.

Past Experience at Achieving 5 mrad Straightness
No past experience known.

Straightness Estimate
This process could produce parts today in the 10 to 15 mrad range. With further development 5 mrad could be obtained. This would most probably require post processing operations.

Direction of Effort To Improve Straightness
Working closely with Corning will be necessary to obtain acceptable plates. Improved finishing operations may need to be developed.

3.4 Ranking of Fabrication Methods

In order to compare the various methods of orifice array fabrication, eight items were identified. These are listed on the left hand side of Table V. The fabrication methods are listed across the top. Most items were evaluated on a scale from 1 to 5, where 5 is best. Straightness past experience was weighted by using a scale of 1-10, where 10 is the best. Each of the measurement criterion is briefly reviewed below.

Straightness: Past Experience
If a method has produced arrays with straightness better than 5 mrad, it gets a rating of 5. No experience gets a 1.

Straightness: Projected
These estimates are applicable after a hypothetical one year effort to improve the fabrication processes. A rating of 5 indicates a high probability of meeting the 5 mrad specification. A 1 rating indicates a low probability. In these estimates it is assumed that a small number (~1%) of the holes may be plugged.

Manufacturability
This rating gives an indication of the adaptability of the manufacturing process to volume production. A process that produces all the holes at the same time is preferred over a one-at-a-time process. Tooling wear on a one-at-a-time process is a negative. Cleanliness and surface finish are also considered.

Availability
A good source of qualified vendors yields a 5 rating in this category.

Mechanical
A good mechanical rating indicates a stiff plate and a very small structurally induced straightness error. This usually implies the process allows higher t/d orifice plates.

Pressure Drop
The pressure drop rating was obtained by multiplying the pressure coefficient (see section 2.5.0) estimated for each orifice plate by 10. The maximum possible rating was 10, but the maximum in value in this study is 5. Thus a rating of 5 would indicate the lowest pressure drop (best) and a rating of 0 the highest pressure drop (worse).

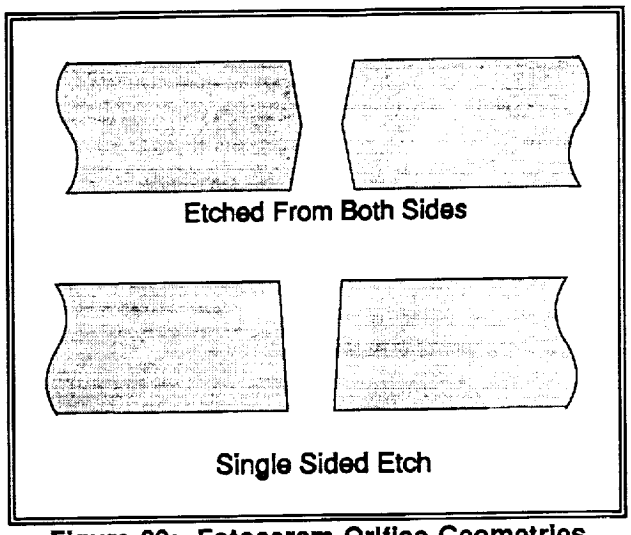

Figure 29: Fotoceram Orifice Geometries

Fluid Flow
This rating contains two characteristics that affect hydrodynamically induced straightness errors. First is the geometry of the orifice cross section which determines the flow properties. Second is the quality and uniformity of the exit surface. Good ratings for both will generate a 5.

Diameter Control
The specification on diameter is ±5%. A process that easily meets specification gets a 5. A process that cannot be controlled to meet the specification gets a 1 rating.

Ranking Result
The results from Table V are summarized below. Past experience brings electroform and soluble core glass fibers to the top of the list. Fotoceram and microchannel plates are rated high because of the orifice geometry, manufacturability, diameter control, and our projections. We feel that processes that form orifices one at time (laser, EDM and mechanical drilling) show potential, but require a finishing process to get clean, smooth surfaces. Using the process described above, the result of ranking of the processes is shown in Table IV.

3.5 Vendor Evaluation

Over fifty companies or organizations were identified and approximately 70% of those were contacted. A list

of the companies identified is shown in Appendix I. Trips were made to visit eleven of these companies. The list of companies identified is given by process type. Where we have enough information to rank companies *in a given process area*, the rankings are shown to the left of the company name. Note that the rankings are relative to *LDR orifice array development only.*

3.6 Recommendations

Based on our evaluation of both the orifice array fabrication methods and specific vendors, the following vendors/processes were recommended for experimental evaluation during Phase II:

Electroform

Because of past experience in achieving jet straightness <5 mrad, high volume manufacturability, and availability of competent vendors, this method has to be at the top of the list. Obtaining parts from both Buckbee-Mears and Stork-Veco was recommended.

Fotoceram

This process has the advantage of being capable of volume manufacturing. If the material is fired to the ceramic form, it has good temperature stability. The orifice configuration has advantages in the fluid flow characteristics *if etched from one side.* Obtaining parts from Corning Glass was recommend. Obtaining two different configurations was also recommended. One would be a single sheet with a cylindrical hole, and the second configuration would utilize a backing layer with a larger hole fused to the primary orifice for added strength.

Microchannel Plates

Microchannel plates have very uniform cylindrical holes with a large t/d ratio. Our past experience has shown that this results in values of jet straightness much better than 5 mrad. Obtaining these parts from Galileo Electro-Optics was recommended because of their experience in dealing with many different configurations and outside customers.

Mechanical Punching

This process produces stainless steel plates of good stiffness and flow characteristics. Based on our experience, Kasen has the best quality parts.

Mechanical Drilling and Finishing

Based upon the reports from Lawrence Livermore National Laboratories, we felt it important to take another look at this process. The advantage of this process is the attendant structural rigidities, the disadvantages are in the area of manufacturability. We recommended that NASA Lewis make some additional orifice plates using the techniques developed at Lawrence Livermore. We also recommended that an outside vendor be found to aid in the finishing operation (electro-polishing).

Table IV: Ranking of Orifice Array Fabrication Methods

1.	Electroform
2.	Soluble Core Glass Fibers
3.	Fotoceram
4.	Microchannel Plates
5.	Punching
	Chemical Milling
7.	Mechanical Drilling and Finishing
8.	Laser Drilling and Finishing
	Mechanical Drilling
10.	Laser Drilling
	EDM and Finishing
12.	EDM
13.	E-Beam Drilling

Chemical Milling

This technology has improved greatly over the last several years, driven by the disk drive industry. Stainless steel prototype parts can be obtained inexpensively and manufacturability is very good. We recommended obtaining parts from Vaaco or Buckbee-Mears.

Table V: Ranking of Fabrication Methods

	Electro-form	Chemical Milling	Laser Drilling	Laser Drill & Finishing	EDM	EDM & Finishing	Mech. Punching	Mech. Drilling	Mech. Drill & Finish	Soluble Core Glass Fibers	Micro-Channel Plate	Electron Beam	Ion Milling	Fotoc-eram
Straightness Experience	10	1	1	1	2	2	4	1	2	10	4	1	1	3
Projected Straightness	5	3	2	3	2	3	3	2	4	5	5	2	2	4
Manufac-turability	10	10	7	7	4	4	5	3	3	6	8	4	1	8
Availability	5	5	5	3	3	3	4	5	3	1	4	2	1	5
Mechanical	2	2	3	3	3	3	4	5	5	2	2	2	2	4
Pressure Drop	5	4	2	2	1	1	3	3	3	1	1	1	4	3
Fluid Flow	3	3	1	3	1	3	4	2	4	4	4	2	2	3
Diameter Control	4	3	2	2	2	2	4	3	3	5	4	2	3	4
TOTAL	**44**	**31**	**23**	**24**	**18**	**21**	**31**	**24**	**27**	**34**	**32**	**16**	**16**	**34**
RANKING	**1**	**5**	**10**	**8**	**12**	**10**	**5**	**8**	**7**	**2**	**4**	**13**	**14**	**3**

4.0 Phase II: Orifice Plate Design; Test System Design and Fabrication; and Orifice Plate Experimental Evaluation

Based on the Phase I results and recommendations, NASA decided that four orifice array fabrication methods would be experimentally evaluated for jet straightness performance:

1. Electroform (two vendors)
2. Fotoceram
3. Mechanically Drilling
4. Microchannel Plate

In addition, two other processes (Lee Company's etched sandwich process and Creare's EDM) were evaluated because they were low cost "targets of opportunity."

4.1 Orifice Plate Design

An orifice plate with 50 orifices of 75μm diameter on 635μm centers was selected as the nominal design. Fifty (50) orifices were selected to be large enough to provide meaningful statistics and a reasonable test of the fabrication process. At the same time, it was limited enough to keep the purchase and testing costs economical.

The 75μm diameter was selected as a compromise. Droplet heat transfer performance increases with decreasing droplet size. However, pressure drop increases, the number of orifices required increases, and contamination related failures increase as the orifice diameter decreases.[7,8]

The rather large orifice-to-orifice pitch (P/d=8.3) was selected to produce an overall plate length significant enough to test the fabrication processes. Also, there was some concern that a smaller pitch would cause some vendors to decline to furnish a quotation.

Figure 30 shows the nominal orifice plate design. The orifice geometry detail shown is that a typical electroformed orifice. For processes other than electroform, appropriate details were substituted.

The electroform orifice plates (Stork-Veco and Buckbee Mears), the Fotoceram orifice plates, and the EDM plates (Creare) were supplied in the nominal configuration. Galileo attempted to supply a Microchannel orifice plate in the nominal configuration, but failed. Mechanically drilled (NASA), Microchannel (Galileo), and etched sandwich (Lee) orifice arrays were supplied in "non-standard" configurations. The geometries of these

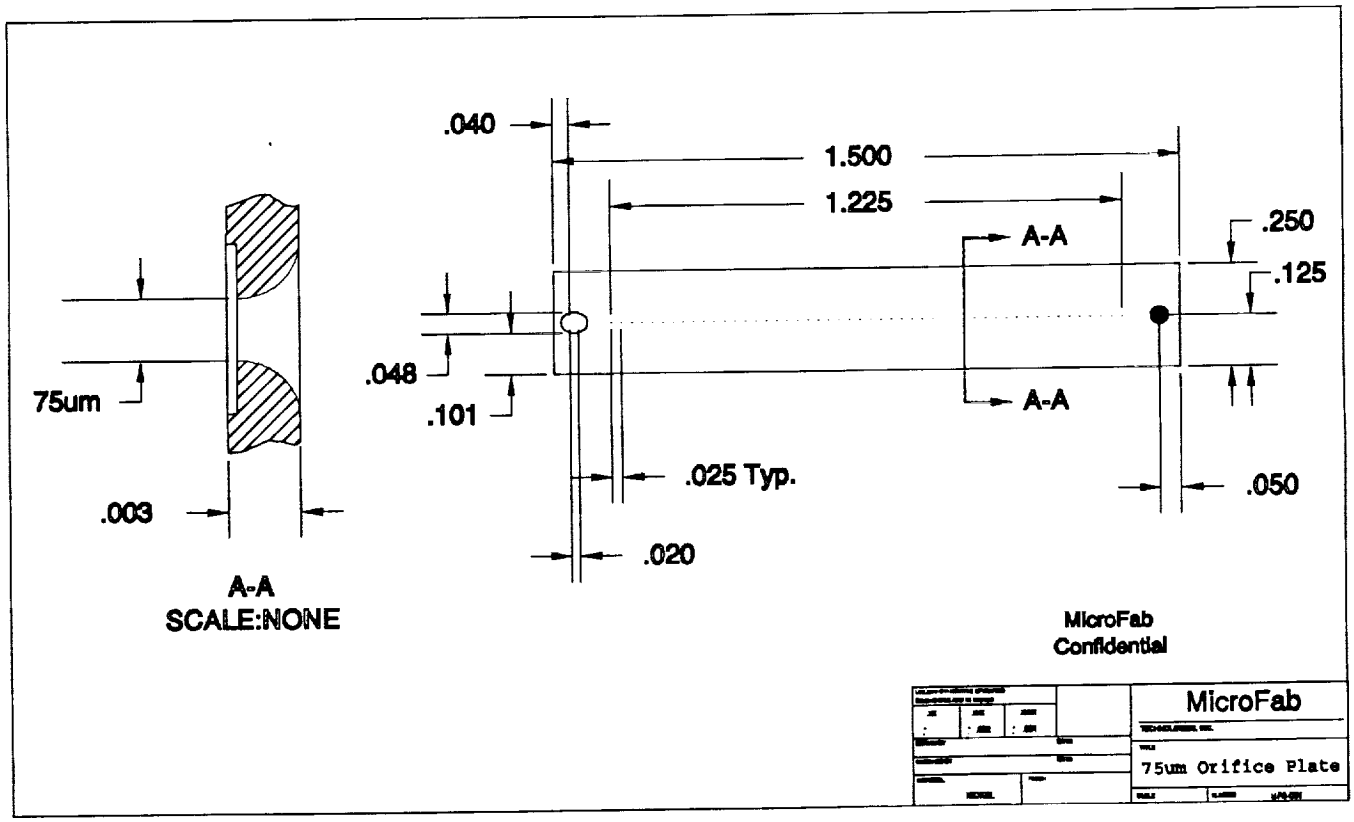

Figure 30: Electroform Orifice Array Drawing

orifice arrays are described below in the sections that discuss the experimental results.

4.2 Orifice Plate Vendor Quotations and Orders

Based on the result of Phase I, quotations were requested from the vendors listed in Table VI (see Appendix I for full company name and address). A larger number of orifice plates were ordered for the electroform and Fotoceram processes because most of the cost was related to tooling charges. No quotations were originally solicited from Lee and Creare since the Lee process was not known to us and EDM ranked low in the Phase I analysis. Both these companies contacted MicroFab after Phase II had begun. The Creare EDM process was being developed as a part of another NASA heat exchanger development project. Both the Creare and Lee plates represented very low cost opportunities to expand the jet-straightness information base generated during Phase II.

4.3 Drop Generator Design

Because of the relatively small size of the orifice plates to be tested, a structurally transmitted stimulation method[9] (as opposed to an acoustic method) was employed. This was accomplished by attaching the orifice plate to an aluminum block that was excited in a length mode (normal to the plane of the orifice plate) by two long aspect ratio piezoelectric sheets attached to each side of the aluminum block. The block was held at its center so as not to restrict the desired motion. A fluid manifold was machined into the block and fluid connectors added to both ends. Two fluid connections were included so that high flow rate purging (or cross-flushing) of the orifice plate could be used for contamination control. Alignment pins, corresponding to the alignment holes in the orifice plates, were pressed into the block. Figure 31 contains a drawing of the drop generator design and Figure 32 shows the drop generator in operation.

Table VI: Orifice Array Vendors, Quotes & Orders

Vendor	Orifice Plate Type	QR	PR	PT
Stork-Veco	electroform	Y	15	4
Litchfield	electroform	N	0	0
Buckbee Mears	electroform	Y	10	4
Corning	Fotoceram	Y	14	3
Galileo	MCP	Y	4	2
NASA	drilled	na	3	2
Lee	sandwich	N	2	2
Creare	EDM	N	2	2

QR = quotation received
PR = number of orifice plates received
PT = number of orifice plates tested

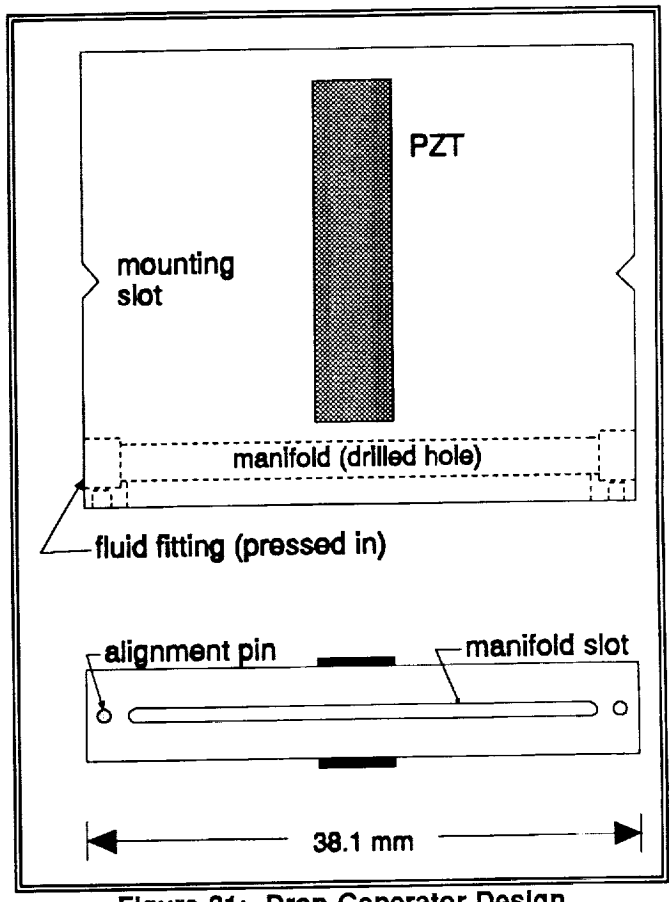

Figure 31: Drop Generator Design

4.4 Orifice Plate Assembly Process

The orifice plate/drop generator designs require that the orifice plate be attached to the drop generator block. Since the orifice plates are generally very thin, adhesive bonding was selected as the attachment method. A B-stage adhesive was selected. An air-brush type sprayer was used to deposit a thin film (less than 15 microns) of epoxy onto the block. The orifice plate was then attached, using the mounting pins for reference. The block with the orifice plate attached was placed into a fixture that applied uniform pressure to the orifice plate. The fixture was then placed in a oven to cure at 170°C for 30 minutes. Operating pressures of up to 60 psig were used without causing failure of the adhesive bond.

4.5 Jet Straightness Test System

To evaluate jet straightness, a test system was designed to hold the drop generator (with assembled orifice plate) in a fixture so that the jets could be observed through a microscope with the field of view defined by the plane of the jets. Figure 33 illustrates the system. As illustrated by Figure 32, electronics to drive the piezoelectric crystals and to stroboscopically observe droplet formation behavior were integrated with the test system. However, jet straightness measurements were made on unstimulated jets. All jet straightness measurements were made using deionized water as the working fluid and a pressure of 35 psig.

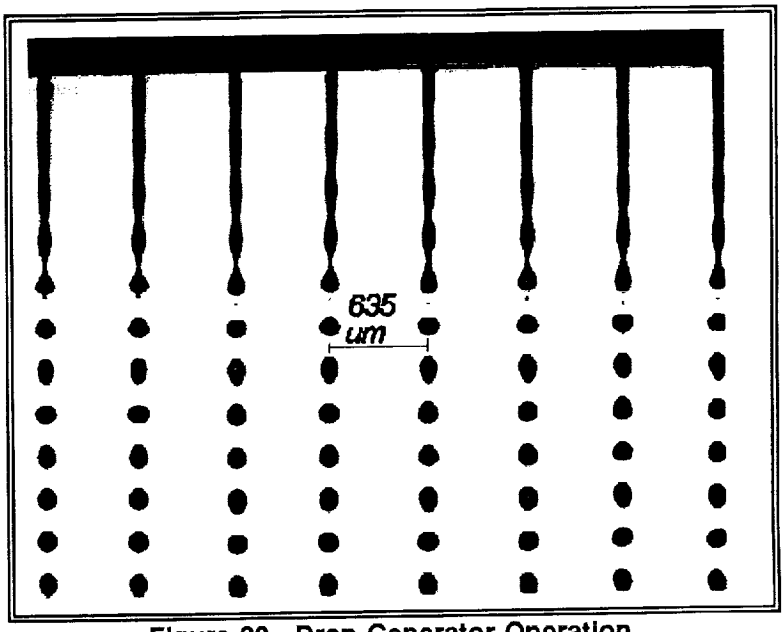

Figure 32, Drop Generator Operation, Stork-Veco Orifice Array Driven at 40kHz

Quantitative jet straightness data was acquired with this system as follows. While the jets were flowing, the image, consisting of 4-6 jets in the field of view, received by a CCD camera attached to the microscope, was captured and stored. A Targa M8 video board and the Java image analysis system were used to accomplish this. The microscope was then traversed to the next field of view, keeping one jet in the field of view as a reference, where the image was again captured and stored. This process was repeated until the images of all the jets had been captured and stored. Each orifice plate thus required 10-11 images. At this point, the jets were shut off and all data reduction occurred off-line.

First, the individual images of the jets were enhanced to improve measurability. Then the centroid of each jet

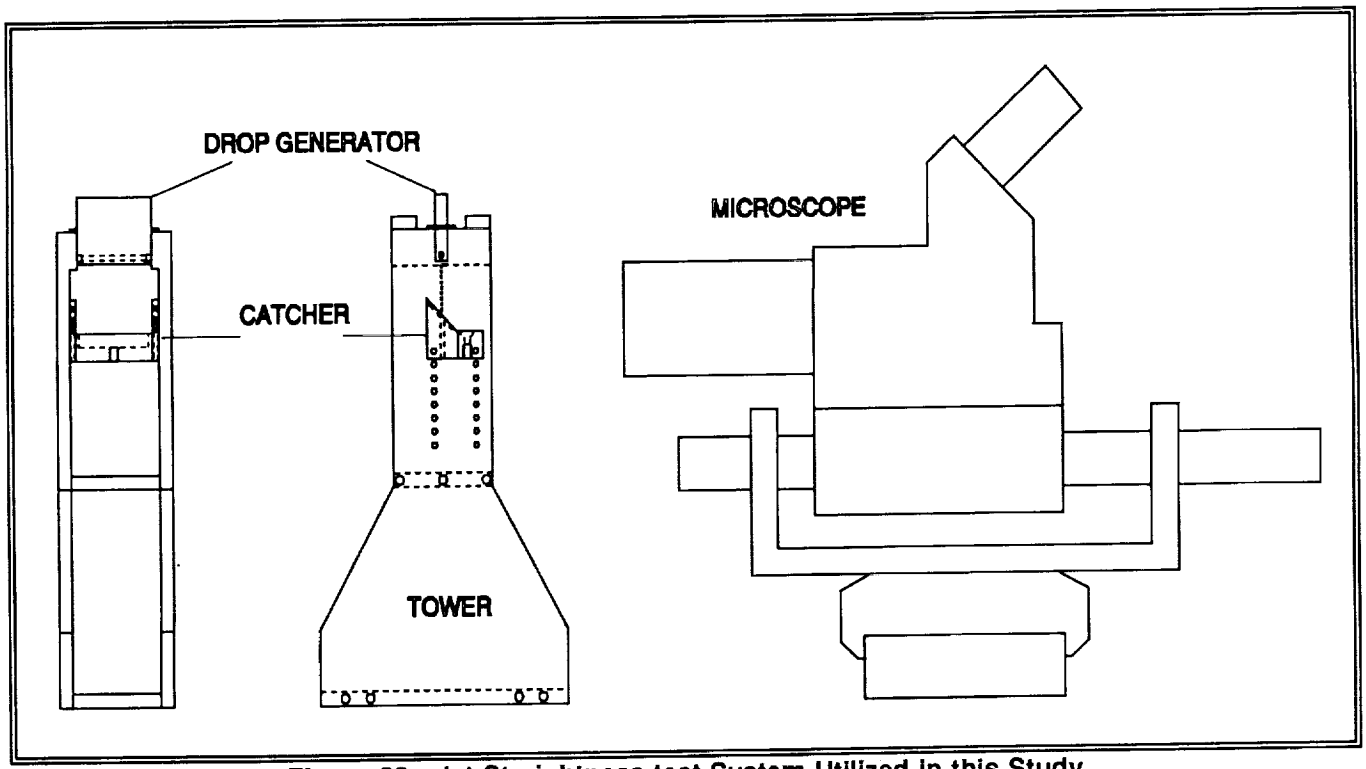

Figure 33: Jet Straightness test System Utilized in this Study

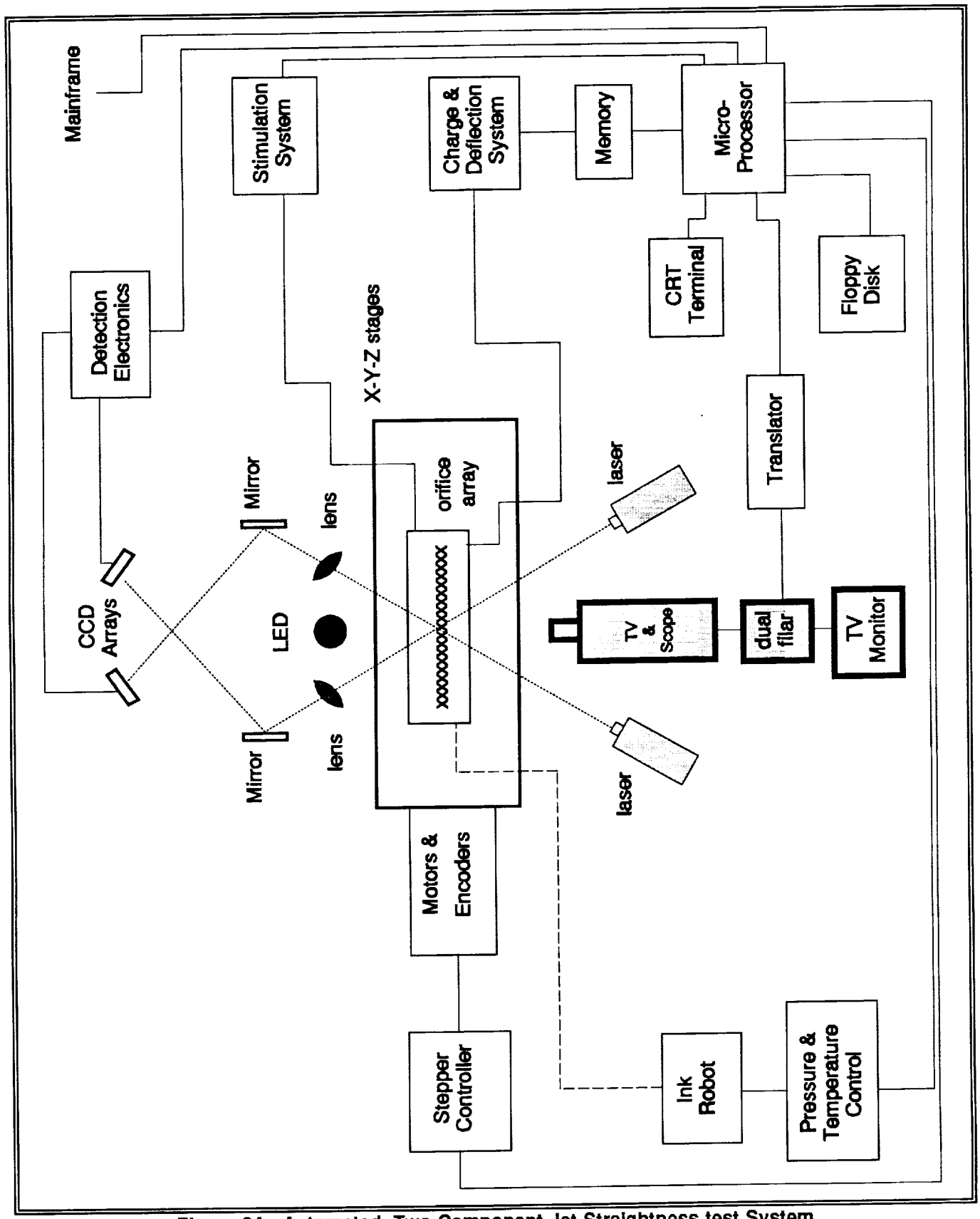

Figure 34: Automated, Two Component Jet-Straightness test System

at a distance of 25.4mm (along the jet) from the orifice was determined in each captured field of view using the object identification function of the image analysis system. Finally, the locations of each jet at 25.4mm from the orifice were computed using the positions calculated in each frame and the jet common to adjacent frames.

The same process of image capture and measurement was used to determine the locations of the orifices on the orifice plate. While the orifice locations were being measured, orifice area and effective diameter was measured.

Given the starting and ending locations of the jets, the relative jet straightness in the plane of the jets was determined. Relative jet straightness is referenced to the mean directionality of the jets whereas absolute jet straightness is referenced to some reference plane, usually a mounting surface of the drop generator. To save money, a system capable of measuring only one of the two (vector) components of jet straightness was employed in this study.

Before acquiring quantitative jet straightness data as described above, every orifice plate that was assembled to a drop generator housing was qualitatively evaluated and given a rating of A, B, or C. The grade of A meant that, at 25.4mm below the surface of the orifice plate, none of the jets merged or crossed. The grade of B meant that, at 25.4mm below the surface of the orifice plate, <2 jets merged or crossed. Finally, the grade of C meant that, at 25.4mm below the surface of the orifice plate, two or more jets merged or crossed. Screening plates in this manner insured that the time consuming quantitative measurements were made on only the best orifice plates.

In our original proposal, both the low cost system described above, and a higher cost/performance system were proposed as options. The higher cost system was based on a system built (by MicroFab personnel) to test ink-jet printer orifice arrays. For completeness and future reference, the higher cost system, which would be required for pilot or production volume manufacturing, is described below.

The system, illustrated in Figure 34, uses two perpendicular collimated light sources to illuminate each jet, one at a time. The resulting diffraction/shadow patterns are then imaged on two separate CCD arrays. The location of the shadow on each CCD array is determined and used, along with the location of the orifice on the array, to determine the vector jet angle. A linear translation stage provides coarse motion (±1μm) to locate each jet at the single focal point defined by the CCD array optics. Location of the orifices can be determined by measuring the orifice plate directly or by duplicating the jet location measurement near the orifice plate. An alternate method, made possible by recent advances in two-dimensional CCD arrays, would determine directionality directly from the shadow/diffraction pattern on the array.

4.6 Stork-Veco (Electroform) Orifice Plates

Fifteen (15) electroform orifice plates were received from Stork-Veco. The overall appearance of the plates was excellent. All of the orifices were very round with sharp edges and smooth surface. Figure 35 shows an SEM of a typical Stork-Veco orifice.

The orifice diameter distributions on five (5) Stork-Veco plates were measured using the image analysis system described above. The results are shown in Figure 36,

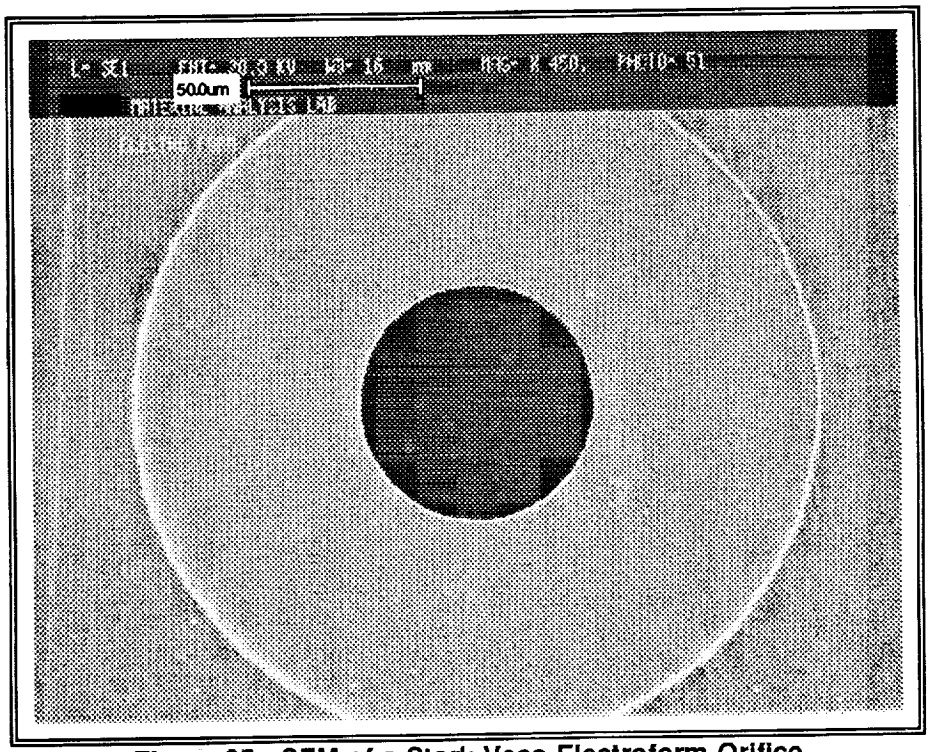

Figure 35: SEM of a Stork-Veco Electroform Orifice

and are summarized in Table VII. The variation of orifice diameter within a given plate is very small (0.3-0.6μm), but the mean orifice diameter varies several microns (3.2μm maximum) from plate to plate. This type of behavior is caused by variations in the plating rate, either over time (batch-to-batch) or at different locations in the plating bath. Both of these causes can be readily addressed by monitoring and controlling the process closely.

Table VII: Summary of Stork-Veco Plates Orifice Diameter Measurements

	SV-1	SV-2	SV-3	SV-4	SV-5	avg
average, μm	69.3	70.5	69.8	72.2	67.3	69.8
std. dev., μm	0.5	0.5	0.6	0.3	0.6	0.5
std. dev., %	0.7	0.6	0.8	0.5	0.8	0.7
std. dev. = standard deviation						

Judgements about orifice diameter variation must be made relative to the measurement uncertainty. Repeated orifice diameter measurements of orifice plate SV-14 were made and the measurement standard deviation was determined (with 50 degrees of freedom) to be 0.18μm. Given the lack of sophistication of the edge detection method employed, this is quite good. However, it will be a strong function of orifice plate quality (i.e., surface finish and edge sharpness), as will be seen with the other orifice plates.

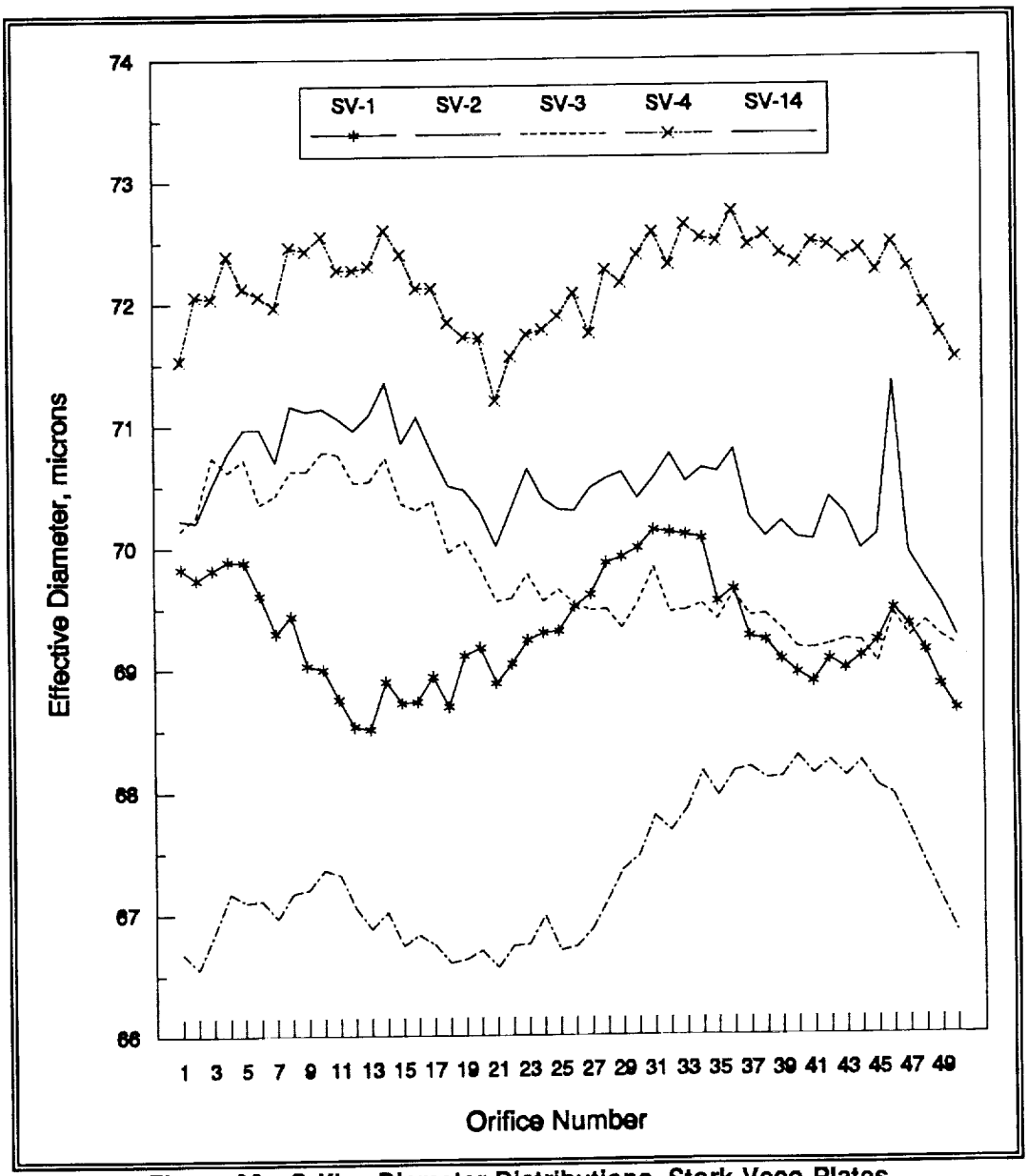

Figure 36: Orifice Diameter Distributions, Stork Veco Plates

Four (4) Stork-Veco orifice plates were assembled to drop generator housings and installed in the jet straightness test system. Orifice plates SV-1, SV-2, and SV-4 received an A rating and plate SV-3 received a B rating (due to two jets merging) from the qualitative evaluation. Quantitative measurements were then made on orifice plates SV-2, SV-3, and SV-4. SV-1 was not

tested because it became degraded by a corrosion problem with the system that was subsequently remedied.

The quantitative jet straightness test results (jet angle for each orifice) for the three Stork-Veco orifice plates are shown in Figure 37 through Figure 39, and are summarized in Table VIII. The data does not show any clearly identifiable trends that might be eliminated or improved by fabrication process modification and/or control. This is confirmed by the histograms of the jet straightness data shown in Figure 40 through Figure 42. Given the number of data points (50), the jet straightness distributions for all three orifice plates are approximately normal.

Only orifice plate SV-2 comes close to meeting the requirements for a LDR orifice array: 99% of the jets <5 mrad. However, the fact that the results are fairly close to the desired goal in the first attempt is encouraging.

Table VIII: Quantitative Jet Straightness Results Summary, Stork-Veco Orifice Plates

Orifice Plate	Standard Deviation of Jet Angle, mrad
SV-2	3.4
SV-3	5.6
SV-4	4.9
average, 3 plates	4.6

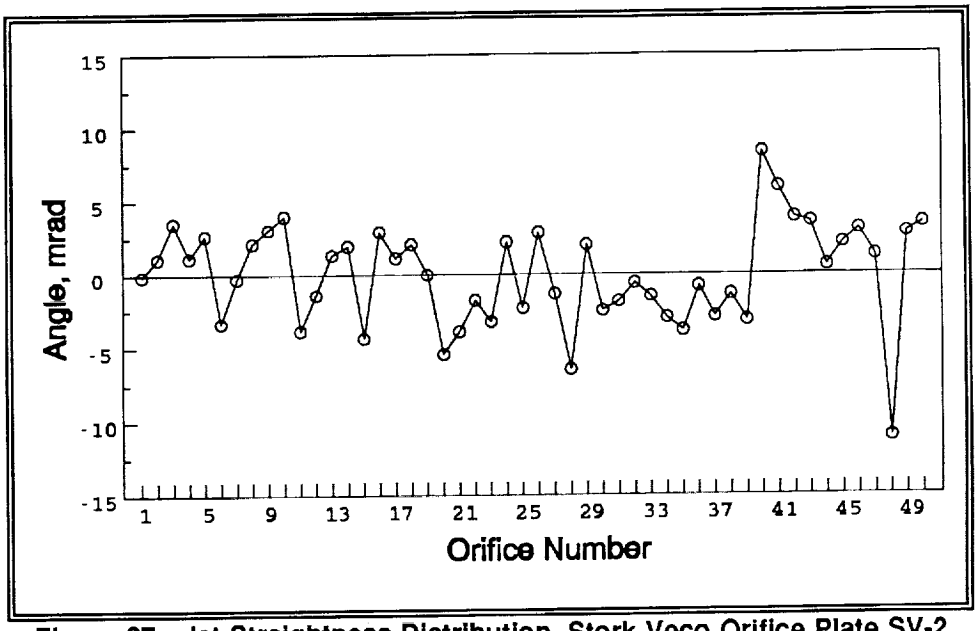

Figure 37: Jet Straightness Distribution, Stork-Veco Orifice Plate SV-2

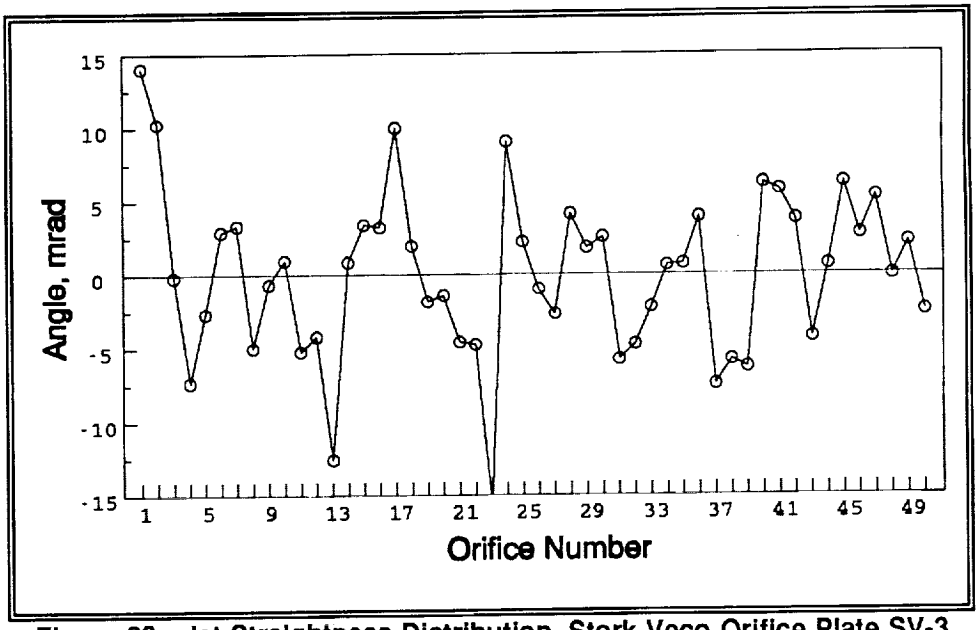

Figure 38: Jet Straightness Distribution, Stork-Veco Orifice Plate SV-3

4.7 Buckbee Mears (Electroform) Orifice Plates

Ten (10) orifice plates were received from Buckbee Mears. The overall appearance of all the orifice plates was good, but was considerably poorer than that of the Stork-Veco orifice plates. The orifices were not as round, the edges of the orifice were not as sharp, and the surface was not as smooth. Some of the orifices had "lumps" of material near the edge. These interfered with the orifice diameter measurements and are a likely cause of jet straightness degradation. It should be reemphasized that the quality of the Buckbee Mears plates was good, and only suffer from the comparison with the excellent quality of the Stork-Veco orifice plates.

Orifice diameter distributions on five (5) Buckbee Mears orifice plates were measured. The results for two (2) of the orifice plates are shown in Figure 43, and the data for all five orifice plates measured are summarized in Table IX. Only two of the five orifice diameter distributions are shown in Figure 43 for clarity. The other three distributions are similar to the two that are shown. The diameter measurement deviation was determined (with 50 degrees of freedom) from repeated measurements of orifice plate BM-6 to be 0.43μm. The increase in measurement devia-

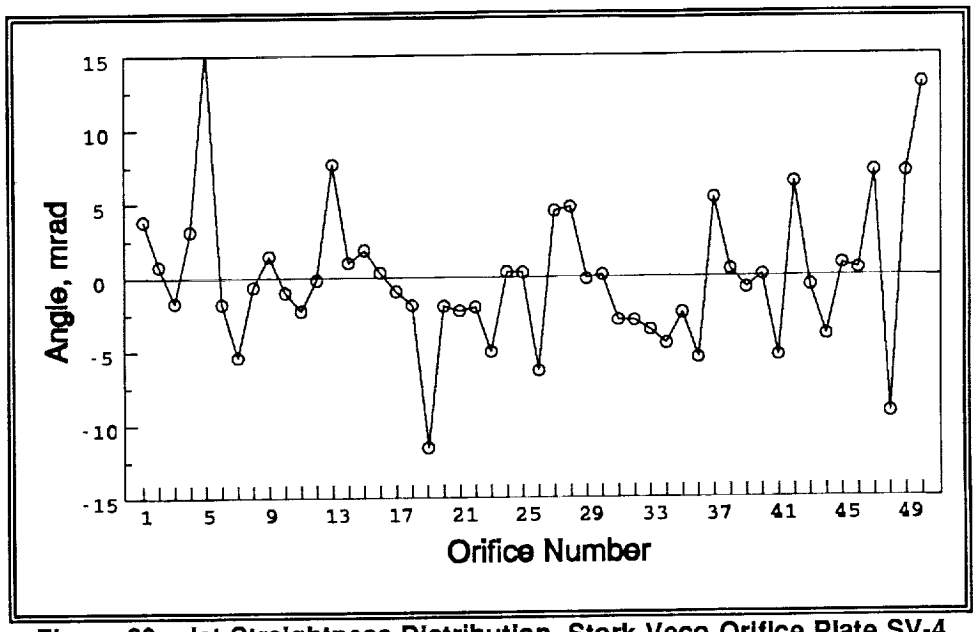

Figure 39: Jet Straightness Distribution, Stork-Veco Orifice Plate SV-4

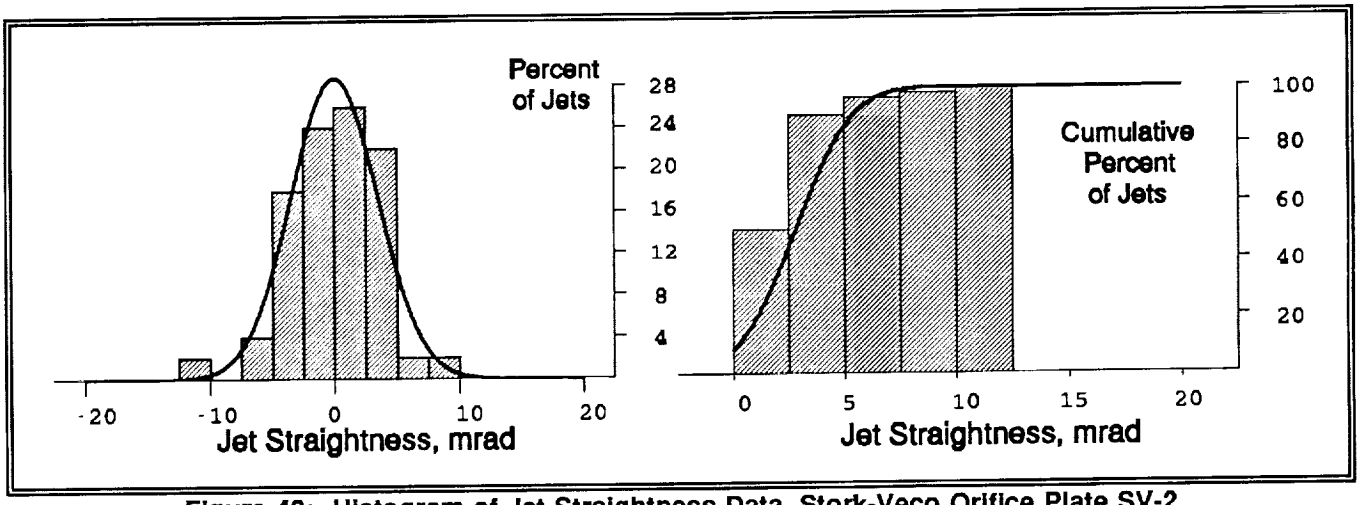

Figure 40: Histogram of Jet Straightness Data, Stork-Veco Orifice Plate SV-2

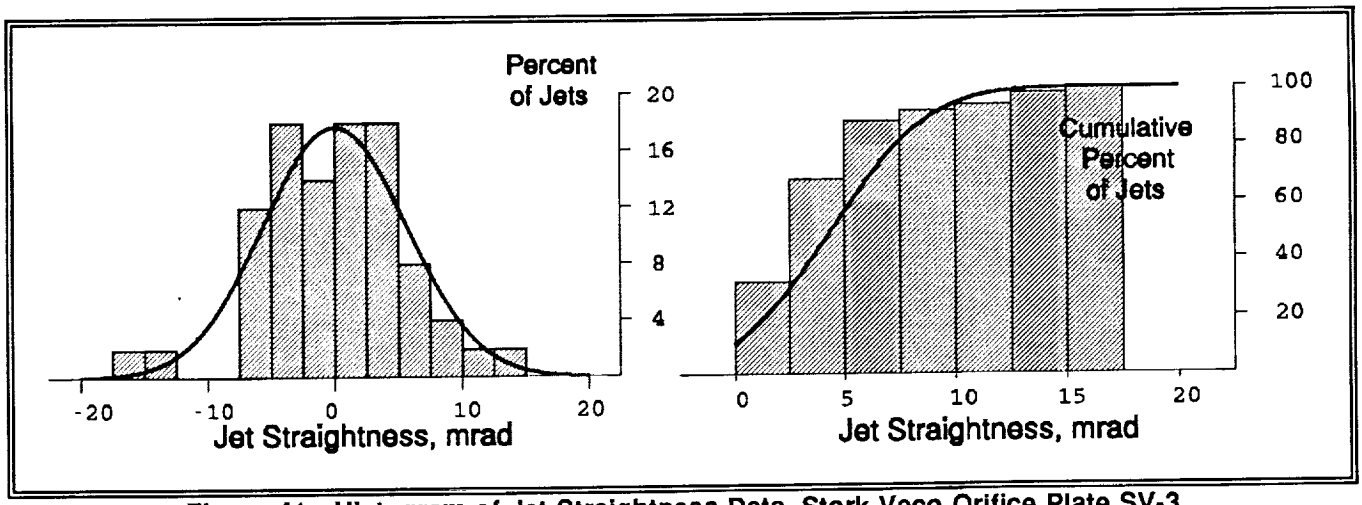

Figure 41: Histogram of Jet Straightness Data, Stork-Veco Orifice Plate SV-3

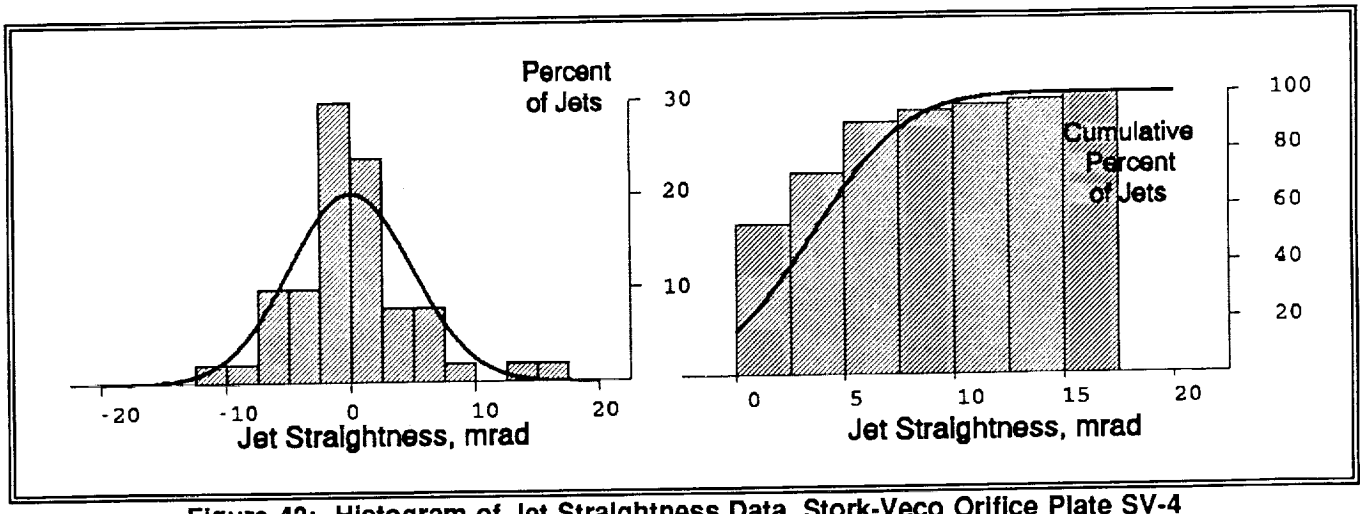

Figure 42: Histogram of Jet Straightness Data, Stork-Veco Orifice Plate SV-4

tion over that of the Stock-Veco orifice plates is attributable to the lower quality of the orifice plate surfaces and the less sharp orifice edges associated with the Buckbee-Mears orifice plates.

The variation of orifice diameter within a given plate is very small (0.6-0.8μm), as was the case with the Stork-Veco orifice plates. Only one of the Buckbee Mears plates had a diameter variation as small as the worst Stork-Veco orifice plate. The average diameter variation from plate to plate (2.6μm maximum) was again greater than the variation on any given orifice plate, but was less than the Stork-Veco plate-to-plate average diameter variation. The comments pertaining to improvement in the plate-to-plate average

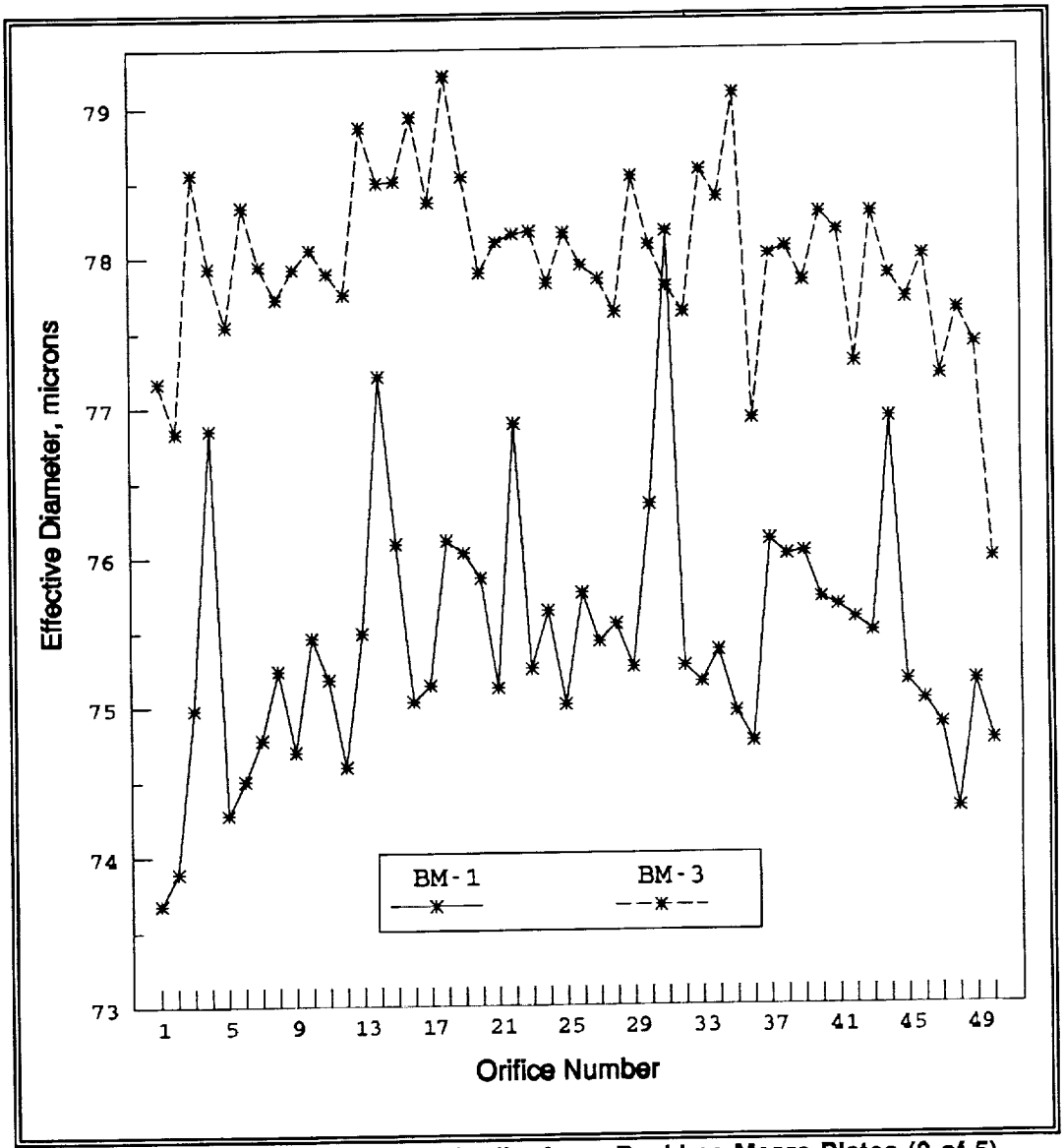

Figure 43: Orifice Diameter Distributions, Buckbee Mears Plates (2 of 5)

diameter variation made in the discussion of the Stork-Veco result also pertain to the Buckbee Mears orifice plates.

Four (4) Buckbee Mears orifice plates were assembled to drop generator housings and installed in the jet straightness test system. Orifice plate BM-2 received an A rating, plate BM-1 received a B rating, and plates BM-3 and BM-4 received C ratings (due to multiple crooked jets) from the qualitative evaluation. Quantitative measurements were then made on orifice plates BM-1 and BM-2.

The quantitative jet straightness test results (jet angle for each orifice) for the two Buckbee Mears orifice plates are shown in Figure 44 and Figure 45, and are summarized in Table X. The result for orifice plate BM-2 would have been as good as those of the best Stork-Veco plate (SV-2) if the four end jets had not had such large angles. Histograms of the jet straightness data are shown in Figure 46 and Figure 47. Again, the jet straightness distributions for both orifice plates are approximately normal.

On average, the Buckbee Mears orifice plates had poorer jet straightness performance compared to the Stork-Veco orifice plates. The performance of the electroform orifice plates from these two vendors was close enough (both to each other and to the ultimate LDR performance goal, 99% of jet <5mrad) that we do not advocate selecting a single vendor for future development at this time.

Table IX: Summary of Buckbee Mears Plates Orifice Diameter Measurements

	BM-1	BM-2	BM-3	BM-4	BM-6	avg.
average, μm	75.4	75.4	78.0	77.4	76.7	76.6
std. dev., μm	0.8	0.7	0.6	0.8	0.8	0.7
std. dev., %	1.1	1.0	0.7	1.0	1.1	1.0
std. dev. = standard deviation						

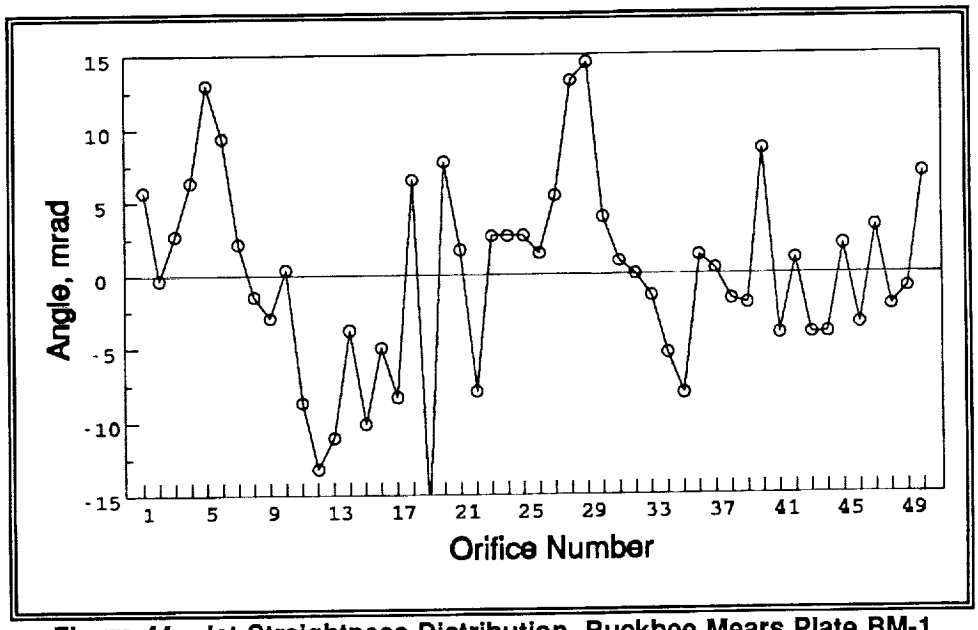

Figure 44: Jet Straightness Distribution, Buckbee Mears Plate BM-1

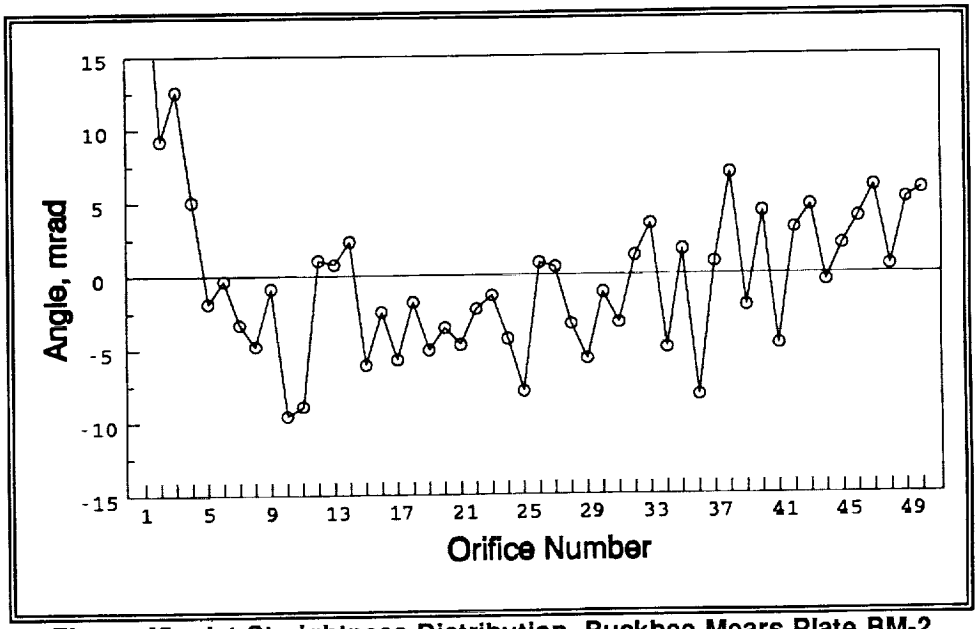

Figure 45: Jet Straightness Distribution, Buckbee Mears Plate BM-2

Table X: Quantitative Jet Straightness
Results Summary, Buckbee Mears Orifice Plates

Orifice Plate	Standard Deviation of Jet Angle, mrad
BM-1	6.6
BM-2	6.0
average, 2 plates	6.3

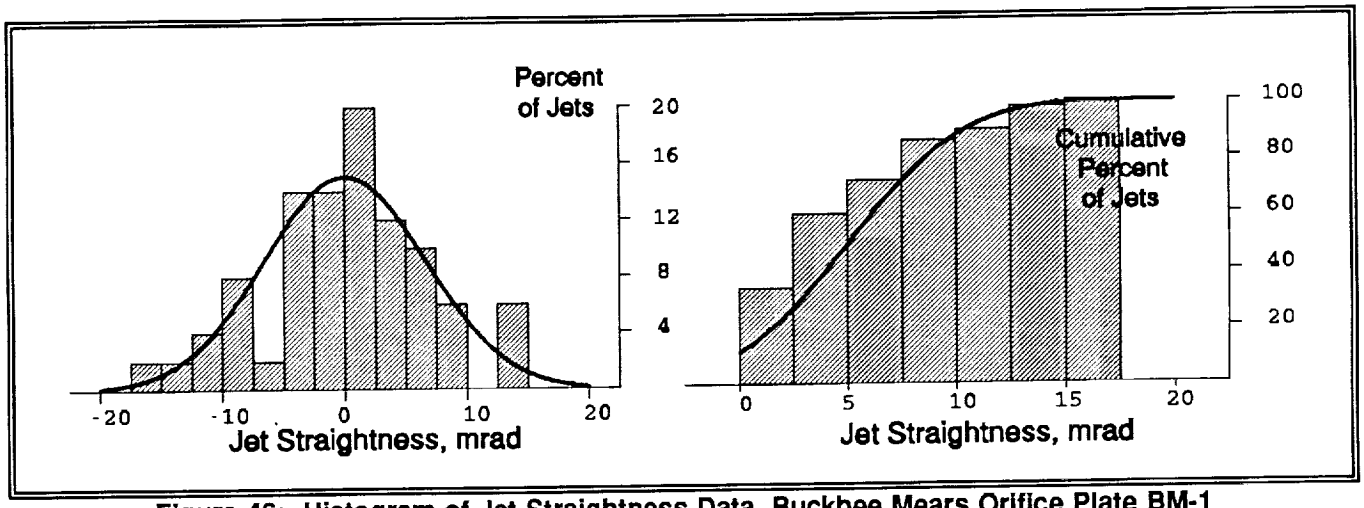

Figure 46: Histogram of Jet Straightness Data, Buckbee Mears Orifice Plate BM-1

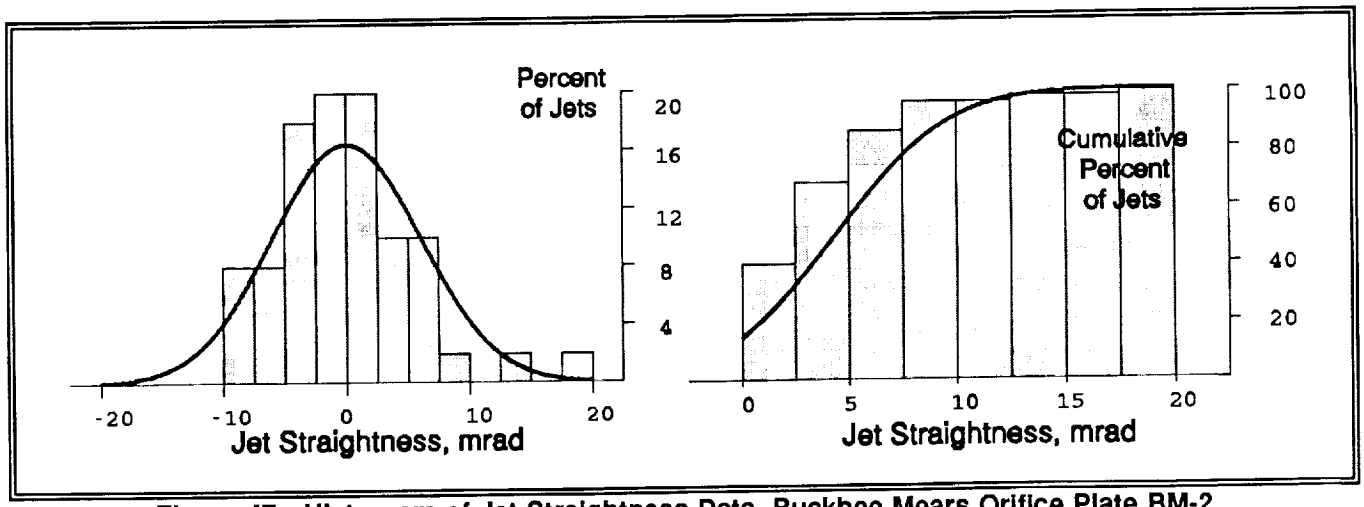

Figure 47: Histogram of Jet Straightness Data, Buckbee Mears Orifice Plate BM-2

4.8 Corning (Fotoceram) Orifice

Fourteen (14) orifice plates were received from Corning. Visual inspection revealed several significant attributes of these plates.

1. Approximately half the orifices were fairly round, while the rest had jagged, sawtooth edges. The edges of the orifices were rounded, not sharp.

2. The orifice diameter could be seen (under a microscope, but without the use of a scale) to vary greatly.

3. The minimum diameter on most of the orifices was not at the orifice exit. This indicated that the orifices were etched from two sides. Having the minimum diameter in the interior of the orifice is a likely cause of the poor straightness performance discussed below.

4. The surface of the Fotoceram plates was granular (as would be expected with this process), flat, and uniform. Figure 49 shows a SEM of a typical Fotoceram orifice.

Orifice diameter distributions on five (5) Corning orifice plates were measured. The distribution for one of the orifice plates is shown in Figure 48, and the data for all five orifice plates measured are summarized in Table XI. The orifice diameter distribution for CO-5, shown in Figure 48, had the least diam-

Table XI: Summary of Corning Plates Orifice Diameter Measurements

	CO-1	CO-2	CO-3	CO-4	CO-6	avg.
average, µm	81.7	81.2	84.5	85.6	80.0	82.6
std. dev., µm	5.7	4.7	4.4	4.4	3.2	4.5
std. dev., %	7.0	5.8	5.2	5.1	4.0	5.4
std. dev. = standard deviation						

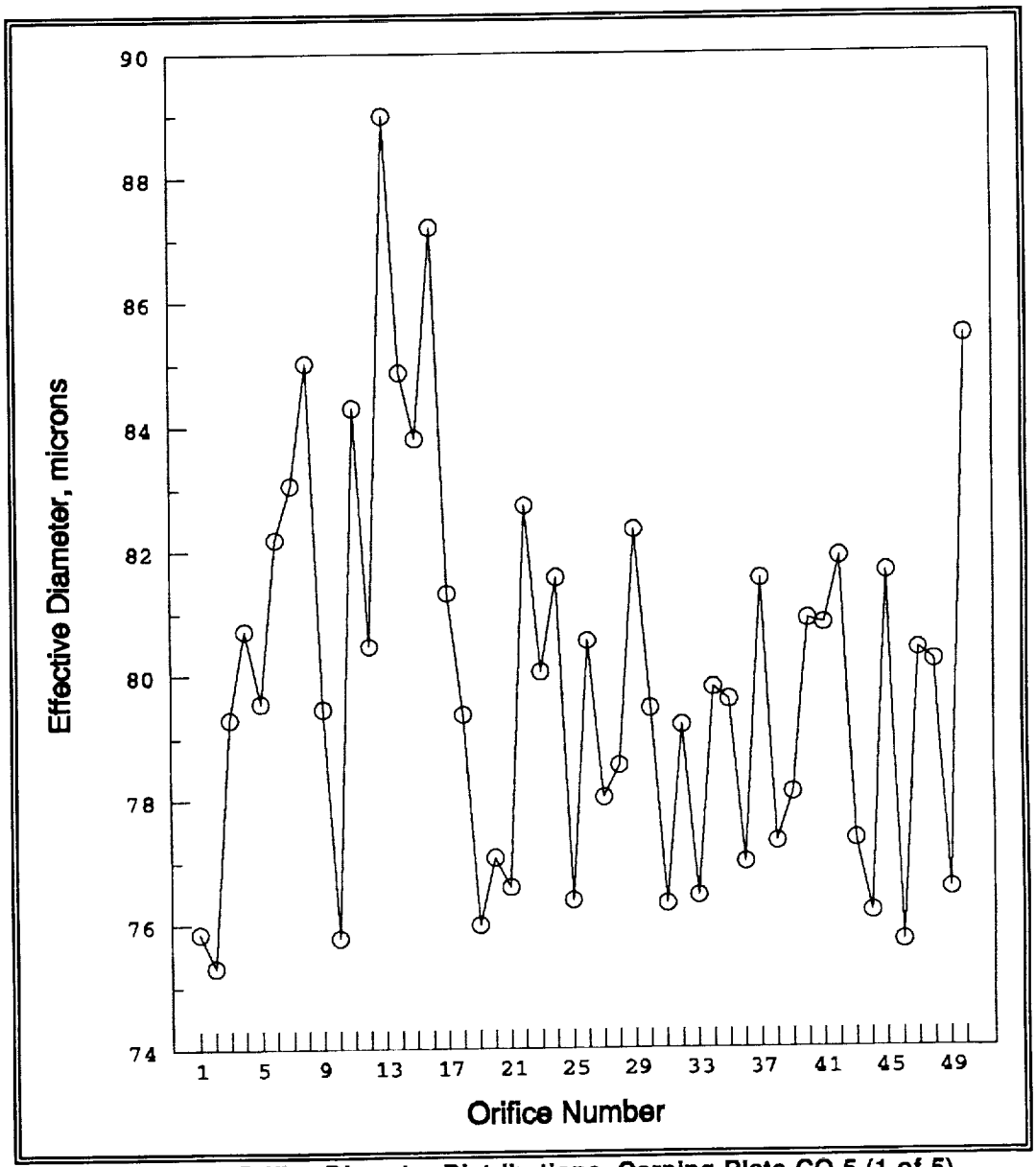

Figure 48: Orifice Diameter Distributions, Corning Plate CO-5 (1 of 5)

eter variation of the five plates measured. The diameter measurement deviation was determined (with 50 degrees of freedom) from repeated measurements of orifice plate CO-1 to be 0.72µm. The large measurement deviation is caused by the minimum diameter occurring interior to the orifice. Although the measurement variation is much larger than those determined for the Stork-Veco and Buckbee Mears orifice plates, it is still quite small compared to the actual diameter variation on the Corning orifice plates.

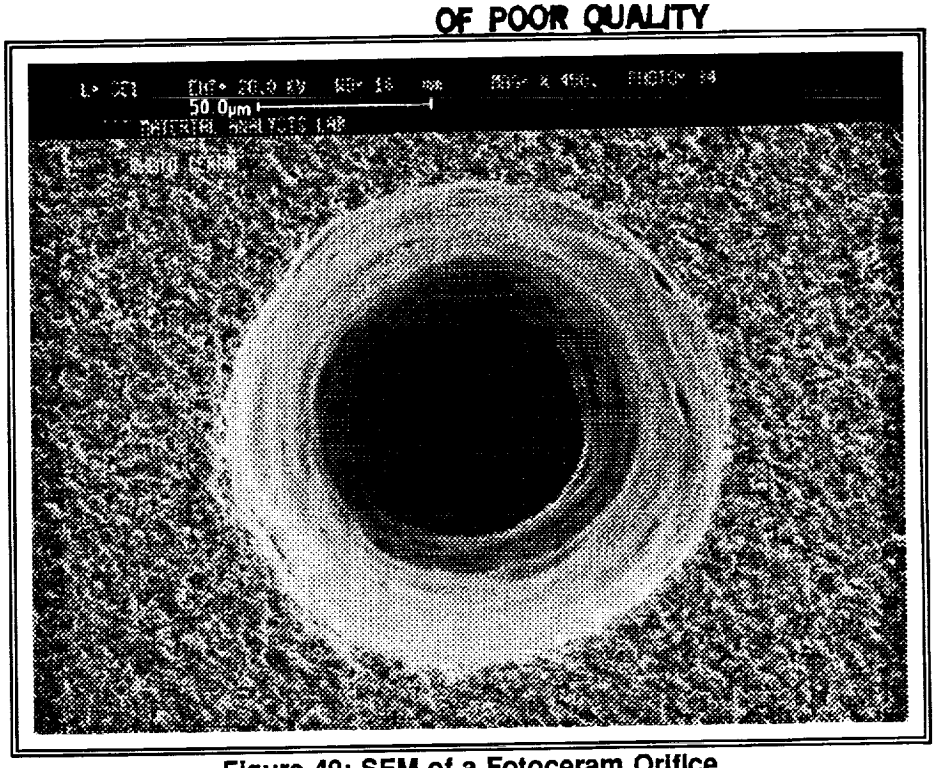

Figure 49: SEM of a Fotoceram Orifice

The orifice diameter distributions for the Corning plates had almost five times the diameter variation compared to those of the Stork-Veco and Buckbee Mears (electroform) orifice plates. Although the amount of variation measured might be acceptable for an LDR application, it is indicative of a process that is not under control, possibly an uncontrollable process. Future LDR orifice array development effort should try to determine, with Corning, if the current results are characteristic of what Corning can achieve, or if the process can be significantly improved.

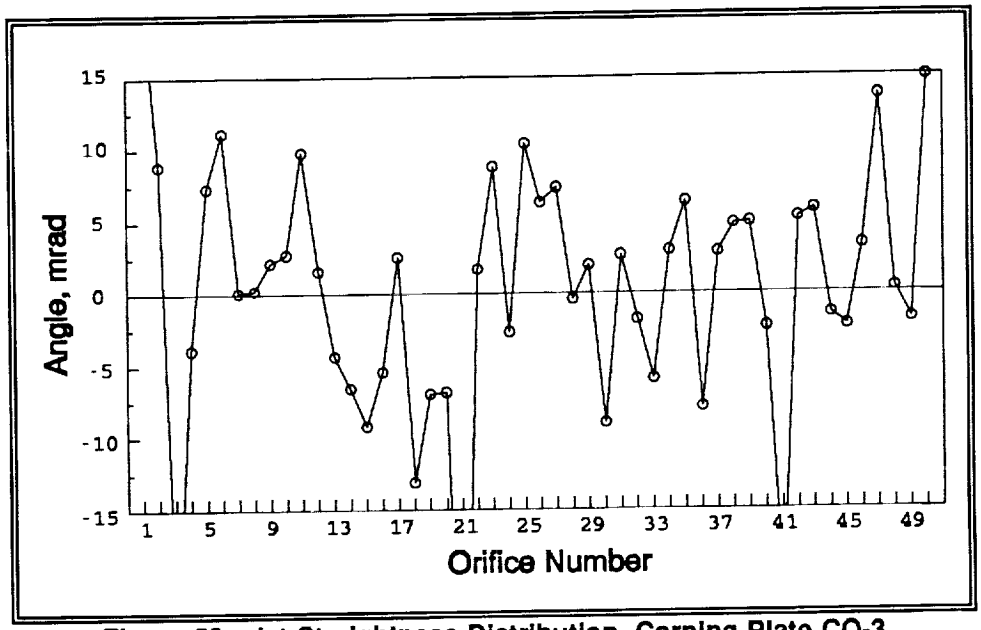

Figure 50: Jet Straightness Distribution, Corning Plate CO-3

Five (5) Corning orifice plates were assembled to drop generator housings. All five cracked during curing (170°C), probably due to thermal expansion coefficient mismatch. However, the cracks on four (4) of the plates were at the edges of the plates (ie., away from the orifices), and three (3) of these did not leak. The cracks on the three plates that did not leak had no effect on jet straightness.

The three (3) surviving Corning orifice plates/drop generator assemblies were installed in the jet straightness test system. All three received C ratings from the qualitative evaluation. In order to have some quan-

Table XII: Quantitative Jet Straightness Results Summary, Corning Orifice Plate

Orifice Plate	Standard Deviation of Jet Angle, mrad
CO-1	9.7

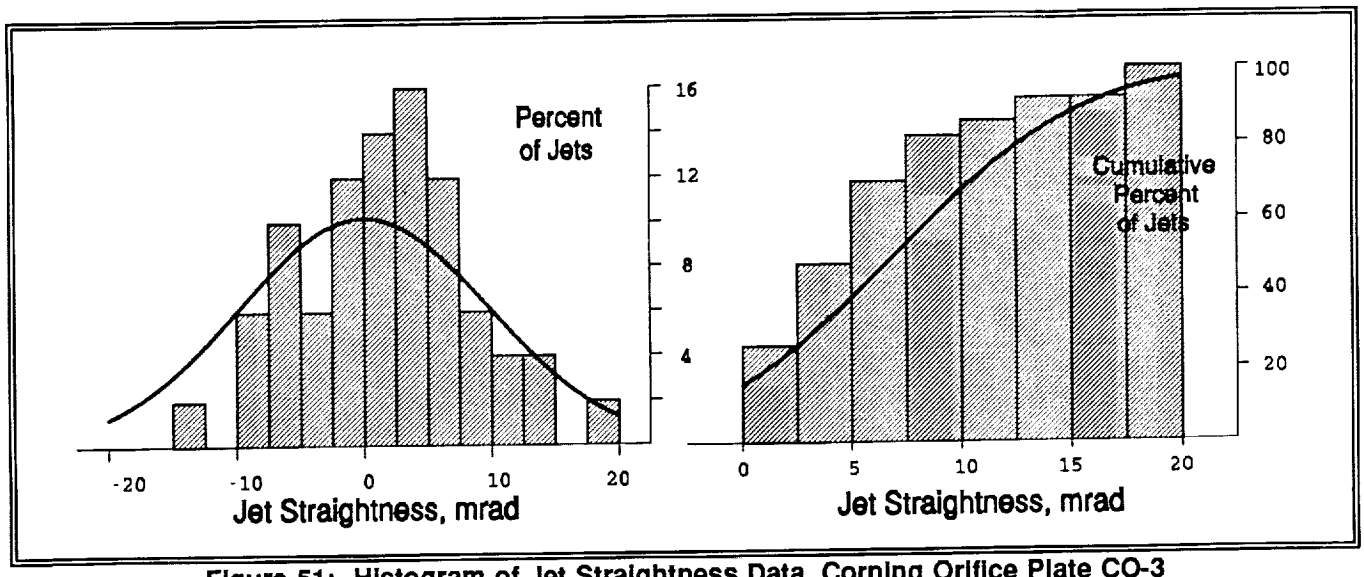

Figure 51: Histogram of Jet Straightness Data, Corning Orifice Plate CO-3

titative jet straightness data base for the Corning orifice plates, plate CO-3 was quantitatively evaluated for jet straightness.

The jet straightness distribution for CO-1 is shown in Figure 50 and the overall results are given in Table XII. Given the large variation in orifice diameters and the negative observations related to orifice shape and the location of the minimum orifice diameter, it is somewhat surprising that the jet straightness is only about ~50% larger (worse) than the average of the Buckbee Mears orifice plates and ~100% larger than the Stork-Veco orifice plates. Figure 51 shows the jet straightness distribution for CO-3.

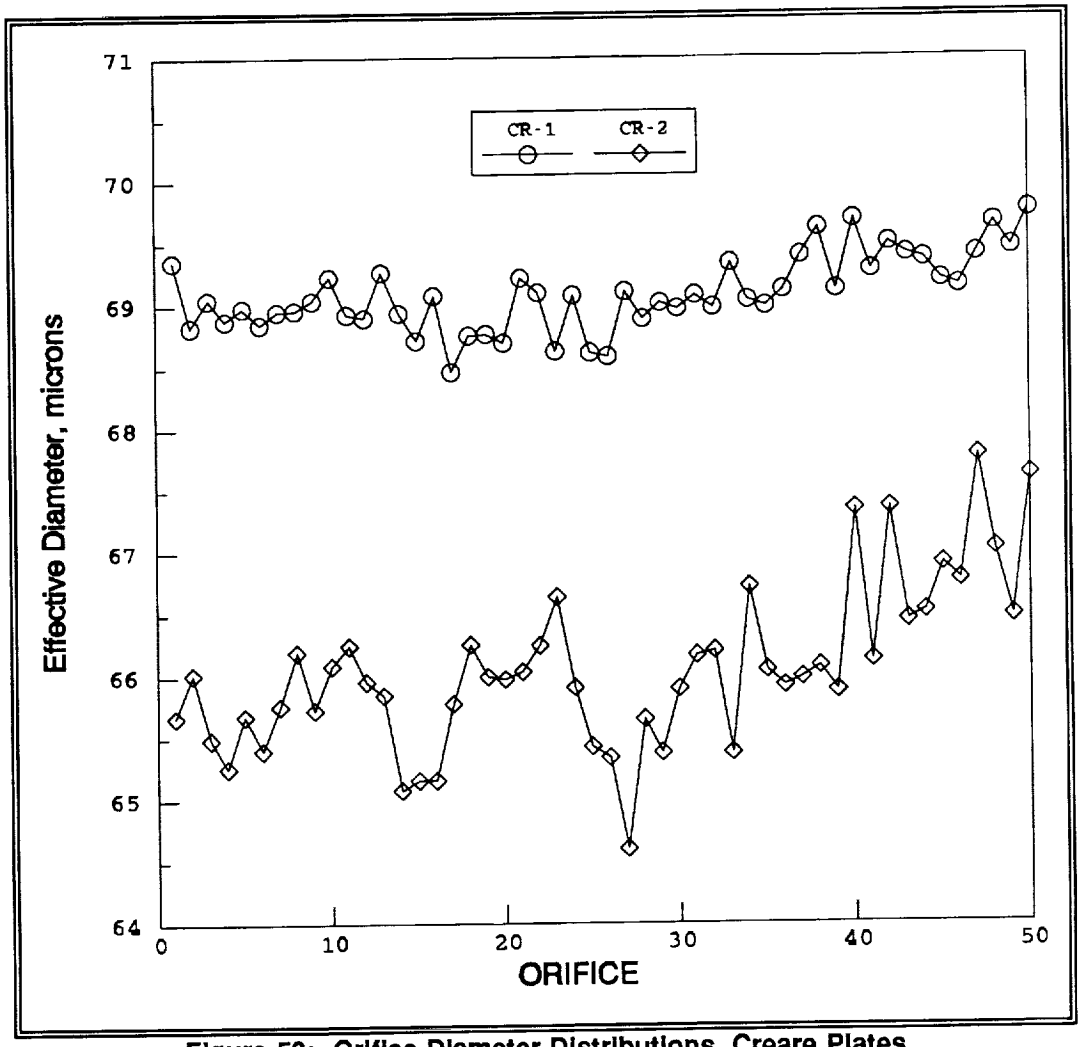

Figure 52: Orifice Diameter Distributions, Creare Plates

Overall, the Corning orifice plates were a surprising disappointment. If the orifice plates had been etched from one side only, the minimum diameter would be at the orifice exit, removing one possible source of jet straightness error. Before eliminating Corning and/or Fotoceram orifice plates from consideration for future LDR development efforts, discussions should be held with Corning to determine the causes the poor orifice quality and diameter control. In addition ,the implications of single sided etching should be discussed.

Table XIII: Summary of Creare Plates Orifice Diameter Measurements

	CR-1	CR-2	avg.
average, μm	69.1	66.1	67.6
std. dev., μm	0.3	0.7	0.5
std. dev., %	0.4	1.0	0.7
std. dev. = standard deviation			

4.9 Creare (EDM) Orifice Plates

Electro-discharge machining (EDM) was not rated very highly during Phase I and, originally, there were no plans to evaluate EDM orifice plates in Phase II. However, Micro-Fab was contacted during Phase II by Creare Inc. personnel interested in providing orifice plates for our evaluation. They had developed an EDM orifice fabrication process for their High Heat Flux Cold Plate for Space Applications project, a Phase II SBIR contract (NAS9-17574). Two orifice plates (with the correct number of orifices and pitch) were provided free of charge. Since this represented a very low cost opportunity to increase the number of orifice plate types experimentally evaluated during Phase II, both of the Creare EDM plates were measured for diameter distribution and jet straightness performance.

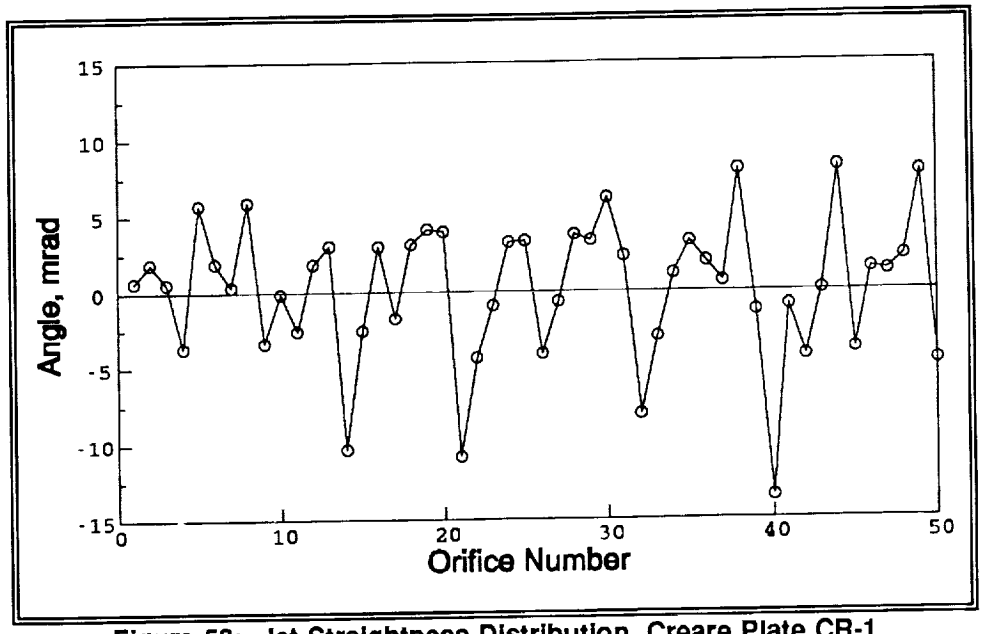

Figure 53: Jet Straightness Distribution, Creare Plate CR-1

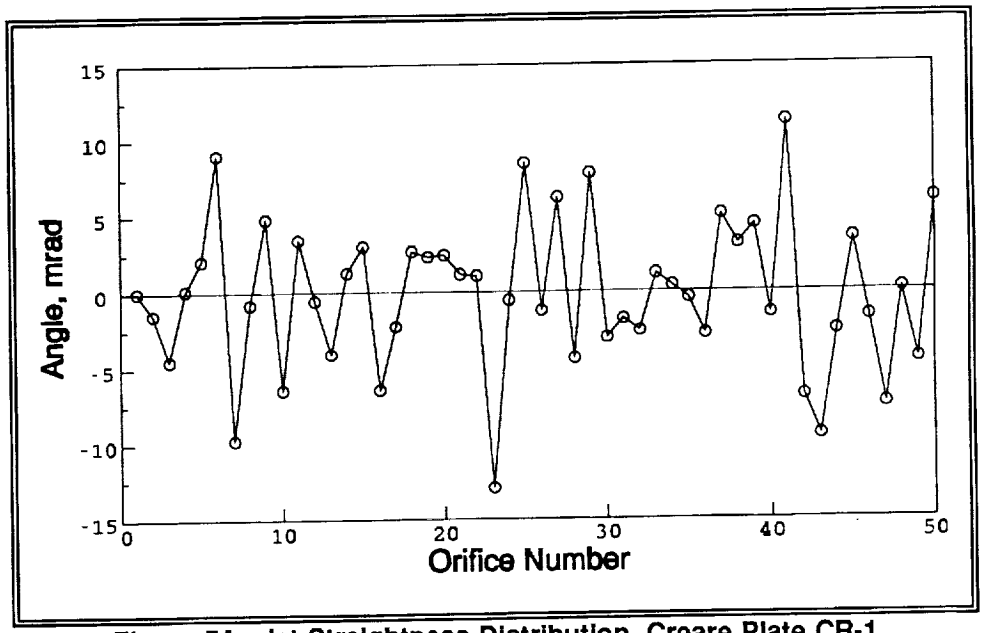

Figure 54: Jet Straightness Distribution, Creare Plate CR-1

The orifice diameter distributions for the Creare plates are shown in Figure 52 and are summarized in Table XIII. The diameter variation for CR-1 was the lowest (best) of the 50 hole plates measured in this study. Taken together, the two Creare plates had the lowest diameter variation of the orifice plate types evaluated in this study, along with the Stork-Veco (electroform) orifice plates. Diameter mea-

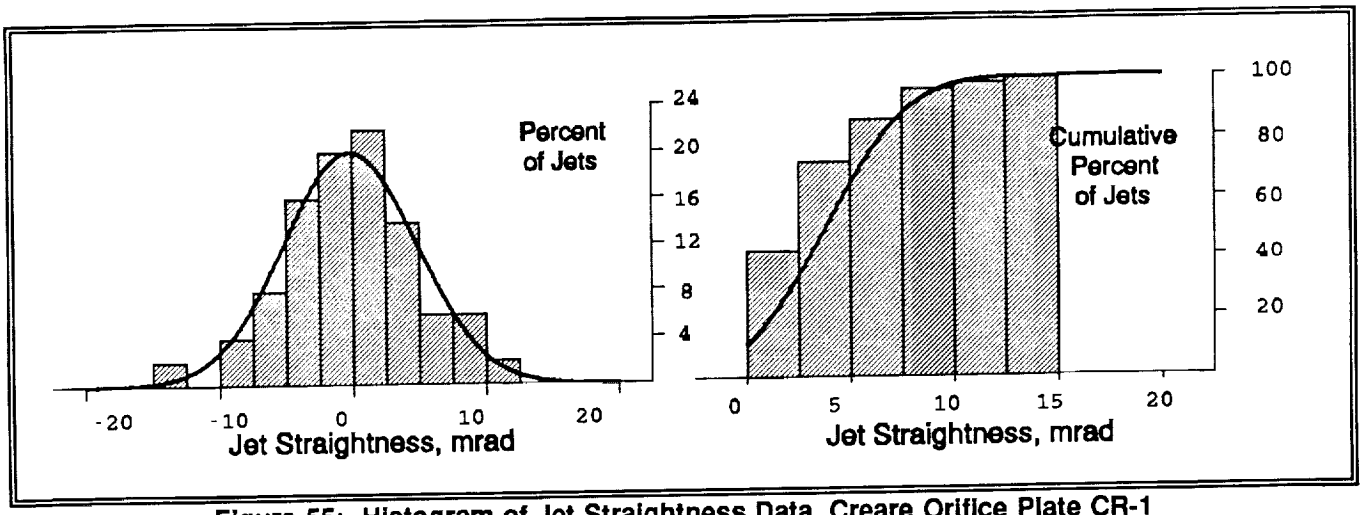

Figure 55: Histogram of Jet Straightness Data, Creare Orifice Plate CR-1

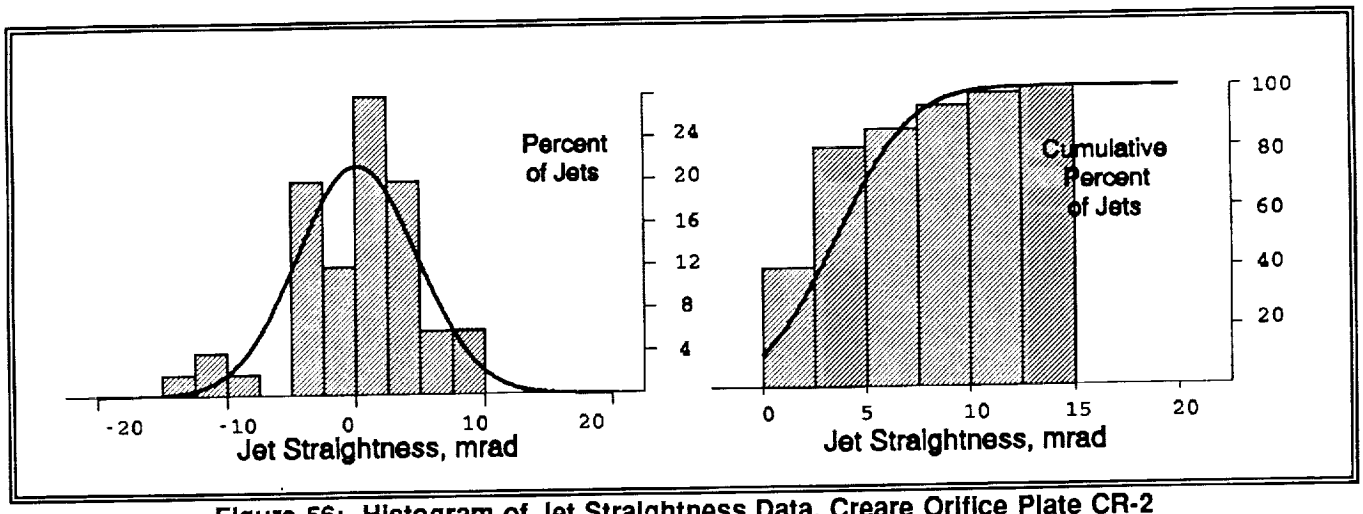

Figure 56: Histogram of Jet Straightness Data, Creare Orifice Plate CR-2

surement deviation was not determined for the Creare orifice plates, but based on the quality of the surface finish and sharpness of the orifice edges, it is estimated to be similar to that of the Buckbee Mears orifice plates (0.44μm).

Both Creare orifice plates were mounted to drop generator housings and evaluated for jet straightness. Both plates received an A qualitative jet straightness. Jet straightness distributions for the two plates are shown in Figure 53 and Figure 54, and the data are summarized in Table XIV. Histograms of the jet straightness distributions for both Creare orifice plates are shown in Figure 55 and Figure 56. The average jet straightness deviation for the Creare plates was the second lowest (best) of the orifice plate types evaluated and was only 0.2% higher (worse) than the Stork-Veco orifice plates.

Table XIV: Quantitative Jet Straightness Results Summary, Creare Orifice Plates

Orifice Plate	Standard Deviation of Jet Angle, mrad
CR-1	4.9
CR-2	4.6
average, 2 plates	**4.8**

4.10 Lee (Etched Sandwich) Orifice Plates

During Phase II, a representative of the Lee Company contacted NASA and MicroFab regarding their multiple orifice ink-jet bar code printer. The print head has 64 orifices on 508μm (0.020") centers in two rows. Lee representatives would not discuss the fabrication process, but by observing the orifice plate, the following description was surmised.

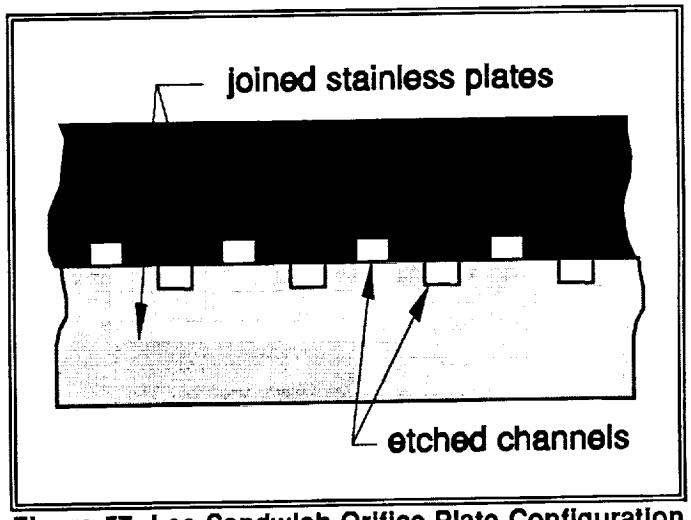

Figure 57: Lee Sandwich Orifice Plate Configuration

The orifices are fabricated by joining (method unknown) thin metal plates, each with etched slots. A photomasking process is probably used to control the etched geometry. The slots in each plate are offset from each other by half the pitch when the plates are joined, producing a staggered array. After joining, the front surface of the orifice plate is lapped, which removes any indication of the parts line. A sketch of the orifice plate design is shown in Figure 57.

This fabrication method was not known to us previously, and was not evaluated in Phase I. As with the Creare orifice plates, adding the Lee orifice plates to the Phase II evaluation represented a very low cost opportunity to expand the experimental jet straightness database. Two standard orifice plates were ordered and received from Lee.

The Lee orifices were rectangular (with a 2:1 aspect ratio) and the orifice edges were very rounded. Both orifice plates were measured for orifice diameter distribution, and the results are shown in Figure 58 and summarized in Table XV. The mean orifice diameters are seen to be almost double the desired nominal value, 75μm, due to the use of a standard

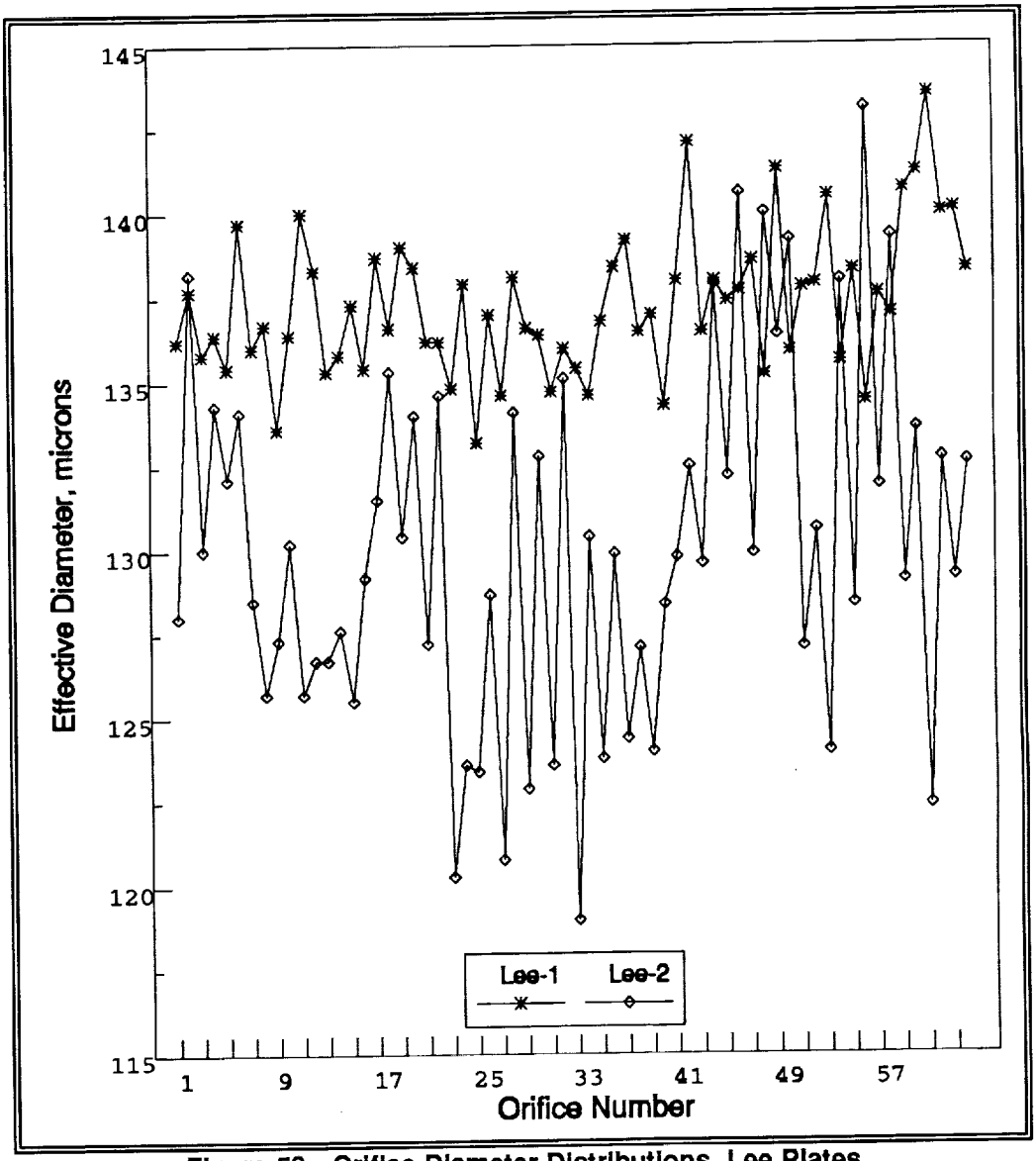

Figure 58: Orifice Diameter Distributions, Lee Plates

part. Obtaining parts with the desired orifice diameter would not have been difficult, if the straightness results had been good (they were not). The diameter variation for one of the two plates is fairly low (1.5%), while the diameter variation for the other plate is almost 3 times greater.

Table XV: Summary of Lee Plates Orifice Diameter Measurements

	Lee-1	Lee-2	avg.
average, μm	137.3	130.1	133.7
std. dev., μm	2.1	5.3	3.7
std. dev., %	1.5	4.1	2.8
std. dev. = standard deviation			

Table XVI: Quantitative Jet Straightness Results Summary, Lee Orifice Plate

Orifice Plate	Standard Deviation of Jet Angle, mrad
Lee-1	7.6

Because the Lee orifice plates came already assembled to their own drop generator housing, a special holding fixture was designed and fabricated to adapt the Lee drop generator to the jet straightness test system. Both plates were mounted in the jet straightness test system and both were given a C qualitative jet straightness rating. For completeness, one of the two Lee orifice plates was quantitatively evaluated for jet straightness. Figure 59 and Table XVI show the jet straightness test results for Lee-1. Figure 60 gives a histogram of the jet straightness distribution for orifice plate Lee-1. As can be seen, the straightness results were very poor. Based on our current understanding of the fabrication process and on the test results of this study, we do not recommend pursuing further development efforts with the Lee orifice plates.

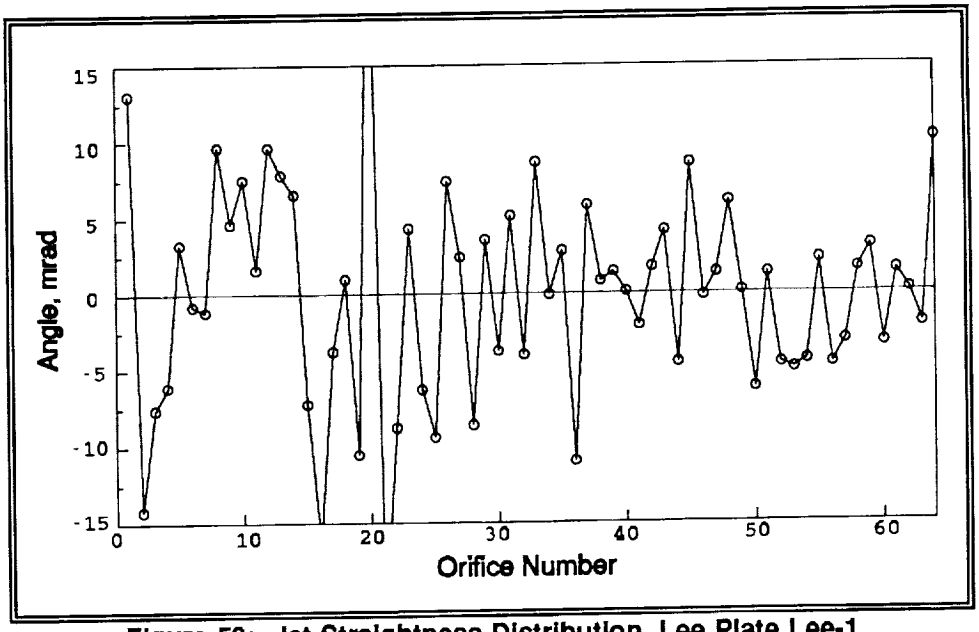

Figure 59: Jet Straightness Distribution, Lee Plate Lee-1

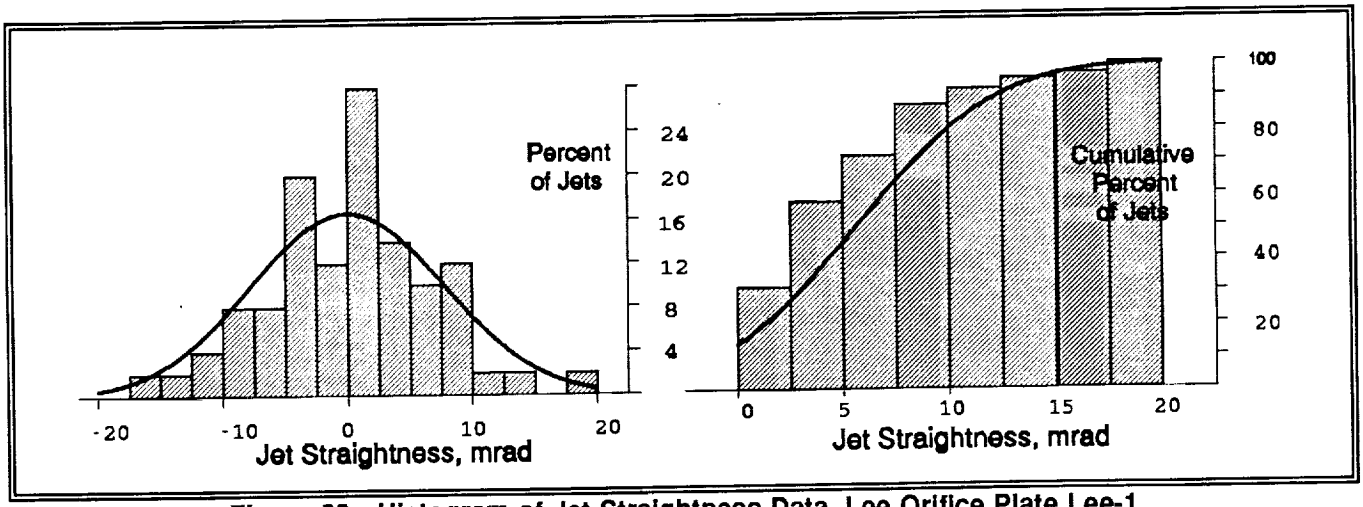

Figure 60: Histogram of Jet Straightness Data, Lee Orifice Plate Lee-1

4.11 Galileo (Multichannel) Orifice Plates

The Microchannel Plate (MCP) fabrication process described in section 3.3.8 was developed specifically to produce a very high density of orifices in a small area. For their normal electronic, optical, and internal hydrodynamic applications, the high orifice density of MCP's is very advantageous. However, if used as an orifice plate whose function is to produce distinct jets, as is the case for this study, the very high orifice density has two drawbacks. First, jet merging can occur at very short distances from the orifice exit, even if the jets are all <5 mrad, making jet identification and straightness measurement difficult, if not impossible. Second, transient wetting of the orifice plate during start-up can cause two or more jets to merge in a pool of fluid at the orifice plate. Some of these jet groups will not separate after the start-up transient, again making jet identification and measurement difficult. Both these conditions are also undesirable for an operational LDR array.

In light of the above, discussions were held with Galileo personnel to define a configuration that would be both testable and manufacturable at a reasonable cost (and time) in small quantities. To produce a custom orifice plate for this study from stock microchannel material, Galileo planned to mask off most of the fibers before the etching process. Only fibers that were approximately in the desired locations would then have the core glass etched out to produce an orifice. Total cost was quoted at $2,100 per orifice plate. Because of the high cost in small quantities, only two orifice plates were ordered from Galileo.

To insure that a MCP orifice plate would be available for testing even if the custom orifice plate was not delivered, two standard configuration orifice plates (glass capillary arrays in Galileo's terminology) were ordered. The standard configuration arrays (circular) were 13mm in diameter, 1mm thick, and contained 100μm diameter orifices. The 100μm diameters were the closest available stock parts. Galileo normally makes this product in much smaller diameters (10-20μm).

Table XVII: Summary of NASA Plates Orifice Diameter Measurements

	NASA-1	NASA-2	avg.
average, μm	67.3	90.2	na
std. dev., μm	0.9	1.9	1.4
std. dev., %	1.4	2.1	1.8

std. dev. = standard deviation
note: 15 orifices per orifice plate

No functional custom parts were received from Galileo, due to problems they had with the etching and laser cutting processes they were using. Four (4) "best effort" parts were received, but after assembling three (3) to drop generator housings, it was discovered that none of the holes were open. In addition, we noted that the overall orifice quality was much poorer (out of round orifices, rounded edges, and large variation on diameter) than what we had expected, both from previous experience and from Galileo's literature. We were informed that Galileo uses two types of glass fibers in their production. The fibers used in the parts sent to us (soda lime glass) do not have the precise diameter control that the other fibers have. Any future work with Galileo should specify the type of fiber used and a resultant orifice quality.

Since no custom plates were received from Galileo, special drop generator housings were fabricated for the 13mm diameter standard parts. The drop generator housing had a slot with dimensions 0.8mm x 32mm over which the array was mounted. It was hoped that a sheet of jets <4-5 jets thick would be produced and some individual jets would be distinguishable enough to make jet straightness measurements. However, even at 60 psi, no individual jets could be produced using either Galileo standard arrays: the jets coalesced immediately into one large "jet."

MicroFab personnel have fabricated soluble core glass arrays, using Galileo optical fibers, with 220 orifices and having all the jets <3 mrad. The current results are therefore both surprising and disappointing. It appears that producing quality glass fiber orifice plates for evaluation for an LDR application will require a much more time consuming (and expensive) effort than anticipated. Based on the degree of difficulty Galileo experienced in trying to modify their high density arrays to produce a lower density array, as is required by an LDR application, we recommend that future efforts with soluble core glass fibers be directed toward arrays fabricated in the manner described in section 3.3.7.

4.12 NASA (Mechanically Drilled) Orifice Plates

Three (3) mechanically drilled orifice plates were received from NASA Lewis. Each had only 15-16 orifices on 635μm centers, due to fabrication difficulties. One of the plates had some form of contamination in seven (7) of the orifices which could not be removed, even with vigorous and extended cleaning. One of the two remaining orifice plates had a nominal orifice

diameter of 70μm and the other a nominal diameter of 90μm. Visual inspection of the orifice plates indicated that the orifice quality was good, with round holes and sharp edges.

The two (2) uncontaminated orifice plates were measured for diameter distribution. The results are shown in Figure 61 and are summarized in Table XVII. The variation in diameter for the mechanically drilled orifice plates was fairly low (good), but greater than the diameter variation for the electroform and EDM orifice plates. Because of the low number of holes (15, as opposed to 50 on the standard orifice plates), care should be taken in comparing the mechanically drilled orifice plate results (both diameter and straightness) with the other orifice plates.

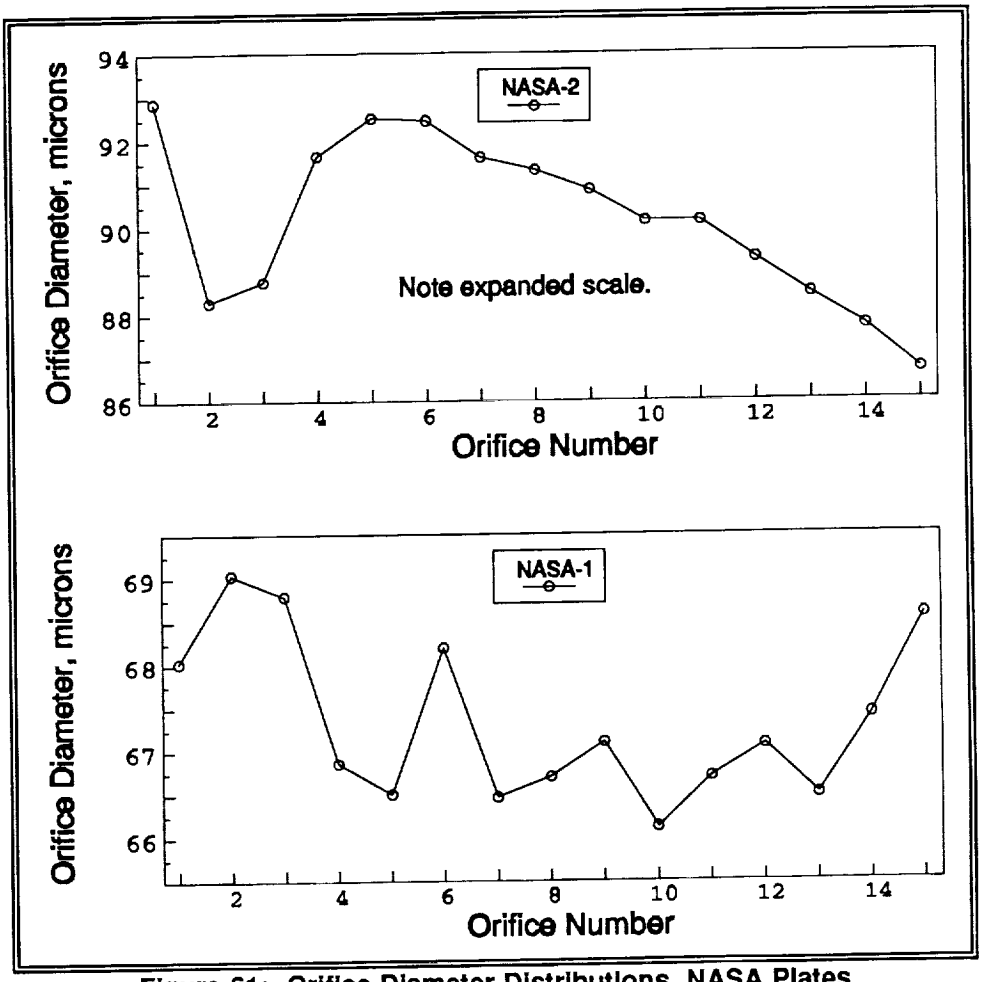

Figure 61: Orifice Diameter Distributions, NASA Plates

Table XVIII: Quantitative Jet Straightness Results Summary, NASA Orifice Plate

Orifice Plate	Standard Deviation of Jet Angle, mrad
NASA-1	5.7
NASA-2	4.0
average, 2 plates	**4.9**

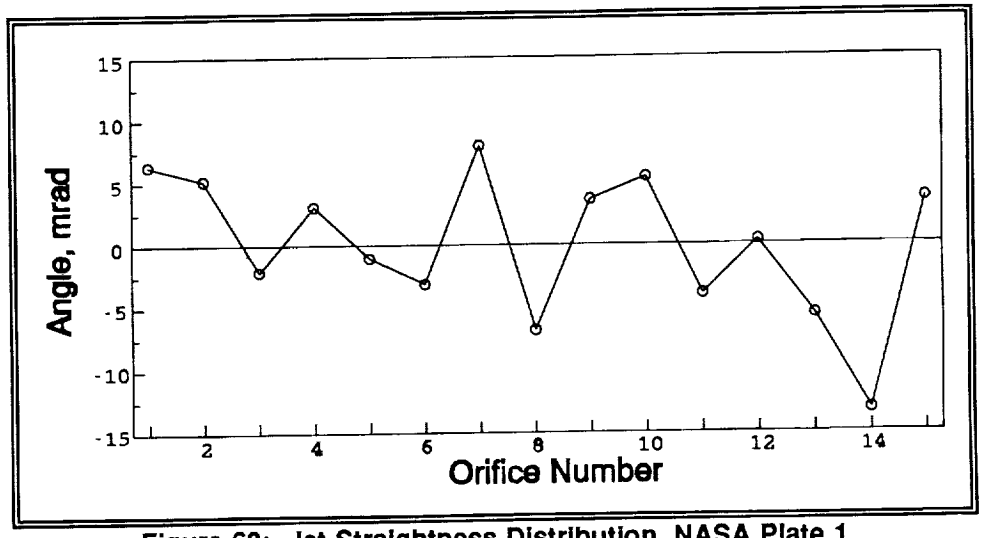

Figure 62: Jet Straightness Distribution, NASA Plate 1

Both NASA orifice plates were mounted to drop generator housings and evaluated for quantitative jet straightness and both received an A qualitative rating. The straightness distributions measured for each orifice plate are given in Figure 62 and Figure 63, and are summarized in Table XVIII. No histograms of the jet straightness distributions are given because of the low number of jets. Overall, the straightness of the NASA

orifice plates was as good as any of the orifice plates tested, but the low number of jets tempers this result somewhat.

4.13 Summary of Orifice Plate Testing Results

Diameter measurements for the seven (7) orifice plates resulted in a very clear distinction between orifice plates with good orifice diameter control and those with poor orifice diameter control. Both types of electroform (Stork-Veco and Buckbee Mears) plates, the EDM (Creare) plates, and the mechanically drilled (NASA) plates had average diameter standard deviations <1.5μm. In contrast, the Fotoceram (Corning), etched sandwich (Lee), and Microchannel Plate (Galileo) plates all had average standard deviations >3.5μm for the orifice diameters. The orifice diameter measurement results are summarized in Table XIX. Note that the Galileo plates were not actually measured for orifice diameter and are included in the >3.5μm average standard deviation category on the basis of visual inspection of the orifice plates. Also note that inclusion of the NASA orifice plates in <1.5μm average standard deviation category is based on much less statistically significant data (15 orifices per plate as opposed to 50 or greater on the other orifice plates).

Table XIX: Orifice Diameter Measurements, Summary of Results for All Seven (7) Orifice Plate Types

Orifice Plate Type & Vendor	Number of Plates Measured	Average Diameter, μm	Average Standard Deviation, μm
Electroform, Stork-Veco	5	69.8	0.5
Electroform, Buckbee Mears	5	76.7	0.7
Fotoceram, Corning	5	82.6	4.5
EDM, Creare	2	67.6	0.5
Etched Sandwich,Lee	2*	133.7	3.7
Multichannel Plate Galileo	0**	na	na
Mechanically Drilled, NASA	2***	na	1.4
TOTAL	21		

* *Nonstandard arrays (64 orifices), but very similar to standard array.*
** *Nonstandard, high density orifice arrays.*
*** *Nonstandard arrays, 15 jets per, 70μm and 90μm nominal diameters.*

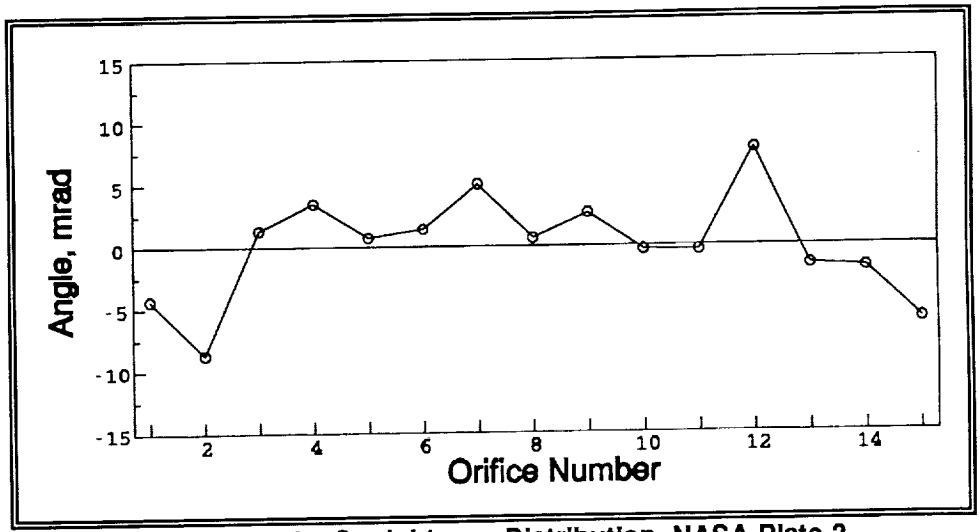

Figure 63: Jet Straightness Distribution, NASA Plate 2

The jet straightness performance of the seven (7) orifice plate types generally followed the orifice diameter results, but did not produce as clear a division in quality. The best orifice plates, the Stork-Veco electroform, the Creare EDM, and the NASA mechanically drilled orifice plates, all had average jet straightness standard deviations <5mrad for the one component of jet straightness measured. Although having a one component σ<5mrad is respectable for a first attempt, the LDR requirement that 99% of the jets be <5mrad is equivalent to

Table XX: Jet Straightness Measurements, Summary of Results for All Seven (7) Orifice Plate Types

Orifice Plate Type & Vendor	Number of Plates Evaluated for Qualitative Jet Straightness	Qualitative Ratings	Number of Plates Evaluated for Quantitative Jet Straightness	Average Standard Deviation, mrad
Electroform, Stork-Veco	4	3 - A 1 - B	3	4.6
Electroform, Buckbee Mears	4	1 - A 1 - B 2 - C	2	6.3
Fotoceram, Corning	3	3 - C	1	9.7
EDM, Creare	2	2 - A	2	4.8
Etched Sandwich,Lee	2*	2 - C	1	7.6
Multichannel Plate Galileo	2**	2 - C	0	na
Mechanically Drilled, NASA	2***	2 - A	2	4.9
TOTALS	19		11	

* *Nonstandard arrays (64 orifices), but very similar to standard array.*
** *Nonstandard, high density orifice arrays.*
*** *Nonstandard arrays, 15 jets per.*

σ<1.9mrad for a normal distribution. For a rectangular sheet LDR configuration,[3] only the jet straightness component normal to the line of centers of the orifice rows need be considered for all but the end jets. Therefore, the σ<1.9mrad requirement applies to that component only. For a triangular sheet configuration,[3] both components of jet straightness are important and the σ<1.9mrad criterion applies to the total jet straightness error. Assuming the two components of jet straightness are independent, a total σ<1.9mrad would be equivalent to each component having σ<1.3mrad. Thus, even the best orifice plates in this study have a long way to go before achieving the required straightness.

The rest of the orifice plates tested fell into two groups: the Buckbee Mears electroform and Lee etched sandwich orifice plates had straightness standard deviations in the range 6-8mrad, and the Corning Fotoceram and Galileo Multichannel plates had straightness standard deviations >9.5mrad. Although the jet straightness for the plates in both these categories was poor, these plates had jet straightness performance as close to the performance of the best plates as the best plates were to the ultimate goal, the Galileo plate being the only exception!

The jet straightness test results are summarized in Table XX. Note that the Galileo plates were not actually measured for jet straightness and are included in the >9.5mrad average standard deviation category on the basis of visual observations. Also note that inclusion of the NASA orifice plates in <5mrad average standard deviation category is based on much less statistically significant data (15 orifices per plate as opposed to 50 or greater on the other orifice plates).

5.0 Discussion and Conclusions

The results of this study would seem to indicate further development efforts be concentrated on electroform, EDM, and possibly mechanically drilled orifice plates. Before proceeding along these lines, the results of this study should be shared and discussed with the vendors. Both EDM and mechanical drilling received low ratings for manufacturability in the Phase I evaluation and, unless these vendors have significantly improved their processes, the favorable jet straightness results in Phase II do not in themselves make these processes candidates for further study. When manufacturability is considered along with the experimental results, the only fabrication process clearly recommended for further development efforts is electroform, with Stork-Veco being the preferred vendor.

As discussed above, the results for the Fotoceram (Corning) and Multichannel Plates were extremely disappointing. The Fotoceram process is one of the most appealing for an LDR array application because of its suitability to volume production of large arrays. The Microchannel Plates are the commercially available process closest to the soluble core glass fiber process, which is the only process to have demonstrated the ability to produce arrays with 100% of the jets <5mrad (<3mrad in some cases). Therefore, before dropping Fotoceram from further consideration, discussions should be held with Corning personnel to see if minor modifications to their process can significantly improve jet straightness. In particular, modifications to improve hole quality and to insure the minimum orifice diameter is at the orifice exit should be addressed. In addition, discussions should be held with Galileo personnel to explore the possibility of their generating a low density, high quality orifice array for the LDR application.

6.0 Recommendations

Most of the orifice arrays evaluated in Phase II were single row, 50 hole arrays of 75μm diameter on 625μm centers (nominally 3.2cm long). As currently envisioned, a subassembly of a Liquid Droplet Radiator (LDR) system will consist of a 4000 hole drop generator configured in a 20x200 array of 75-100μm diameter with the orifice pitch/diameter in the 4-6 range. The next logical step in the development of an LDR orifice array would be to obtain orifice plates with:

More rows

The most straightforward approach would keep the number of orifices at 50, orifice diameter at 75μm, and the orifice pitch at 625μm, while increasing the number of rows to 5. Depending on the response of the vendors selected and the data obtained from 5 row arrays, the number of rows might be increased to 10.

More orifices in one row

The length of a 200 hole per row array with 75μm diameters and a pitch/diameter ratio of 4 (300μm) would be nominally 6cm. This represents a minimum array length because of the small orifice diameter and the low pitch/diameter. As a first step, this array length would be used with the current 75μm orifice diameter and 625μm pitch. Rounding up, this would result in 100 holes in a row. As this is not a large increase in the 50 holes used in the present study, two rows would be desirable.

Smaller pitch/diameter

The pitch/diameter ratio affects the overall size, and thus weight, of the drop generator. In addition, structurally induced jet straightness effects are a function of pitch/diameter. In both cases, low values are better, up to the point where heat transfer performance is degraded. A simple extension of the current work would be to obtain arrays of 100 orifice with 75μm diameters on 300μm centers. These arrays would require no modification of the existing jet straightness tester.

Based on the above, the following future effort is recommended:

Task I: Low Pitch/Diameter Orifice Plate Evaluation

From each of 2 vendors, obtain 5-10 single row orifice plates, each with 100 holes with diameters of 75μm on 300μm centers. Fabricate drop generator housings, measure orifice diameters, assemble the orifice plates to the housings, measure jet straightness, and reduce and analyze the data. Compare the results with the Phase II results with single row, 50 hole plates with 75μm diameters on 300μm centers.

Task II: Multiple Row Orifice Plate Evaluation

From each of 2 vendors, obtain 5-10 multiple row orifice plates (4-6 rows, depending on vendor response to the RFQ), each row having 50 holes with diameters of 75μm on 625μm centers. Design and fabricate drop generator housings, design and fabricate modifications to jet straightness tester mechanical and fluid systems, measure orifice diameters, assemble the orifice plates to the housings, measure jet straightness, and reduce and analyze the data. Compare the results with the Phase II results with single row, 50 hole plates with 75μm diameters on 300μm centers.

Task III: Full Length Orifice Plate Cost Estimate

From each of 2 vendors, obtain estimates for the cost of producing 5-10 orifice plates with 5-10 rows, each row having 100 holes with diameters of 75μm on 625μm centers.

7.0 References

1. Roark and Young, *Formulas For Stress and Strain*, 5th edition, Niagara Hill, New York, 1975.

2. Peterson, R.F., *Stress Concentration Factors*, John Wiley and Sons, New York, 1974.

3. Mankamyer, M.M., R.E. Snyder, R.T. Taussig, "Liquid Droplet Radiator System Investigation," AFRPL-TR-85-080, November 1985.

4. Filmore, G.L., "Drop Velocity from an Ink-Jet Nozzle", *IEEE Trans. on Ind. App.*, Vol. 6, pp. 1098-1103, Dec. 1983.

5. Wallace, D.B., "A Method of Characteristics Model of a Drop-On-Demand Ink-Jet Device Using an Integral Drop Formation Method," ASME publication 89-WA/FE-4, December 1989.

6. Kretz, M., editor, *Mechanical Engineers' Handbook*, John Wiley & Sons, New York, pp. 1527-1529, 1986.

7. K.A. White, "Liquid Droplet Radiator Development Status," 22nd Thermo-physics Conference, AIAA, July 1987.

8. Mattick, A.T., and A. Hertzberg, "Liquid Droplet Radiators for Heat rejection in Space," *Energy to the 21st Century,* Vol. 1, AIAA, New York, 1980. pp. 143-150.

9. Braun, H., "Fluid Jet Print Head," U.S. Patent #4,606,104, 1987.

Appendix I: Vendor List

Over fifty companies or organizations were identified and approximately 70% of those were contacted. The list of companies identified is shown below. Trips were made to visit eleven of these companies. The list of companies identified is given by process type.

Where we have enough information to rank companies *in a given process area*, the rankings are shown to the left of the company name. Note that the rankings are relative to *LDR orifice array development only.*

Electroform - Plating

1 Stork-Veco
68 Harvard Street
Brookline, MA 02146

2 Buckbee Mears
245 E. 6th Street
St. Paul, Minnesota 55164

EMF
3025 Janitell Road
Colorado Springs, CO 80901

Optical Radiation Corporation
1300 Optical Drive
Azusa, California 91702

GAR Electroforming
Augusta Drive
Danbury, Connecticut 06810

3 AMT - Xerox
Jefferson Road
Rochester, New York

A.J. Tuck Company
10 Tuck Road
Brookfield, Connecticut 06804

GAR Electroforming
Augusta Drive Commerce Park
Danbury, Connecticut 06813

T.V. Jay Company
1771 W. Sunnyside Avenue
Chicago, Illinois 60640

Hanovia
100 Chestnut Street
Newark, New Jersey 07105

Chemical Milling

Optifab, Inc.
1550 W. Van Buren
Phoenix, Arizona 85007

Photo Milling Inc.
2437 Radley Court
Hayward, California 94545

Litchfield Prec. Comp., Inc.

MECH - TRONICS Corp.
1635 N. 25th Ave.
Melrose Park, Illinois 60160

Photo Fabrication Eng. Inc.
2 Granite Park
Millford, Massachusetts 01757

Tech - Etch, Inc.
45 Aldrin Road
Plymouth, MA 02360

1 Vacco Industries
10350 Vacco Street
South El Monte, CA 91733

Hutchinson Technology Inc.
40 West Highland Park
Hutchinson, Minnesota 55350

Laser Drilling

EBTEC
630 Silver Road
Agawam, Massachusetts 01001

Laser Fare Ltd., Inc.

1 Industrial Drive South
Lan Rex Industrial Park
Smithfield, R.I. 02917

Precision Aperture
P.O. Box 10863
Fort Wayne, Ind. 46854

Raytheon Company
4th Avenue
Burlington, MA 01803

Control Laser
7503 Chancellor Drive
Orlando, Florida 32809

Chicago Laser Systems, Inc.
4034 North Nashville Avenue
Chicago, Illinois 60634

2 Lumonics
12163 Globe Road
Livonia, MI 48150

Coherent General Inc.
1 Picker Road
Sturbridge, MS 01566

1 Image Micro Systems
900 Middlesex Turnpike
Billerica, MA 01821

XMR
5403 Betsy Ross Dr.
Santa Clara, CA 95054-1102

Electro-Discharge Machining

2 Panasonic
One Panasonic Way
Secaucus, New Jersey 07094

1 Creare
Etna Road, P.O. Box 71
Hanover, NH 03755

Electrocut - Pacific
1058 Terminal Way
San Carlos, California 94070

Aerospace Techniques, Inc.
5-A Pasco Hill Rd.
Cromwell, CT 06416

West Hartford Tool & Die Co.
840 Holmes Road
Newington, Connecticut 06111

New England Die Co., Inc.
49 Ford Ave.
Waterbury, Connecticut 06111

Spectrum Manufacturing, Inc.
140 Hintz Road
Wheeling, Illinois 60090

F.D. Miller Tool Company
RD 1 Box 282
Brodbecks, Penn. 17329

Mechanical Punching/Broaching
Accurate Products Company
404 Hillside Avenue
Hillside, New Jersey 07205

Chatham Precision Inc.
342 Union Street
Stirling, New Jersey 07980

Fairview Machine Company
427 Boston Street
Topsfield, MA 01983

Nikkoshi Co., Ltd.
151 East Post Road
White Plains, New York 10601

Dupont

2 Celanese

1 Kasen
Japan

National Jet

Nippon Nozzles, Japan
Frey, German
Ceccheo, Italian

Mechanical Drilling
2 NASA
Lewis Research Center
Cleveland, Ohio

1 Lawrence Livermore Labs

National Jet
10 Cupler Drive
LaVale, Maryland 21502

Ted Pella Inc.
P.O. Box 510
Tustin, California 92681

M.A. Ford Company
Davenport, IA

International Carbide
Jamesville, WI

Soluble Core Glass Fibers
None available

Multichannel Plates
Varian Image Tube Division
Microchannel Plate Operation
601 California Avenue
Palo Alto, California 94303

1 Galileo Electro-Optics Corp.
Galileo Park
Sturbridge, MS 01518

Electron Beam Machining
M.G. Industries, Systems Div.
9427 Fountain Blvd.
Memomonee Falls, WI. 53051

Laybold Inc.
120 Post Road
Enfield, CT. 06082

Ion Drilling
Commonwealth Scientific Corp.
500 Pendleton Street
Alexandria Virginia 22314

IICO
3350 Scott Blvd.
Santa Clara, California 95051

Fotoceram
1 Corning Glass Works
MP 21- 3- 4
Corning, New York 14831

Hoya Glass
Japan